University of Tuscia

Department for innovations in Biological, Agri-food and Forest systems

Ph.D. Program

XXXIV Cycle

New Technologies for Forest Monitoring in Alpine Region

(S.S.D. AGR/05)

Ph.D. candidate

Dott. Shahla Asgharinia

Ph.D. Program Coordinator

Prof. Andrea Vannini

Supervisor

Prof. Riccardo Valentini

Co-supervisor

Dr. Damiano Gianelle

A.A. 2020/2021

University of Tuscia

Department for innovations in Biological, Agri-food and Forest systems

Corso di Dottorato di Ricerca in Sciences, Technologies and Biotechnologies for Sustainability

Curriculum “Environmental technologies and Forest ecology”

XXXIV Ciclo

New Technologies for Forest Monitoring in Alpine Region

(S.S.D. AGR/05)

Tesi di dottorato di:

Dott. Shahla Asgharinia

Coordinatore del corso

Prof. Andrea Vannini

Tutor

Prof. Riccardo Valentini

Co-tutor

Dr. Damiano Gianelle

A.A. 2020/2021

Dottorato di ricerca in

“Technologies and Biotechnologies for Sustainability” Curriculum: “Environmental technologies and Forest ecology”XXXIV CICLO

TITOLO TESI DI DOTTORATO DI RICERCA

New Technologies for Forest Monitoring in Alpine Region

Docenti tutor:

Prof. Riccardo Valentini

Dottorando:

Shahla Asgharinia

Anno accademico 2020/2021

Dedication

I dedicate this dissertation to my family. I love you deeply with all my heart. To my husband Jim, you have been a listener and a supporter of all my endeavours. Your partnership, steadfastness, and love sustain me. To my son, Dante Soren, remember all things are possible. Never be afraid to pursue your dreams and goals. To my parents, and siblings especially Mansour, I love you without measure.

New Technologies for Forest Monitoring in Alpine Region

Abstract

The science of forest digitalization via technological innovation offers an opportunity to develop new methods for mass monitoring forest resources. A key constraint is the ability to collect data, store and analyze said retrieved data. The TreeTalker® (TT+) is a multisensory IoT-driven platform designed to detect and collect information on individual trees where its nested sensor approach captures several key eco-physiological parameters autonomously and in semi-real-time. Key parameters are: 1) tree radial growth, as an indicator of photosynthetic carbon allocation in biomass; 2) sap flux density, as an indicator of tree transpiration and functionality of xylem transport; 3) stem water content as an indicator of hydraulic functionality 4) light penetration in the canopy in terms of fractional absorbed radiation 5) light spectral components related to foliage dieback and phenology and 6) tree stability parameters to allow real time forecast of potential tree fall. The focus of this study is to design/calibrate and validate sensors for stem water content and sap flow measurement using the TreeTalker platform with the application of these platforms for monitoring ecophysiological parameters at a single tree scale providing time series data for forest monitoring.

i. Stem water content

To demonstrate the capability of the TreeTalker, a three-phase experimental process was performed including (1) sensor sensitivity analysis, (2) sensor calibration, and (3) long-term field data monitoring. A negative linear correlation was demonstrated under temperature sensitivity analysis, and for calibration, multiple linear regression was applied on harvested field samples, explaining the relationship between the sample volumetric water content and the sensor output signal. Furthermore, in a field scenario, TreeTalkers were mounted on adult Fagus sylvatica L. and Quercus petraea L. trees, from June 2020 to October 2021, in a beech-dominated forest near Marburg, Germany, where they continuously monitored sap flux density and stem volumetric water content (stem VWC). The results show that the range of stem VWC registered is highly influenced by the seasonal variability of climatic conditions. Depending on tree characteristics, edaphic and microclimatic conditions, variations in stem VWC and reactions to atmospheric events occurred. Low sapwood water storage occurs in response to drought, which illustrates the high dependency of trees on stem VWC under water stress. Consistent daily variations in stem VWC were also clearly detectable. Stem VWC constitutes a significant portion of daily transpiration (using TreeTalkers, up to 4% for the beech forest in our experimental site). The diurnal–nocturnal pattern of stem VWC and sap flow revealed an inverse relationship.

ii. Sap flow: an empirical approach

Here, a new IoT-based multisensing device, TreeTalker® with its tailored firmware is exploited to input different heating duration to capture high-frequency data of both heating and cooling phases. Using this advance in technology, its application, we aim to assess the applicability and thus merit of the TreeTalker toward sap flux density measurement and computation. Capability analysis of TT+ is verified both under a lab scenario using an artificial hydraulic column of sawdust and a stem segment of *F. sylvatica* L. in the field via mounted TT+ devices and with the comparison of commercial sap flow sensors on different species. Installing a TT+ on the artificial flow system, temperature evolution data from heating and reference probes are recorded both in heating and cooling phases to compute values of different flow indices under different flux densities.

Applied continuous heating mode and a transient regime with four different combinations of heating and cooling times (in minutes) 10/10, 5/10, 15/45, and 10/50 are tested by TT+ and calibration of flux density vs flow indices conducted by applying optimal fitting curve on the source data up to 8 (L dm-2 h-1).

Nonetheless, comparing TT+ set on the transient regime (10H/50C) performance across different species of Norway spruce, European beech, and oak in situ with well know thermal approaches (TDP: Continous Heating and HPV: Heat Pulse Velocity method) proved that the TT+ is capable to measure sap flow with reasonable accuracy (≈80%) for network-based mass monitoring in remote areas with low power consumption.

iii. Semi-analytical solution for transient regime

Measurement of xylem sap flow via thermal dissipation probes (TDP) and the transient regime (TTD), which is essentially derived from the TDP system, are two widely accepted and applied methods for estimating whole-tree transpiration. So far, thermal dissipation approaches use empirical equations to estimate sap flow and although robust,

by nature, are limited by their accuracy. To overcome the limitations typically associated with the empirical approach, a novel method is introduced to solve the heat partial differential equation driven by the mechanisms of conduction/convection for the transient thermal dissipation method (TTD) with heating/cooling cycles. Also, a simple semi-analytical method was developed to exploit the convolution integral of the heat flow equation. The capability of the novel solution is approved by comparing its results with observations under the controlled condition as well as the output of the available well-known empirical equations under field circumstances. An essential feature of the TreeTalker platform, therefore, is to capture the full heat flow curve at the microprocessor level and integrate a semi-analytical approach to mathematically evaluate the amount of sap velocity and thermal diffusivity at a large scale and in real-time.

iv. TT+ applications at forest monitoring

In this investigation, two sites (Molveno and Val Canali) are established with a total of 84 TT+ in the Alpine zone, Northern Italy. The Italian Alps are important ecosystems supporting rich landscapes and biodiversity with their forests supporting several key ecosystem services. Thus, monitoring these ecosystems is of critical importance to track the variation of individuals' ecological demands in different species. For this study, we focus on two of the most dominant tree species across the Central European Forest, *Fagus Sylvatica* L. and *Picea Abies* L., to evaluate the TT+ as a novel biosensing platform for mass monitoring. Furthermore, we explore the relationships between site characteristics and abiotic factors using collected TreeTalkers data. Although not a complete substitute for field data collection, platforms such as the Treetalker can enhance established methods for mass monitoring, offers big data solutions on individual trees, and further the pursuit of forest digitalization. Yet, as with any new technology challenges remain related to obstacles such as sensor green character, durability, flexible design, maintenance, precision, and accuracy.

***Keyword**: TreeTalker, IoT, Forest digitalization, Time series data, Stem water content, Sap flow, Alpine region*

Table of Contents

General Summary

Introduction

Forests cover about 30% of the land area and provide a number of ecological services, such as biodiversity, water purification, and carbon sequestration (Sánchez et al., 2019). Recently, tree mortality is increasing in mountain forests due to climate change, which results in species shifts, erosion increase, degradation of ecosystem services, and ultimately changes in landscapes (Gazol et al., 2018). Evidence of species distribution and rearrangements for example, are becoming evident (Illés and Móricz, 2022). With such rearrangements forecasted it is necessary to improve monitoring technologies related to data collection and synthesis. We know from satellite global estimations that there are about 3 billion trees globally (Ehrenberg, 2015), but despite all such efforts, we know very little about their physiological behavior, their interactions with the environment, and ultimately their lives. Thanks to the new developments in IoT and long-range data transmission (LoRa) technologies we have developed a new multi-functional sensing device, the "TreeTalker", able to transmit in quasi-real time (every hour) plant water transport, stem water storage, growth, tree oscillations, leaves spectral parameters and climate data at an extremely low cost. The object of my thesis therefore started with the goal of improving the current capability of the TreeTalker technology to monitor sap flow and tree stem water content. Furthermore, by deploying a network of TreeTalkers connected to a web-cloud, I was able to monitor individual tree responses to climate variability providing big data to assess forest health and trends. The data were analyzed by advanced analytical tools, including machine learning algorithms, to detect trees' environmental stresses and anomalies behavior.

Objectives

The first goal (GOAL-1). is the design, validation, and application of TreeTalker toward stem water content measurement using a frequency domain reflectometry sensor. The objectives linked to GOAL-1 are: – Objective 1.1: Sensor sensitivity analysis under controlled conditions to detect temperature, air humidity, and different matrix impact on the sensor signal output. – Objective 1.2: Collection of fresh-cut stem samples across different species to provide calibration equations and convert reported frequency values to stem volumetric water content. –Objective 1.3 Investigate TT capability on a daily, and seasonal scale for measuring stem water content for several individuals under climate variability in a beech site.

The second goal (GOAL-2). is the design, validation, and application of TreeTalker toward sap flow measurement. The objectives linked to GOAL-2 are: – Objective 2.1: Providing an empirical calibration equation for the TT sap flow sensor using a hydraulic bench filled with sawdust and freshly harvested stem segment of European beech in the lab. – Objective 2.2: Characterize and explore TT capability in sap flow measurement across different species in comparison with different well-known methods (heat pulse velocity method, Granier approach, and cyclic regime) in situ. – Objective 2.3: Propose a semi analytical solution to estimate sap flow based on the full heat dissipation curve captured by TT.

The third goal (GOAL-3) of this study is to establish an innovative in-situ monitoring network on mountain forest ecophysiological responses under climate variability, with the following characteristics: it is based on a new tool (called TreeTalker) measuring tree ecophysiological variables at an individual level, in quasi real and in situ time; it is cost-effective if compared to the current more common in situ monitoring systems. The objectives linked to GOAL-3 are: – Objective-3.1: Install a sample of TT+ in the alpine forest as a prototype for an innovative in-situ monitoring network on forest ecophysiology and response to climate and site variability. – Objective-3.2: Exploit the quasi-real-time data continuously collected by the TT+ in-situ monitoring network transmitted on a web-cloud platform through the long-range data transmission technology (LoRa), to demonstrate a path toward forest digitization. – Objective-3.3: Explore and compare the seasonal ecophysiological responses of beech and spruce specifically focused on water related indicators, transpiration rate and stem humidity. – Objective-3.4: Implement data analytics and machine learning algorithms to elaborate the continuously collected TreeTalker data with the aim of distinguishing the two species, European beech (*F. sylvatica* L.) and Norway spruce (*P. abies*) in two different sites.

Methodology

The following section is an introduction to methods applied throughout the dissertation. however, a comprehensive description for each topic is presented in the following chapters within these relevant sections. In summary, the TreeTalker (TT+) device technology developed by our team, was tested and applied under differing research projects as reported by (Matasov et al., 2020; Valentini et al., 2019) and the device is currently patented. Each TT+ is connected wirelessly (using a new LoRa low power chipset) to a node managed by another micro-controller serving the cluster of individual TT+ devices of the plot (typically 30 trees per node). The microcontroller is connected via a modem/router to a telephone network and internet connected to the computer cluster center facility at UNITUS. Pooling of data and requests of services are directly forwarded at the single tree level using our internal protocol. Data are collected every 60 minutes for each TT+ and transmitted to the server database. Currently, the battery system supports such operation mode for about 100 days.

Overall, the TT+ device has the following features associated with monitoring: 1) tree radial growth as an indicator of photosynthetic carbon allocation in biomass; 2) the tree sap flow, as an indicator of tree transpiration and functionality of xylem transport 3) the water content of the stem xylem; 4) light transmission in 12 spectral bands to infer the quantity and quality of tree canopy light absorption 5) The tree stability through an accelerometer sensor (accuracy ± 0.01 degrees) which measure the deviation of the position in respect of the gravity vector. 6) climate and soil parameters (air and soil temperature and humidity). Please note that the focus of this thesis, however, is toward water-related indicators for forest monitoring using the TT+ platform.

Executive summary

Chapter 1. The focus of chapter 1 was an investigation into sensor sensitivity and applied ecological compatibility using the IoT platform ‘Treetalker’ referred here on as TT+. Therefore, the

principal emphasis here was practical research into the TT+'s frequency domain reflectometry sensor. Through my research, I observed different sensor responses to different matrices with my findings ultimately leading to the creation of new species-specific calibration equations facilitating the conversion of sensor frequency signal to stem water volumetric water content. In addition, I was able to successfully demonstrate the TT+'s capability to detect several parameters at daily, and seasonal scales for measuring stem water content for several individuals under climate variability in a beech site. In support of such findings, I observed stem water fluctuations up to 4 % on a daily scale and seasonal variation up to 35% for a *Fagus Sylvatica L.* high forest in Germany. In addition, and as expected, rainfall events have a positive correlation with stem water content, whereas drought is negative.

Stem water content: a. I have investigated temperature and matrix-type effects on sensor performances. b. I have created new calibration equations provided for beech and oak species as well as pine sawdust to convert the recorded frequency signal to stem volumetric water content. c. application of the sensor hosted by the TT+ platform was successful in monitoring stem water content to collect mass data and detect individual and population responses under climatic variabilities. d. stem water fluctuations were detected up to 4 % on a daily scale and seasonal variation up to 35% for a beech high forest in Germany. e. as expected rainfall events have a positive correlation with stem water content, whereas drought is a negative as detected by the TT+.

Chapter 2. The goal of the second chapter in this thesis dissertation focuses on the design, validation, and application of TT+ toward sap flow measurement. Taking advantage of tailored firmware, I demonstrated the ability of the TT+ platform to easily perform as continuous heating, or a cyclic system with customizable measurement time intervals. This information allowed the application of empirical calibration equations provided for different flow indices using a hydraulic bench filled with pine sawdust in the lab. My principal findings in this section followed a logical method of comparing TT+ set on the transient regime (10 min Heating/50 min Cooling) performance across different species Norway Spruce, European Beech, and Oak in situ comparison with well know thermal approaches (TDP: Continuous Heating and HPV: Heat Pulse Velocity method). My results proved that the TT+ is capable to measure sap flow with reasonable accuracy (80 %) for network-based mass monitoring in remote areas with low power consumption. TreeTalker underestimates approximately 20% midday max sap flow rate and has a weak performance under low flux (< 0.5 l dm-2 h-1), however, the latter weakness is reported across most thermal approaches. This common weakness may be negated where a TDP approach is applied at a higher energy consumption cost. Finally, the role of stem water content is not banal and is highly important for capturing accurate temperature differences (Delta T, Heater Probe – Reference probe) between sap flow probes.

Chapter 3. The chapter follows research into sap flow measurement using TDP and transient regime methods. My goal in this section was to propose a semi-analytical solution to estimate sap flow based on the heat flow equation based on the full heat dissipation curve captured by TT+. As far as I am aware, this is the first time that such an approach has been constructed. My results suggest that by performing convolution integration, I was able to completely reproduce the heat flow curve optimizing with TT+ captured data and evaluation thermal diffusivity as well as flow

velocity. This result will be applied to new versions of the sap flow probes under construction as well as being fully applicable to the current and older versions of the TT+

Chapter 4. Ultimately, the TT+ is designed for the mass monitoring of individual trees within forests to obtain quasi real-time measurements of several dynamic tree ecophysiological processes. Therefore, in this chapter, I focused on a proof of concept toward mass monitoring using the TreeTalker. To demonstrate the proof of concept, we installed 82 devices on trees within a forest across two sperate sites mounted on two species, European beech and Norway spruce in the Trentino Province of Italy. In addition to the proof of concept for mass monitoring, I also focused on defining each species by way of the captured ecophysiological data from the TreeTalker and by both sites. I illustrate that over two consecutive years species behavior to seasonal climatic dynamics and some other abiotic features are clearly discernable from the captured data. By applying both unsupervised Principal Component Analysis and supervised Linear Discriminant Analysis my results explain that beech and Norway spruce behave differently across the season complementing the general and current excepted research on the behavior of each species. This result is most clearly demonstrated in Sap Flux Density and Stem Water Content aligning with the isohydric and anisohyrdic characteristics of each species, spruce and beech, across the growing period, respectively. Furthermore, the results from the TT+ on board spectrometer concur with the canopy phenological characteristics of each species with well-defined light use time series capture across 12 spectral bands. Whoever, in Alpine case study focusing on mountainous remote forests, big data collection was mainly limited by weak signal strength of IoT nodes, therefore, data were collected manually from backup internal memories of each single devices especially in Molveno site. And consequently, data quality check, validation and data analysis were challenging due to accumulated big data.

Conclusion

Across this research dissertation, I have investigated the application of the novel IoT platform ‘TreeTalker®’ and its application to forest and plant sciences. My work on the two sap flow sensors, that is, the frequency domain reflectometry sensor and the heating sensor, have helped to improve the overall platform’s capacity to collect meaningful and correct data related to stem water processes in tree stems. The data and analysis I performed led to some insightful moments, where confirmation of mass deployable IoT platforms can deliver big data at individual tree scale with a relatively low cost. In addition, the performance of the sensors via strict calibration experiments was improved, thus allowing the implementation of such calibrations across all deployed TT+ currently in more than 10 countries globally. Indeed, the semi analytical solution I solved for the heater probe and heat curve may prove to be a breakthrough in plant sciences as it avoids empirical approach and allows the optimization of the TT+ system saving battery power. As demonstrated in chapter 4, systems such as the TT+ offer novel and dynamic insights into tree behavior which in the future could be included in establishing empirical and deterministic models toward the fine tuning of these models and responses in stem water processes under dynamic climate change along with offering big data digitalization of forest monitoring data.

Breakthrough of this study:

1. We designed and developed a novel stem water content sensor along with a sap flow sensor for water status detection in living trees. Exploiting the developed sensor for mass monitoring, we were able to demonstrate seasonal fluctuation of stem water content. A caveat for this study was the importance of wood anatomical structure impact on sensor. To improve stem water sensor functionality for future research we are investigating the application of an impedance spectroscopy by inputting a different range of frequency from 70 to 600 MHz to detect both stem water content and stem water potential, in real time and continuously.

2. Different sap flow techniques were characterized and tested in the lab and field. Results highlight that the TTD system is outperforming regarding power consumption but limited under low flux rate. The TDP system is limited by power consumption and the HPV method having a theoretical base, using a very low energy for introducing pulses, has more capability for reverse, zero and positive flow detection. However, the accurate estimation of the heat velocity (reverse, zero, slow and fast) and proceeding further to convert it to sap flux density, requires evaluation of thermal diffusivity and sapwood moisture content. Overall, thermal approaches are known to underestimate sap flux density. Biological properties of conducting tissue, wound effects, radial flow and sapwood area should be considered to reduce possible errors in measuring sap flow rate.

3. The concept of a new semi analytical algorithms for a theoretical solution of the heat flow equation based on convolution integral under transient regimes (TTD) opens new potential for estimation of sap flow theoretically rather than the traditional empirical approach. Furthermore, our semi analytical solution improves the accuracy of computation of heat velocity under pulse system when the duration of pulse surpasses the instantaneous term. For instance, exploiting heat pulse methods with a single probe, to overcome the limitation of the slow flow measurement, pulse duration increased from an instant pulse (2 to 6 sec) to 30 sec. The proposed semi analytical solution attempts to reduce the error of sap flow estimation due to the uncertainties propagated through the empirical correlation equations. However, the influence of wounds, radial flow, sapwood area and stem moisture content on sap flow rate remains challenging.

4. The previous phases for testing and validating of TreeTalker toward sap flow and stem water content measurement provided the foundation for a novel approach for individual monitoring in an Alpine area at a reasonable cost. The objective being a focus on the exploitation of collected TreeTalker data and a meaningful ecological derivate. Here continuous real-time ecophysiological data were collected for different species (beech and Norway spruce) under different climatic conditions. By applying Machine Learning algorithms (PCA, LDA), most notably, we found that the ecological variables monitored by the TreeTalker and collected via their IoT capability can discriminate each species under investigation. In addition, collected TreeTalker data lead to the site discrimination as a function of light transmitted radiance primarily. However, species-based discrimination driven predominantly by sap flow, stem water content and near infrared parameters, has a higher classification accuracy rather than the site-based discrimination analysis. Keeping in mind that species based discrimination was conducted between beech and spruce which are distinctly different species. Indeed, it would be challenging to investigate the model response between species that are from the same family. The model accuracy can increase by linking remote sensed data such as elevation, slope, canopy volume etc… and field observations.

Article 1: Stem water content

Towards Continuous Stem Water Content and Sap Flux Density Monitoring: IoT-Based Solution for Detecting Changes in Stem Water Dynamics

Shahla Asgharinia [1,2,*], Martin Leberecht [3], Luca Belelli Marchesini [2], Nicolas Friess [4], Damiano Gianelle [2], Thomas Nauss [4], Lars Opgenoorth [3], Jim Yates [1,2] , and Riccardo Valentini [1]

1. Department for Innovation in Biological, Agro-Food and Forest Systems (DIBAF), Tuscia University, Via San Camillo de Lellis snc, 01100 Viterbo, Italy; jim.yates@unitus.it (J.Y.); rik@unitus.it (R.V.)

2. Forest Ecology Unit, Research and Innovation Centre, Fondazione Edmund Mach, Via E. Mach 1, San Michele All'adige, 38010 Trento, Italy; luca.belellimarchesini@fmach.it (L.B.M.); damiano.gianelle@fmach.it (D.G.)

3. Department of Biology, Philipps-Universität Marburg, Karl-von-Frisch Strasse 8, 35043 Marburg, Germany; martin.leberecht@biologie.uni-marburg.de (M.L.); opgenoor@staff.uni-marburg.de (L.O.)

4. Department of Geography, Philipps-University Marburg, Deutschhausstr. 10, 35037 Marburg, Germany; nico.friess@posteo.de (N.F.); nauss@staff.uni-marburg.de (T.N.)

- Correspondence: asgharinia@unitus.it

Forests

Received: 29 May 2022

Accepted: 28 June 2022

Published: 1 July 2022

DOI

https://doi.org/10.3390/f13071040

Towards Continuous Stem Water Content and Sap Flux Density Monitoring: IoT-Based Solution for Detecting Changes in Stem Water Dynamics

Abstract

Taking advantage of novel IoT technologies, a new multifunctional device, the “TreeTalker”, was developed to monitor real-time ecophysical and biological parameters of individual trees, as well as climatic variables related to their surrounding environment, principally, air temperature and air relative humidity. Here, IoT applied to plant ecophysiology and hydrology aims to unravel the vulnerability of trees to climatic stress via a single tree assessment at costs that enable massive deployment. We present the performance of the TreeTalker to elucidate the functional relation between the stem water content in trees and respective internal/external (stem hydraulic activity/abiotic) drivers. Continuous stem water content records are provided by an in-house-designed capacitance sensor, hosted in the reference probe of the TreeTalker sap flow measuring system, based on the transient thermal dissipation (TTD) method. In order to demonstrate the capability of the TreeTalker, a three-phase experimental process was performed including (1) sensor sensitivity analysis, (2) sensor calibration, and (3) long-term field data monitoring. A negative linear correlation was demonstrated under temperature sensitivity analysis, and for calibration, multiple linear regression was applied on harvested field samples, explaining the relationship between the sample volumetric water content and the sensor output signal. Furthermore, in a field scenario, TreeTalkers were mounted on adult *Fagus sylvatica L.* and *Quercus petraea L.* trees, from June 2020 to October 2021, in a beech-dominated forest near Marburg, Germany, where they continuously monitored sap flux density and stem volumetric water content (stem VWC). The results show that the range of stem VWC registered is highly influenced by the seasonal variability of climatic conditions. Depending on tree characteristics, edaphic and microclimatic conditions, variations in stem VWC and reactions to atmospheric events occurred. Low sapwood water storage occurs in response to drought, which illustrates the high dependency of trees on stem VWC under water stress. Consistent daily variations in stem VWC were also clearly detectable. Stem VWC constitutes a significant portion of daily transpiration (using TreeTalkers, up to 4% for the beech forest in our experimental site). The diurnal–nocturnal pattern of stem VWC and sap flow revealed an inverse relationship. Such a finding, still under investigation, may be explained by the importance of water recharge during the night, likely due to sapwood volume changes and lateral water distribution rather than by a vertical flow rate.

Overall, TreeTalker demonstrated the potential of autonomous devices for monitoring sap density and relative stem VWC in the field of plant ecophysiology and hydrology.

Keywords: *IoT, TreeTalker, sap flux, stem water content, transient thermal dissipation, capacitance sensor*

Introduction

Severe water stress can result in both hydraulic failure and carbon starvation contributing to the greater phenomena of tree mortality (Sevanto et al., 2014). Tree physiological parameters like sap flow and stem water content perform as plant-based water stress indicators (Nadezhdina, 1999; Salomón et al., 2020). Variation in sap flow and stem water content of a tree plays a biologically significant role in tree status and function with respect to internal and external drivers such as anatomical wood anatomy and vapor pressure deficit (WARING and RUNNING, 1978). Under water deficit, stem water storage contributes to transpiration thus helping to achieve a balance between root water uptake and water transpiration (Čermák et al., 2007; Dzikiti et al., 2007; Goldstein et al., 1998; Hernández-Santana et al., 2008; Malavasi et al., 2016; McDowell, 2011; Nadler and Tyree, 2008). Variation of stem water content in trees may depend on multiple factors such as species, growth form, size, competition, phenology, and abiotic environmental conditions (López-Bernal et al., 2012; Matheny et al., 2015; Wullschleger et al., 1996). Several studies have reported on the diurnal, nocturnal, seasonal, and annual dynamics, and ranges of stem water content by applying different methods to living trees (Constantz and Murphy, 1990; Hernández-Santana et al., 2008; Irvine and Grace, 1997; López-Bernal et al., 2012).

To measure stem water content, many direct and indirect approaches were developed including the oven drying method (Boone and Wengert, 1998), gamma-ray attenuation (EDWARDS and JARVIS, 1983), nuclear magnetic resonance (Byrne et al., 1986; van As et al., 2009), electrical conductivity, and time-domain reflectometry (TDR) (He et al., 2021a; Lane et al., 2002; Nadler et al., 2006, 2003; Nadler and Tyree, 2008), as well as using heat as a tracer in the tangential direction of the stem (López-Bernal et al., 2012; Vandegehuchte and Steppe, 2012a; Vergeynst et al., 2014).

However, many of the available techniques to measure stem water content exhibit limitations and specific drawbacks as addressed appropriately by (Dietsch et al., 2015; He et al., 2021a; Malavasi et al., 2016). For instance, the kiln-dry or oven drying method (Boone and Wengert, 1998), delivers precise results which are used to calibrate measurement equipment. However, these sampling methods necessitate the destructive extraction of a physical wood specimen, and furthermore, its application is time-consuming (Dietsch et al., 2015). Indirect approaches such as the TDR probe and the microwave method in turn, although non-invasive and very accurate, are quite expensive for continuous monitoring (Constantz and Murphy, 1990; Hardie, 2020; He et al., 2021a; Irvine and Grace, 1997; Nadler et al., 2006, 2003; Stott et al., n.d.).

Thermal approaches are another category for determining both sap flux density and the stem water content in living trees (Alizadeh et al., 2021; Vandegehuchte and Steppe, 2012a). A non-empirical heat-pulse-based method, Sapflow+ (Vandegehuchte and Steppe, 2012a) was developed to measure temperature changes around a linear heater in both axial and tangential directions after the application of a heat pulse from a sensor within the stem. However, despite this being a method for continuous stem moisture monitoring, it only provides stem moisture in zero flux conditions (i.e., usually during nighttime) (Vergeynst et al., 2014). In general, there is an increasing interest in having continuous parallel measurements of sap flow and stem moisture, since the latter is a fundamental parameter to correctly detect thermal equilibrium point or zero-flux conditions (Looker et al., 2016; Vergeynst et al., 2014).

Capacitive sensing by rapidly charging and discharging a positive and ground electrode (capacitor) has gained increasing importance in the last decades in the industrial and automotive sectors. Its application to detect moisture content in materials (i.e., wood) and soils has been proven to be effective (Chetpattananondh et al., 2017; Fares and Polyakov, 2006; Fuchs et al., 2009; He et al., 2021a; Korkua and Sakphrom, 2020; Matheny et al., 2017), however, its application to tree physiology is still at the beginning (Araújo et al., 2021; Cheng et al., 2021; Hao et al., 2013; He et al., 2021a; Irvine and Grace, 1997; Liang et al., 2020; Saito et al., 2016; Zhou et al., 2018, 2015) and there are limited articles available on the simultaneous stem water detection with sap flow monitoring at the same time scale (López-Bernal et al., 2012; Ren et al., 2020; Vandegehuchte and Steppe, 2012a; Windt and Blümler, 2015).

To address these issues, we have developed a new capacitive sensor to continuously monitor stem water content in parallel with sap flux measurements in order to provide long-term measurements across daily and seasonal time scales. In addition, the sensor is connected to an IoT platform (Matasov et al., 2020; Valentini et al., 2019; Zorzi et al., 2021) to transmit data in nearly real-time to the cloud and from there to the desktop. The main aim of the paper is to present a novel capacitance probe for continuous stem water monitoring and to integrate such capability into a sap flow monitoring device already developed by our group.

The study is based on a combination of two separate but related experiments. Firstly, we analyze experimental results on the temperature sensitivity of the sensor and the related species-specific stem moisture calibration responses. Secondly, the sensors were integrated with the TreeTalker platform and installed on trees in the field to monitor both sap flow and stem water content dynamics under field conditions.

Material and methods

The TreeTalker platform

The present study is based on the integration of a new capacitance probe for stem water detection into the existing TreeTalker platform (TT+) for tree physiology research. The TreeTalker is an IoT platform which is able to measure tree physiology parameters such as sap flow, canopy transmitted light spectra (12 bands), stem growth, tree stability (via an accelerometer sensor), and basic climate parameters (air temperature and humidity) (Matasov et al., 2020; Valentini et al., 2019; Zorzi et al., 2021).

The TT+ sap flow measurement technique is based on the temperature difference between a pair of probes, the reference (Ref) probe and the Heater probe, which are inserted radially in the tree trunk with a vertical separation of 10 cm, facing north and covered by a reflective shield to avoid direct solar heating which may impact registered temperatures (GRANIER, 1985). One of the probes is heated while the other is used to measure the stem temperature, and stem water content using a thermistor and capacitance sensor with frequency band of 50 KHz, respectively (Fig.1). TT+ sap flow measurement is designed based on the transient thermal dissipation (TTD) technique with a cyclic heating system (by default: 10 minutes of heating/50 minutes of cooling) to measure

sap flow (Do et al., 2018, 2011; Isarangkool Na Ayutthaya et al., 2010; Masmoudi et al., 2012; Nhean et al., 2019a). The transient signal (dT) is the relative change in temperature over the heating period, calculated as the temperature difference between the probes reached at the end of the heating phase (ΔT_{on}) and that just before the heating phase (ΔT_{off}) (Do et al., 2011):

$$1. \quad \boldsymbol{dT\ (°C) = \Delta T_{on} - \Delta T_{off}}$$

The transient signal is normalized by its value at zero flow to estimate a transient index K:

$$2. \quad \boldsymbol{K = \frac{dT_0}{dT_u} - 1}$$

where $dT_0$is the maximum transient signal obtained under zero flow conditions and dT_u is the measured signal at a given sap flux density.

To estimate the sap flux density (SFD ($l\,dm^{-2}\,h^{-1}$)), a non-species-specific calibration equation is conducted by utilizing transient index (K) (Do et al., 2018).

$$3. \quad \boldsymbol{SFD\ (l\,dm^{-2}\,h^{-1}) = \left(11.3 * \frac{K}{1-K}\right)^{0.707}}$$

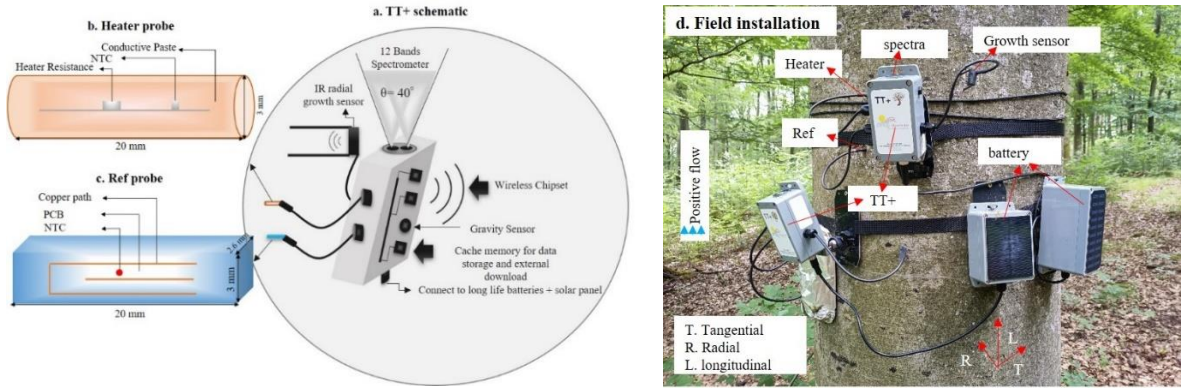

Figure 1. a. TT+ layout, b. heater probe including a thermistor (NTC) and a heater resistance which are placed in a conductive paste, c. Ref probe including a thermistor (NTC), and a copper path as capacitance oscillator, d. Installation of two TreeTalkers (TT+) on a beech tree.

Sensor design for stem water content monitoring

The principal idea was to modify the Ref temperature probe of a classic sap flow sensing device, as in the TreeTalker system, to include a new capacitance sensor for sensing wood water content.

A capacitance sensor can capture the change in the electric capacitance of stems, exposed to an electromagnetic field, by detecting the change in the dielectric properties. This method delivers an acceptable accuracy for wood moisture contents from 2 % up to fiber saturation point (Dietsch et al., 2015) whereas it may lead to be incorrect records for values above the saturation point. At a

low frequency of the generated electromagnetic field, the value may lead to be incorrect, owing to short circuit currents in the wood (Korkua and Sakphrom, 2020). Material density, material temperature, and voltage frequency are the main influences on measurements (Whalley et al., 1992). The development of capacitance sensors may offer flexibility and efficiency regarding indirect stem water content measurement.

In this study, the Ref probe has been realized with a copper PCB design with two traces forming the electrodes (one grounded and one signal) which are separated by 1.5 mm. The sensor has a rectangular cross-section and therefore implanting it inside the stem wood requires a properly engraved 2 mm deep cut (fig 2).

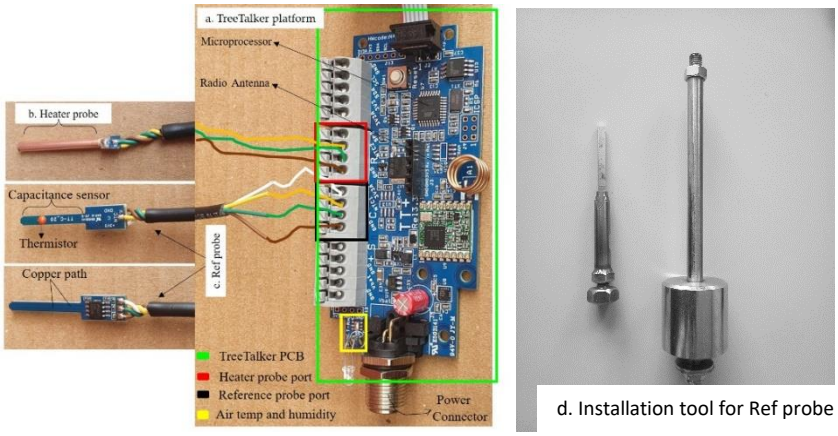

Figure 2. a. TreeTalker platform based on ATMEGA 328P processor-8-bit AVR RISC 8 MHz, b. Heater probe 0.2 watt, c,d. Ref probes including capacitance sensor and a thermistor, front and backside, respectively, d. installation tool for Ref probe.

Usually, the capacitance probe is inserted in an RC circuit which is a low pass filter whose cutoff frequency ECfc (Hz) is defined as:

4. $ECf_c = \frac{1}{2}\pi\ R\ C$, R = resistance (Ω), C = capacitance (F)

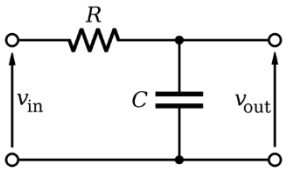

Figure 3. RC filter Circuit.

At the cutoff frequency the input signal (V_{in}) is attenuated by 70.7%. In general, the output signal amplitude (V_{out}) is attenuated in the function of frequency (ECf) as follow:

5. $V_{out} = V_{in}\frac{1}{ECf\ R\ C+1}$

This setting is applied in most of the available commercial sensor for soil moisture sensing (Dean et al., 1987; Hardie, 2020; Whalley et al., 1992; Zhu et al., 2019) where a fixed frequency is applied (usually > 1MHz). We have however used a different approach where the capacitance of the moist wood is integrated with an astable oscillator and the output frequency is variable in relation to the change in capacitance (see fig.4 where C is the wood moisture wood capacitance).

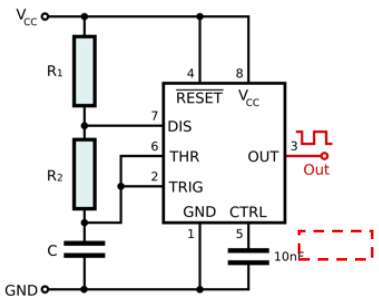

Figure 4. TreeTalker oscillator circuit using 555 Timer.

In this case, the variable frequency output (ECf) is given by:

$$6. \quad ECf = \frac{1.44}{(R_1+2R_2)C}$$

In the first case, the main parameter is voltage sensing, which is acquired as an analog signal. In the second approach, the main output is an oscillating signal (square wave) whose frequency is measured by the time counter digital pin of the TreeTalker microprocessor. For the sake of simplicity throughout the paper, we report the frequency data as the parameter related to capacitance changes. For this reason, also the calibration is performed between stem moisture data and frequency. The advantage of the proposed new scheme is that the sensitivity of changes in frequency in relation to capacitance is higher in the frequency domain than in the voltage one.

Lab experiments

Temperature dependence of Ref probe

Dielectric moisture sensors are known to respond to temperature variations (Fares et al., 2016; Kizito et al., 2008), therefore a temperature sensitivity analysis was conducted under controlled conditions using a climatic chamber with a selected temperature range from 5 to 35 °C with temperature steps of 5 °C/30 minutes to detect the temperature influence on the probes' frequency output when the signal is stabilized. For the temperature sensitivity tests, the capacitance probe was placed in different substrates: distilled water, water-saturated pine sawdust, and fresh-cut wood samples of *Fagus. sylvatica*, *Populus nigra* L., and *Pinus sylvestris* L. For each substrate, three temperature repetitions were conducted respectively, where wood moisture content was assumed constant during each repetition since the samples were sealed with parafilm.

Species-specific calibration

Fresh-cut wood samples from different species were collected from the Marburg Open Forest of the Philipps-Universität Marburg (Friess et al., 2019) to conduct the species-specific calibration for recorded frequency data (ECf (Hz)) by Ref probe in comparison with the oven-drying method (Boone and Wengert, 1998) as a reference technique of measuring wood water content. The species-specific calibration was conducted on *F. sylvatica*, *Quercus petraea* L, and pine sawdust with different densities of 0.52, 0.53, and 0.18 g/cm^3, correspondingly. Wood samples of *F. sylvatica* and *Q. petraea* were harvested from the same trees at DBH in different directions, North (beech-1), South (beech-2), and for the *Q. petraea*, North (oak-1), and East (oak-2), respectively (fig 5).

Previous studies have reported wound impacts on measurements from sensors measuring sap flow and stem water content (Wiedemann et al., 2016). Damaged vascular tissue response to probe insertion presents a problem that can last a few hours to a few days, dependent on wound occlusion, and as such, impacts sensor signal normalization in both lab and field experiments. To avoid air gap and wound impact on the data, Ref probes were installed in living trees on 21.10.2020 and harvested on 02.11.2020 to establish the passage of wound occlusion (fig 5). The harvested samples were analyzed in the lab where, using a TT+ connected to the Ref probe, continuous temperature, and frequency (ECf (Hz)) data were recorded. In parallel, sample weight loss was recorded by a digital balance for each sample as a standard technique to determine volumetric water content. Sample data was continuously collected via the balances and TT+ until the specimen mass stabilized at the approximate constant value. Each sample with and without a Ref probe is weighed at the end of the drying procedure in the laboratory. The differences considered, i.e., those pertaining to the with/without Ref, equates to the net mass of the sample during the experiment. Subsequently, dry mass was determined after wood samples were oven-dried for 48 h at 75°C. Such a temperature is considered to be sufficient to allow complete water evaporation and at the same time avoid significant destruction of the wood structure (Boone and Wengert, 1998). Ultimately, the gravimetric and volumetric water content were calculated using the following equations:

7. $$Gravimetric\ Water\ Content\ (g\ g^{-1}) = \frac{fresh\ weight - oven_{dry} weight}{oven_{dry} weight}$$
8. $$Volumetric\ Water\ Content: VWC\ (\%) = \theta_g * \frac{\rho_{wood\ sample}}{\rho_{sap}} * 100$$

Where the term ρ_{wood} is the basic density of the wood sample and ρ_{sap} is the sap density assuming its equality to water density. In fact, the density of water is close to 1 and is often ignored (Wolf, 2008). ρ_{wood} is the ratio of wood oven-dry mass to sample fresh volume. Fresh volume was calculated by carefully measuring the dimensions of the samples with digital calipers with an accuracy of 0.01 mm.

Figure 5. a. Installation of Ref probe at DBH, 10 days before harvesting wood samples, b. harvesting beech and oak trees to collect fresh-cut wood samples including Ref probes, c. Using harvested samples to conduct the species-specific calibration for Ref probe-TT+.

Field experiments

To assess the TreeTalker (TT+) capability under field conditions, a managed, beech-dominated forest in the lower mountain ranges of Western Germany near Caldern (8°40´E; 50°50´N) was chosen. The forest is owned by Philipps-Universität Marburg and is an experimental site for the biodiversity monitoring project Nature 4.0 (Friess et al., 2019) and is characterized by a forest covering an area of 1,5 km², dominated by *F. sylvatica* and *Q. petraea* (Mattuschka) Liebl of different age classes. Elevation level ranges from 260 to 410 m a.s.l. The predominant soil type is Cambisol. Historical data on air temperature, humidity, and precipitation is measured via the MOF climate station. Using air temperature and humidity data, vapour-pressure deficit (VPD) is analyzed for 2020 and plotted vs precipitation in fig 6. The average annual air temperature and precipitation for 2020 in the selected site were reported at 9.7°C and 374 mm, respectively. As reported in the previous study about the European heatwave impact on western Germany (Neuwirth et al., 2021), correspondingly, in this site, from July, 15 to August, 15, we show an increasing trend in VPD up to a maximum of 3.8 KPa due to high temperatures and few rainfall events (fig 6). The maximum recorded rain event was 21.2 mm which occurred on 17 June. Here, in spring 2020, TT+, n = 59, are mounted at 1.30 m or diameter at breast height (DBH) to monitor the dynamics of sap flux and stem water content (Fig. 7). In particular, TT+ demonstrates the applicability and functionality of the Ref probe in distinguishing plant hydraulic functionality under different meteorological circumstances.

Table 1., displays the ancillary variables associated with the selected trees to discuss the diurnal fluctuation of water-related indicators for the MOF area.

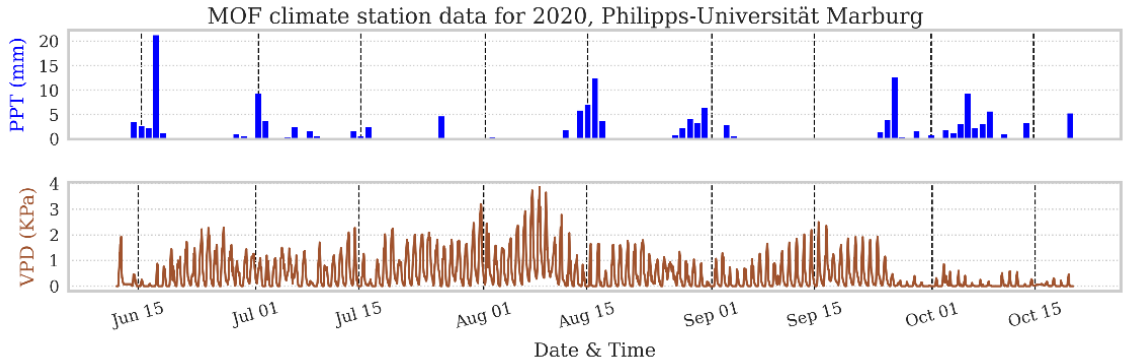

Figure 6. Precipitation (PPT (mm)) & vapour pressure deficit (VPD (kPa)) for 2020 based on data from the climate station in the Marburg Open Forest (MOF) study area.

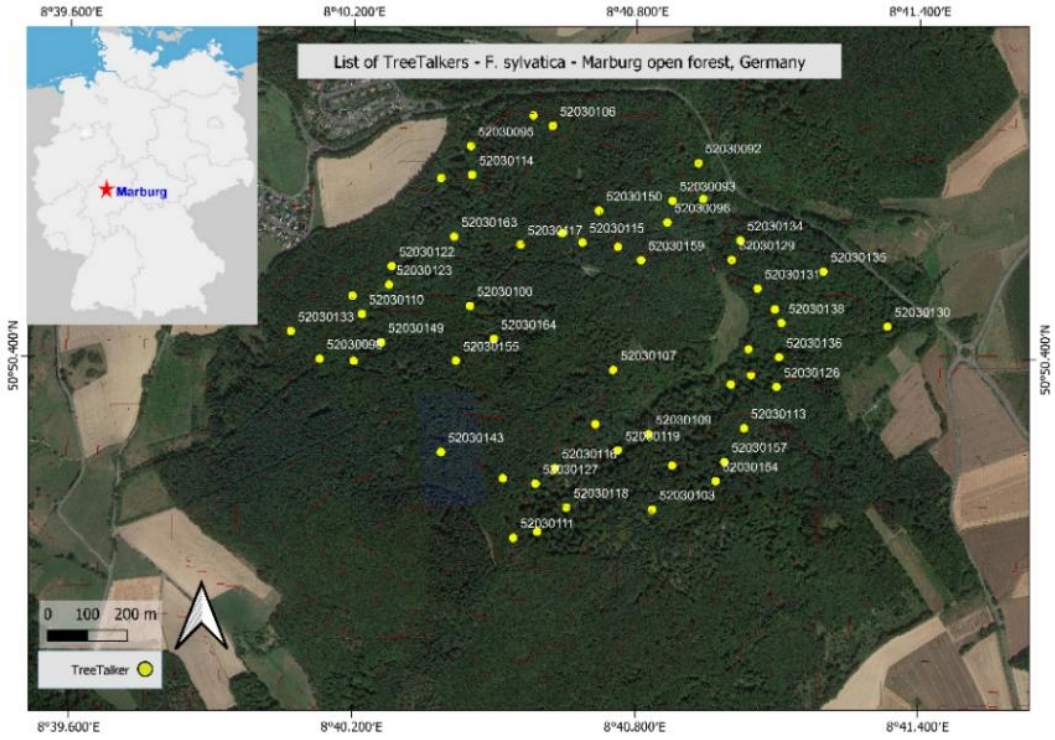

Figure 7. Map of the study area, Marburg Open Forest (MOF), showing the location of the mounted TreeTalkers on beech trees.

Table 1. Kraft class, vitality, height, diameter at breast height (DBH), sapwood area, and canopy volume for the selected trees for individual responses.

TT+ No.	Kraft-class	Vitality	Height (m)	DBH (cm)	Sapwood area (cm2)	Canopy volume (m3)
TT25	2	2	29.9	53	685	879
TT54	2	2	32.7	56	806	1017
TT62	2	2	29.5	53	615	1801

Results and Discussion

Lab experiments

Temperature sensitivity analysis of Ref probe

The temperature sensitivity analysis results show a negative correlation between capacitance sensor data (ECf (Hz)) and wood sample temperature (T (°C)) (fig 8). The relationship between ECf (Hz) and T (°C) is assessed by a linear regression model (y = m_1x+ b_1) assuming a constant moisture content during the experiment (fig 8). The coefficients 'm_1', the slope of the linear model, and 'b_1' the intercept, are presented in table 2 for each substrate.

Table 2. Temperature sensitivity analysis for TreeTalker's Ref probe exposed to different substrates. Coefficients '$\boldsymbol{m_1}$' and ' $\boldsymbol{b_1}$' are presented for a linear equation in the standard form of $\boldsymbol{ECf_T = m_1 * T + b_1}$.

Var	**Water**	**Sawdust**	***F. sylvatica***	***P. nigra***	***P. sylvestris***
Slope (m_1)	-81	-87	-43	-84	-78
Intercept (b_1)	13867	18519	21834	33283	27555
R^2	0.98	0.88	0.94	0.98	0.81
p-value	< 0.01	< 0.01	< 0.01	< 0.01	< 0.01
stderr	0.53	0.92	0.45	0.41	1.28

Our empirical findings show that not only temperature affects the performance of the Ref probe, but also matrix types and their physical properties. Although results are clearly displaying a negative linear relationship between material temperature and ECf, the slope of the linear regression model, m_1, across the various substrates, is neither constant nor similar. This demonstrates that textural features of our samples have a remarkable impact on frequency data recorded by the Ref probe (fig 8).

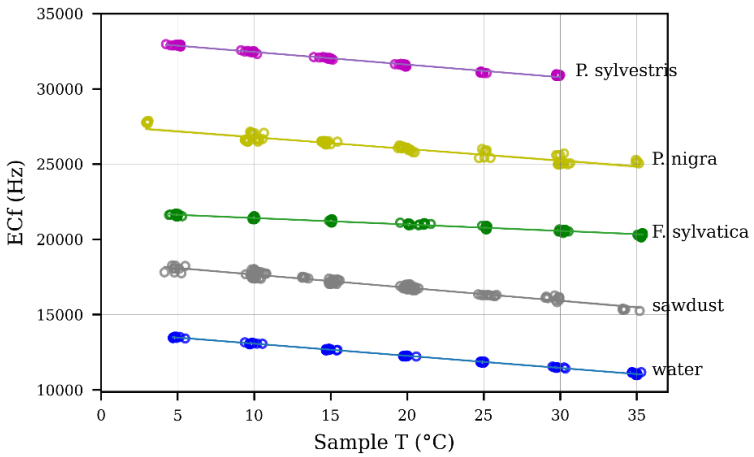

Figure 8. Temperature sensitivity analysis for the capacitance sensor used in the Ref probe_TT+ across different substrates.

Species-specific calibration

The calibration equations for two wood types (beech and oak) and the pine sawdust sample (fig 9) were determined using multiple linear regression models considering the impacts of frequency records (ECf (Hz)) and stem temperature (T °C). The multiple linear regression model takes the volumetric water content of samples using the reference gravimetric data as one parametric component with stem temperature T and Ecf as the Ref probe's output. The below equation can be used to determine stem volumetric water content (stem VWC) in percentage using the Ref probe's raw records in living trees.

$$9. \quad stem\ VWC\ \%_{(T,ECf)}^{Matrix} = \beta_0 + \beta_1 \times T + \beta_2 \times ECf + \epsilon$$

Where, β_0 is the intercept, β_1 and β_2 are the slope coefficients of T and ECf records, respectively. ϵ is the model's error term. (see table 3). The multivariate analysis for beech and Oak are displayed in fig 9 a. and b. for combined data of beech-1 and 2 as well as oak-1 and *2*. The objective was to provide a general equation for each species

Therefore, to derive the combined data, we extracted the temperature and ECf (Hz) output where stem VWC was equal for both trials.

Table 3. Calibration equations to estimate stem volumetric water content for the different samples. Coefficients 'β_0', 'β_1', and 'β_2' are presented for multiple linear equations in the standard form:
$stem\ VWC\ (\%) = \beta_0 + \beta_1 \times T + \beta_2 \times ECf$

Samples	β_1	β_2	β_0	R^2	P>|t|	RMSE	No. Obs
Beech	-0.23	-0.0021	93	0.996	<0.001	0.86	1430

Oak	-0.56	-0.0042	150	0.996	<0.001	0.61	889
Pine sawdust	-0.61	-0.0013	96	0.969	<0.001	2.4	8263

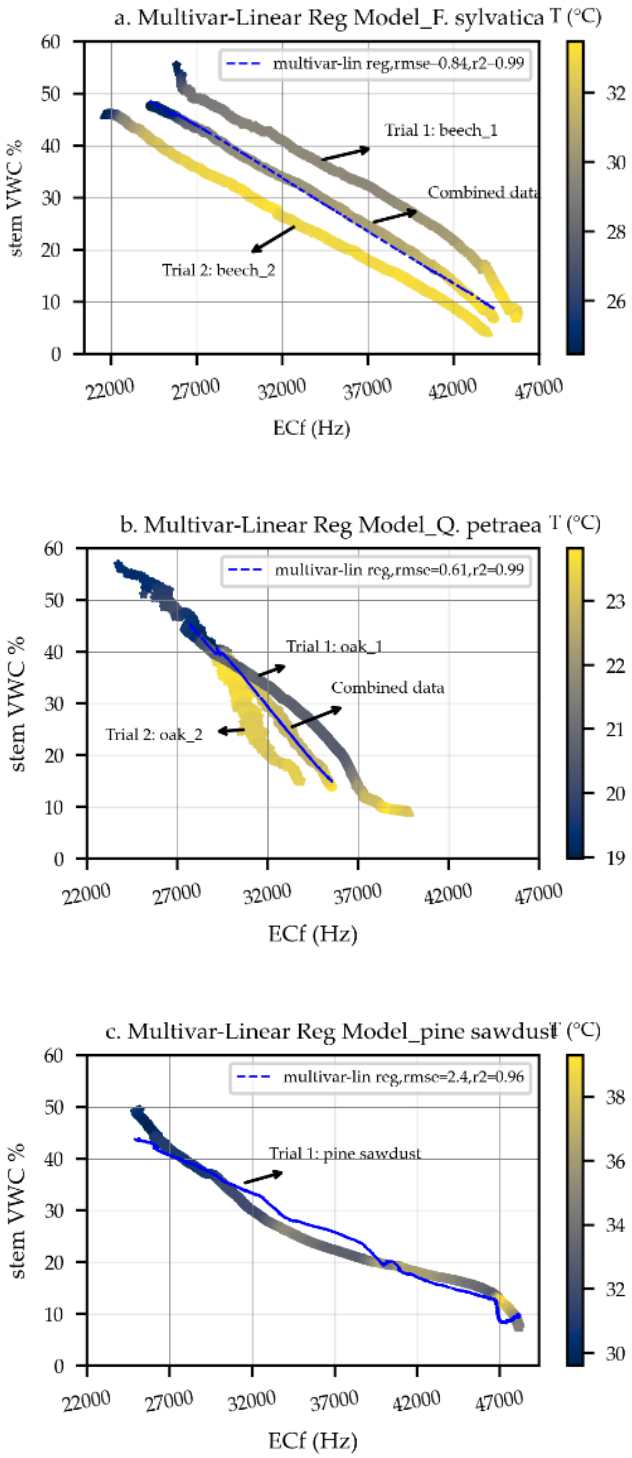

Figure 9. Relationship between Ref probe's output: ECf, and sample temperature versus the digital balance output: Stem Volumetric Water Content across the selected samples, a). *F. sylvatica*, b). *Q. petraea*, and c). pine sawdust.

In fig 10, the predicted values from the multivariate linear regression model (table 3) are displayed on the y-axis, while the actual values from the dataset are displayed on the x-axis. The statistical analysis for regressions of each substrate demonstrates that the accuracy of predicted stem VWC% data is rather high considering the R-squared and p-values (Schermelleh-Engel et al., 2003). However, considering the respective RMSE for each result, both regression models of beech and oak suggest an acceptable explanation (~ RMSE < 0.8) for describing the trends between predicted and actual stem VWC% data (Schermelleh-Engel et al., 2003). For the pine sawdust, however, the model reflects a poor ability to predict stem VWC% (table 3).

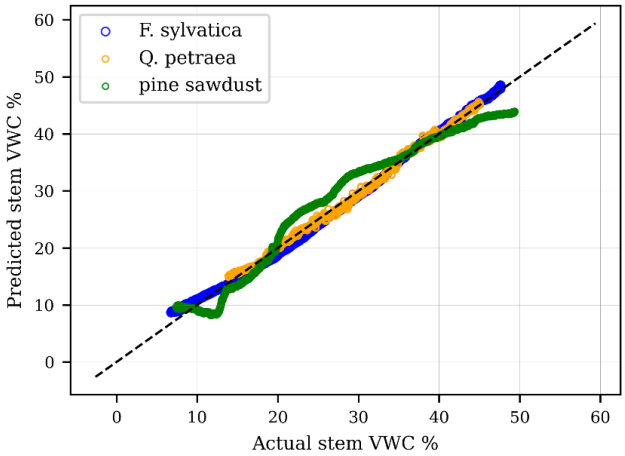

Figure 10. Predicted stem VWC % values (multivariate linear regression model output) versus actual stem VWC% (digital balance records) for the selected samples.

To conduct species-specific calibration equations, instead of a model of best-fit approach, multiple linear regression is applied to compare the variability of slope (β_1, and β_2) across the samples. Intraspecies variability was rather limited. However, interspecies variability is more pronounced, especially for those samples collected from northern sides of the stems. The observed differences in slope (β_2) between species can be explained by the differences between species in terms of area of living tissue, freely available water in plant tissue, water molecular bounding condition, water potential, wood anatomical structure (small vs larger vessels), etc which is the objective of future research (Nola et al., n.d.). This result suggests that for the same range of frequency change, *Q. petraea* dries approximately more than two times in comparison with diffuse-porous *F. sylvatica* under the same experimental condition. The reported pine sawdust data are here considered only as a reference since they do not compare with real fresh wood samples.

Relative saturation index

The measurements and calibrations are highly dependent on the material temperature, moisture level, and variability of species wood anatomy requiring, therefore, species-specific calibration to be used in field operations.

To address above mentioned limitations, continuous monitoring and long-term data sets can and should be used to derive a relative index that can represent stem moisture dynamics of time series data.

We propose a procedure to derive such an index as outlined in the following. First, the frequency data (ECf) recorded by the Ref probe decreases as the material temperature increases. Second, the local minimum of frequency reported value occurs at saturation point and the local maximum occurs while the sensor is exposed to the driest conditions in the living tissue. Taking advantage of these two facts, considering the fiber saturation point for each single living tree in a given period of time, the minimum frequency record and corresponding stem temperature are required to determine the expected frequency signal, $ECf_{adj}(Hz)$, by stem temperature effect at the same moisture level.

$$10.\ ECf_{adj}(Hz) = m_1 * (T_i - T_{sat}) + ECf_{sat}$$

Where m_1 is the temperature sensitivity slope, T_i is thetemperature of stem in °C, T_{sat} is the stem temperature associated to ECf_{sat} in °C, ECf_{sat} (Hz) is the minimum raw record of frequency data in one cycle of the growing season.

The relative index of stem saturation % is given as:

$$11.\ \text{Rel stem saturation \%} = \left(1 - \frac{ECf\ (Hz)_i - ECf_{adj}(Hz)}{ECf_{adj}(Hz)}\right) * 100$$

Where $ECf\ (Hz)_i$ is the current frequency record.

One complete growth season is recommended to accurately capture the above event. Furthermore, to convert the relative stem saturation index to the stem VWC, we suggest using tree coring techniques to scale up the results. From our observations, the corresponding date and time of Min_{ECf} and Max_{ECf} denote optimal periods to collect physical stem core samples. By following the oven-drying method, the derived minimum and maximum for stem VWC are established, essentially allowing the evaluation of tree stem water content for any reported ECf value for each individual tree.

Field results

Individual variability in sap-flow rate and stem VWC in *F. sylvatica*

Measurements from installed TreeTalkers in the MOF study area, species *F. sylvatica*, demonstrate the capability of the system to detect individual differences in the hydraulic status of each tree. Seeing available ancillary data, three individuals, TT25-TT54-TT62, were selected giving a snapshot of tree functionality toward stem temperature (fig 11.a), sap flux density rate (fig 11.b), relative stem saturation (fig 11.c), and stem VWC using equation 9_ *F. sylvatica* (fig 11.d) in Mid-June and Mid-September during the vegetation period of 2020.

The variance in sap flux and stem water content in individual trees may be attributed to different parameters such as DBH size class, sapwood area, canopy volume, etc. For example, TT 25 with the lowest canopy volume, among the selected trees, has the highest flux rate. Focusing on diurnal and nocturnal patterns for sap flux, we see that the general pattern holds true for each tree, however, the magnitude remains different for each individual, possibly suggesting individual trees do not demonstrate homogeneous responses to abiotic factors. Indeed, tree cellular structure, hydraulic tissue matrices, physical size, and canopy volume, i.e., leaf area, may be more important factors determining the magnitude and change in flux vs water storage across these individuals.

Diurnal variations in sap flux rates (fig 11.b) versus stem VWC (fig 11.d) indicate that variation in sap flux rate and stem VWC are not strictly related. For example, TT25 with the highest sap flux rate does not necessarily denote the highest stem VWC. Drivers for this observed phenomenon are linked to two possible scenarios. Firstly, hydraulically, trees with higher facilitation of flux rate store less WC content (see fig 11.b and 11.d for TT25) (Barbour and Whitehead, 2003; Bowman et al., 2005; Roderick and Berry, 2001). Secondly, water scarcity, tree health, size, factors of competition, and suppression may all contribute to decreased available water for both flux and stem WC, requiring more investigation (see fig 11.b and 11.d for TT54).

Seasonal rhythm of stem VWC and relative saturation index

Seasonal variability of stem VWC and relative saturation index for several trees of *F. sylvatica* from the MOF area are shown in fig 12.a/b. Results from equations 9_ *beech* and 11 appear in fig 12.a and 12.b, respectively. In fig 12a. specifically, hourly fluctuations of stem VWC are recorded for all individuals in the MOF study from June until November 2020 with the rolling average of all individuals displayed in black color.

September, marking the end of the growing season in the MOF, exhibited higher stem VWC than in June. Although precipitation in June (50.8 mm) was even higher than in September (36.4 mm), reduced transpiration to the end of the vegetation period can explain the observed increase in stem VWC and saturation index (Gebauer et al., 2012; Nalevanková et al., 2020) (fig 12). For the same reason, the diurnal rhythm is less pronounced in September. Due to a later sunrise or reduced photoperiod, approximately 1:45 h later than June, tree transpiration is already reducing in September, and stem VWC contribution is realized later (between 11:00 and 16:00). Recovery starts immediately after a minimum level is reached and this is coupled with limited photosynthesis confined to a small window of a few hours in the late vegetation period. Temporal shifts are matching later sunrise and earlier sunset (fig 12.a/b).

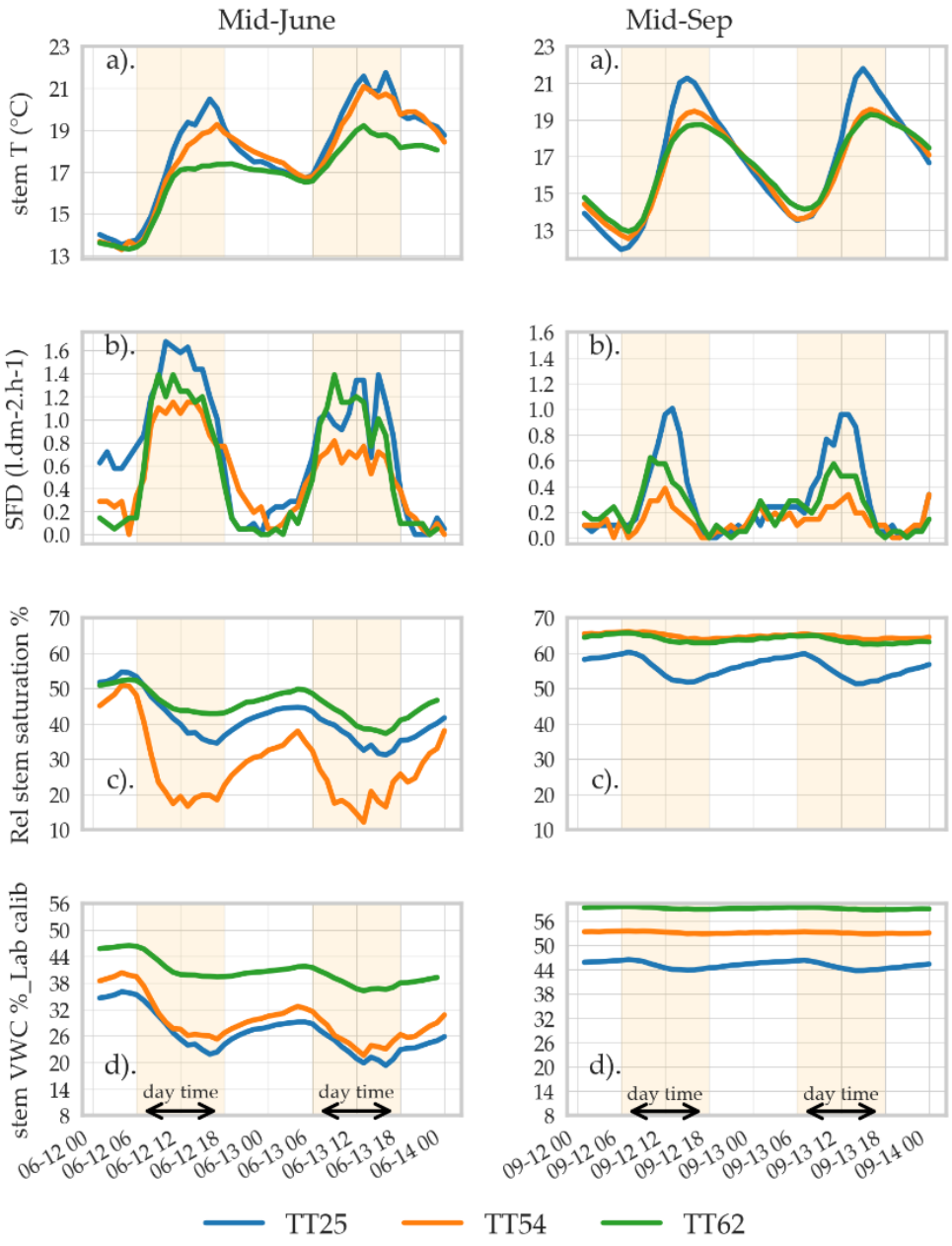

Figure 11. Individuals' behavior for three selected trees (25, 54, and 62) based on available ancillary data toward a). stem temperature, b). sap flux density, c). relative stem saturation index, and, d). stem volumetric water content based on TreeTalker hourly data focused on June vs September 2020.

Observed hourly data captured by the TreeTalkers (fig 12.a/b) for one growing season, accurately reveals the impact of elevated temperature and an acute heatwave from 15 July to 15 August 2020 across Germany. Subsequently, a large impact on the trees' water storage level in beech was evident (fig 12.a/b) and can be explained by (Hafner et al., 2017; Neuwirth et al., 2021).

Based on our observations, we see a general population response to abiotic events such as dry periods and rainfall events (see fig 12.a/b for max VPD and rain events). However, at an individual scale, ecophysiological response to climatic variables varies according to magnitude (see fig 12 a.

colored points). Although general observations are evident, further investigations are required about both population and individual responses to abiotic factors. For instance, the last rainfall event demonstrates a drop in both indices, stem VWC and stem relative saturation index which requires a deeper understanding and analysis.

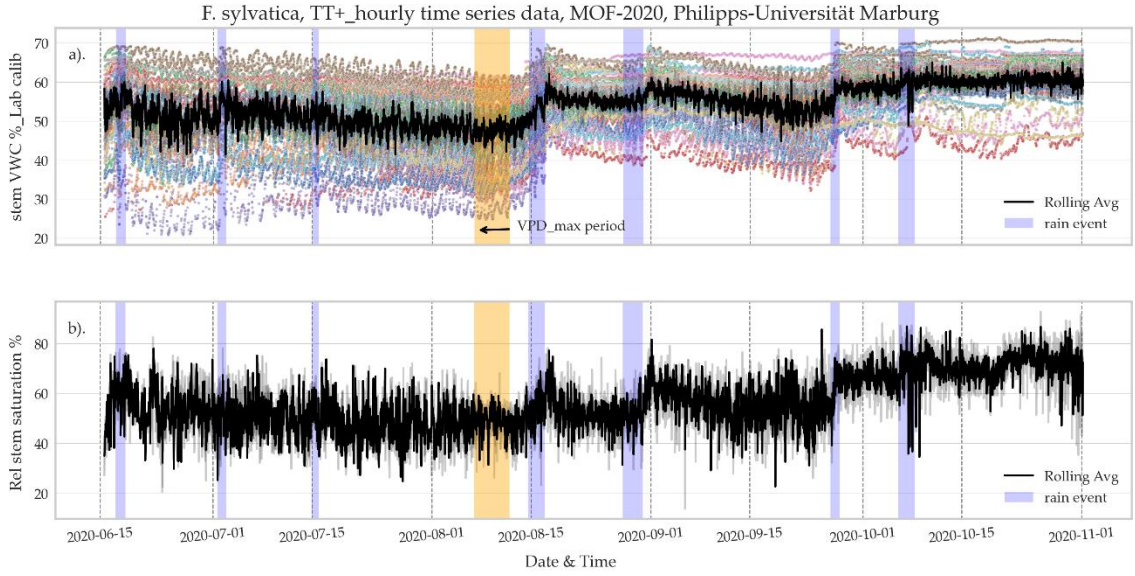

Figure 12. Seasonal variability of a. stem VWC % for all individuals (colored points) and combined rolling average using all data (black, b. relative stem saturation index % based on a combined rolling average across all individual data. All data is derived from hourly data by TT+, species *F. sylvatica* in the MOF study area.

Conclusion

This study confirms that TreeTalker can estimate the time evolution of relative changes in stem water content. According to the experimental results, the following conclusions can be drawn:

I. The TreeTalker, having a capacitive sensor, is an effective IoT-based device for real-time and continuous estimation of relative stem saturation at a single tree level, furthermore, demonstrating a reasonable capacity for capturing a single tree's ecophysiological behavior under differing environmental conditions.

II. The application of continuous and simultaneous monitoring of several trees is showing a remarkable coherent response to climate events (rain and drought). Where precipitation has a positive impact with increased stem VWC and dry periods where decreases are evident.

III. Stem water content varies regularly according to diurnal and nocturnal fluctuation following the overall trend of rising during the night and falling during the day. This observed trend is coherent with stem recharge and increased transpiration rates driven by photosynthesis.

IV. The accuracy of the sensor, however, seems not to be adequate yet for diurnal trend estimation under small water content variations. We are continuously working on improving the

sensor with a high frequency of oscillation (100-500 MHz) to increase the sensitivity to the level requested by daily trends.

V. Individual tree ecophysiological and geometrical characteristics demonstrate a plausible connection to the pattern and amount of stem water content.

VI. For further optimization of Species-specific calibrations of the Ref_probe, we suggest a seasonal sampling campaign to collect wood core samples.

Article 2: Sap Flow-Part I: Empirical approach

Principles And Applicability of Treetalker (TT+): A Two-Needle Transient Thermal Dissipation Enabling Real Time Sap Flux Density Measurement

Shahla Asgharinia [1,2,*], Francesco Renzi [1,] Ilaria Zorzi [3], Martin Leberecht [4], Timo Gebhardt [5], Claudia Cocozza [3], Francesco Niccoli [6], Lars Opgenoorth [4], Mazda Kompanizare [7], Kathy Steppe [8], and Riccardo Valentini [1]

1. Department for Innovation in Biological, Agro-food and Forest Systems (DIBAF), Tuscia University, Via San Camillo de Lellis snc 01100 Viterbo (VT), Italy

2. Research and Innovation Centre, Fondazione Edmund Mach, Via E. Mach 1, 38098 San Michele all'Adige, TN, Italy

3. Dipartimento di Scienze e Tecnologie Agrarie, Alimentari, Ambientali e Forestali, Università degli Studi di Firenze, 50145 Firenze, Italy

4. Department of Biology, Philipps-Universität Marburg, Karl-von-Frisch-Straße 1, 35043 Marburg, Germany

5. Technical University of Munich, School of Life Sciences, Land Surface-Atmosphere Interactions – AG Ecophysiology of Plants, Hans-Carl-von-Carlowitz Platz 2, 85354, Freising, Germany

6. Università degli Studi della Campania "Luigi Vanvitelli Department of Environmental, Biological and Pharmaceutical Sciences and Technologies

7. Global Institute in Water Security, University of Saskatchewan, 11 Innovation Blvd, Saskatoon, SK S7N 3H5, Canada

8. Laboratory of Plant Ecology, Department of Plants and Crops, Faculty of Bioscience Engineering, Ghent University, Coupure links 653, Gent 9000, Belgium

* Correspondence: asgharinia@unitus.it

In preparation

Principles And Applicability of Treetalker (TT+): A Two-Needle Transient Thermal Dissipation Enabling Real Time Sap Flux Density Measurement

Abstract

Because of the low-cost, non-destructive, multifunctional nature of the IoT-based TreeTalker (TT+), both the transient thermal dissipation (TTD) system and constant thermal dissipation method (CTD) methods have become more accessible and interchangeable. Using this advance in technology, its application, we aim to assess the applicability and thus merit of the TreeTalker toward sap flux density measurement and computation. Capability analysis of TT+ is verified both under a lab scenario using an artificial hydraulic column of sawdust and a stem segment of F. sylvatica L. in the field via mounted TT+ devices and with comparison of a commercial sap flow sensors on different species. and in different cyclic TTD systems on Populus nigra L and P. pinea. Installing a TT+ on the artificial flow system, temperature evolution data from heating and reference probes are recorded both in heating and cooling phases to compute values of different flow indices ($K_{Classic}$: (GRANIER, 1985), K1 & K2: (Do and Rocheteau, 2002a; Do et al., 2018), K3: (Mahjoub et al., 2009) under different flux densities. Applied continuous heating mode and a transient regime with four different combinations of heating and cooling times (in minutes) 10/10, 5/10, 15/45, and 10/50 are tested by TT+ and calibration of flux density vs flow indices conducted by applying optimal fitting curve on the source data up to 8 L $dm^{-2}h^{-1}$. Results Employing TT+ and revisiting different thermal approaches, we confirmed that the best possible empirical approach is the transient regime using cooling phase data to value flow index "K3", applying the temperature of probes after the heating current is switched off. The relationship between sap flux and K3 for different cyclic TTD systems was found to be linear with better coefficients of determination in the cooling phase ($R^2 = 0.79 - 0.94$) with respect to the heating phase by valuing K1 and K2 ($R^2 = 0.71 - 0.90$). Obtained calibration equations for sap flux density vs K1 were applied to data from different species across different locations and compared with thermal dissipation and heat pulse velocity methods to validate TT+ ability under field circumstances.

***Keyword**: the transient thermal dissipation, flow index, artificial hydraulic column, heating duration, empirical approach*

Introduction

Sap flow as a proxy for transpiration and as an indicator of plant water status has become increasingly important in plant science (Vandegehuchte and Steppe, 2013). Numerous studies have reported a range of different sap flow measurement methods predominantly based on the application of heat to the sapwood area with the subsequent literature in this field being both broad and robust (Do et al., 2018, 2011; Flo et al., 2019; GRANIER, 1985; Huber and Schmidt, 1937; Isarangkool Na Ayutthaya et al., 2010; Marshall, 1958; Masmoudi et al., 2012; Nadezhdina et al., 2012; Nhean et al., 2019a; Ren et al., 2020; Vandegehuchte and Steppe, 2012a). Transporting heat as a tracer by the ascent of sap within xylem tissue to derive sap flow based on the principles of heat conduction–convection was, in fact, reported 90 years ago by (Huber, 1932). The heat conduction–convection equation in sapwood has been developed by (Marshall, 1958) and is used worldwide as an analytical solution of the heat partial differential equation in a specified isotropic medium. For an instantaneous heat pulse, Marshall (1958) proposed the following analytical solution:

$$1. \qquad \Delta T = \frac{Q}{4\pi kt} \exp\left[-\frac{(x-Vt)^2 + y^2}{4Dt}\right]$$

with ΔT (K) the temperature differences between two sap flow needles at position (x, y), t is the time in seconds, Q (K m2) is defined as the temperature to which the amount of heat liberated per unit length of the line would raise a unit volume of the substance, D the thermal diffusivity (m2 s-1), and V the heat pulse velocity (m/s) (Vandegehuchte and Steppe, 2012b). This heat pulse velocity (HPV) is directly proportional to sap flux density. HPV method as a theoretical approach with the capability of capturing reverse, zero, and positive flow rates, is limited by measuring the flow rate greater than 0.54 m/hr and it is dependent on the thermal characteristics of the wood (D, thermal diffusivity).

Among the available thermal methods to measure sap flux density, the thermal dissipation method (TDP) is the most used in application and research to estimate plant transpiration (Vergeynst et al., 2014). The continuous heating technique was developed by Granier (Granier, 1987; GRANIER, 1985) which comprises two needle-sized sensors, a heater, and reference probes, inserted radially into the sapwood area. The flow rate is estimated from a dimensionless flow index, $K_{classic}$, which is related to the differential measurement of temperature between heated and reference probes in the heating phase.

$$2. \qquad \mathbf{K_{classic}} = \frac{\mathbf{\Delta T_{max} - \Delta T_i}}{\mathbf{\Delta T_i}}$$

Where ΔT_I is the actual temperature gradient between two probes and ΔT_{max} is the maximum temperature gradient between the probes measured during a period of zero flow condition.

TDP method depends on the zero-flux condition and supports low, average, and high sap flux density estimations (P. Lu, 2002; Ping Lu et al., 2004). Granier performed an empirical and species-independent calibration for the TDP system which is valid for various tree species (Cabibel et al., 1991; GRANIER, 1985; Köstner et al., 2017):

3. $$\mathbf{SFD} = \mathbf{119} * \mathbf{K_{classic}}^{\mathbf{1.231}} * \frac{\mathbf{3600}}{\mathbf{100000}}, \mathbf{in\ linear\ form\ SFD} = \mathbf{4.28} * \mathbf{K_{classic}}$$

Where SFD is the sap flux density (l dm-2 h-1).

However, the TDP method is not capable of measuring reverse flow, often underestimates the sap flux density by increasing wound impact due to continuous heating resulting, has a dependency on zero-flux, and is limited by high power consumption (Cermák et al., 1973; Čermák and Kučera, 1981; Granier, 1987; GRANIER, 1985; Lu, 2002; Lu et al., 2004; Sakuratani, 1984; Siqueira et al., 2020; Vandegehuchte and Steppe, 2013). Moreover, natural temperature gradients (NTG) in stems of trees growing in open stands give rise to errors when measuring sap flow by the continuous thermal dissipation probe method (Do and Rocheteau, 2002a; Lubczynski et al., 2012). The influence of NTG on the TDP method has been extensively studied and has been shown to lead to errors of over 100% if not corrected (F. Do & Rocheteau, 2002b, 2002a; Ping Lu et al., 2004; Lubczynski et al., 2012; Vandegehuchte & Steppe, 2013). Therefore, a novel cyclic heating system with a new flow index was developed by Do and Rocheteau to reduce significantly the influence of NTG (F. Do & Rocheteau, 2002b).

Cyclic heating system works in transient thermal dissipation (TTD) conditions by introducing a relatively short cycle of heating and cooling (a minimum of 10 minutes heating and 10 minutes cooling) (F. C. Do et al., 2011). The transient signal (dT) is the relative change in temperature over the heating period, between the differential cooled temperature (ΔT_c, after cooling) and the maximum differential temperature reached after the period of heating (ΔT_h):

4. $$\mathbf{dT} = \mathbf{\Delta T_h} - \mathbf{\Delta T_c}; \quad \mathbf{given} \quad \mathbf{K_1} = \frac{\mathbf{dT_{max}} - \mathbf{dT_i}}{\mathbf{dT_i}}$$

Where dT_{max} is the maximum transient signal obtained under zero-flux conditions and dT_I is the measured signal at a given sap flux density.

The transient signal is normalized by its value at zero-flux and a non-species-specific calibration method is used to derive the sap flux density equation in (l dm-2 h-1) (Do and Rocheteau, 2002a, 2002b; Isarangkool Na Ayutthaya et al., 2010).

5. $$\mathbf{SFD} = \left(\mathbf{11.3} * \frac{\mathbf{K_1}}{\mathbf{1 - K_1}}\right)^{\mathbf{0.707}}, \mathbf{\ in\ linear\ form: SFD} = \mathbf{12.95} * \mathbf{K_1}$$

To improve the TTD system, (Nhean et al., 2019b) proposed using the incremental rise of temperature from 30 to 300 s time window after commencement of heating to derive K_2 while normalizing as $K_2 = \frac{dT_{max} - dT_i}{dT_{max}}$. The assessd linear calibration for K_2 yielded:

6. $$\boldsymbol{SFD} = \mathbf{6.42} * \boldsymbol{K_2}$$

The possibility of measuring sap flow density (SFD) by a single heated probe using the transient regime (TTD) just after the heating current is switched off was proposed by (Mahjoub et al., 2009; Masmoudi et al., 2012). A new flow index (K_3) is presented, which involves the transient

signal (dT) at the beginning and intermediate times of the cooling kinetics. The recorded temperature at the end of the cooling phase where the equilibrium point is considered as the stem temperature.

$$7. \qquad K_3 = \frac{1}{t_i} ln \frac{dT_{t_0}}{dT_{t_i}}$$

Where, t_0 when the heating current is switched off, t_I is $intermediate\ time\ after\ kinetics \approx 20\ seconds$, dT_{t_0} is temperature decrease at the initial time of kinetics and dT_{t_i} is the temperature decrease at $intermediate\ time$. Using an olive stem segment, a non-species-specific calibration method is used to derive the sap flux density equation in (l dm-2 h-1) having K_3 from cooling phase data.

$$8. \qquad SFD = a K_3 + b \qquad \text{WHEN } t_i = 20 \text{ sec A= 180 AND B= -8.7}$$

The above equation applies the classic 10/10 cyclic regime as introduced by (Do and Rocheteau, 2002a) and it is only valid for the positive flow when $K_3 > -\frac{b}{a}$.

Transient thermal dissipation (TTD) systems provide a simple way to measure xylem sap flux with a dual or a single Granier-type probe (F. C. Do et al., 2011, 2018; Mahjoub et al., 2009; Masmoudi et al., 2012; Ren et al., 2020b), but the possibility of reducing the heating duration (minimum 5 minutes) while keeping enough sensitivity and accuracy in the response to flux density as well as lower energy consumption as suggested by (Nhean et al., 2019; Ren et al., 2020b). However, TTD system has weak performance under low flux rates (< 1 l dm-2 h-1) since with the minimum heat input, the system 95% is sufficient to reach dT_{max} (maximum temperature gradient under zero-flux) due to the nocturnal hydraulic activity of trees regarding the stem water content (Do and Rocheteau, 2002). Stem water content may decline during the day to contribute to transpiration rate and as such dT_{max} increases when WC decreases (0.1 to 2°C) (Vergeynst et al., 2014). Consequently, the sap flow measurement methods based on dT_{max} under zero-flux (TDP and TTD) might introduce errors from 16 to 68.2% in daily sap flow measurement (Vergeynst et al., 2014).

Although the above-mentioned sap flow measurement methods, the heat pulse method (HPV) (Marshall, 1958), continuous heating (TDP) (GRANIER, 1985), and cyclic regime (TTD) (Do and Rocheteau, 2002a) are well-established, exploiting an innovative in-situ IoT monitoring network for a fast assessment of forest transpiration rate with real-time data, low power consumption at very low cost is still under discussion (Ren et al., 2020a; Siqueira et al., 2020; Smith & Allen, 2007; Vandegehuchte & Steppe, 2013). Thus, a new tool (called TreeTalker) developed with UNITUS, offers a unique feature of tailored firmware to measure plant water transport (Asgharinia et al., 2022; Tomelleri et al., 2022; Matasov et al., 2020; Valentini et al., 2019; Zorzi et al., 2021). TreeTalker (TT+) is the automated setting of both described methods TDP and TTD, respectively. In TTD method, TreeTalker can accept the manipulation of any preferred heating/cooling durations to suit climatic variability and species-independent preference. Furthermore, the TT+ platform permits the recording of high-frequency data of heat dissipation in the sapwood area. This demonstrates a novel approach to the application of both methods cost-effectively and conveniently furthering scientific precision and accurate based measurements of sap flux density. By default,

TreeTalker is designed on a non-steady-state regime utilizing the transient thermal dissipation (TTD) method (Do and Rocheteau, 2002; Do et al., 2011, 2018; Isarangkool Na Ayutthaya et al., 2010) which by theory is very close to thermal dissipation probe (TDP) method (Granier, 1985). However, the TTD method has been chosen for the TreeTaker development for the lower energy consumption which is a critical issue for the long-term operation of large sensor networks in remote areas.

The main purpose of this study is the validation of TreeTalker performance toward sap flux density measurements using hydraulic bench experiments and a beech stem segment in the lab, comparing with TDP and HPV methods as established throughout topical literature. Additionally, the proposition of a numerical solution to estimate sap flux density based on heat flow equation capturing full heat dissipation curve by TT+. Fig 1 shows a flowchart with step-by-step processing of this study.

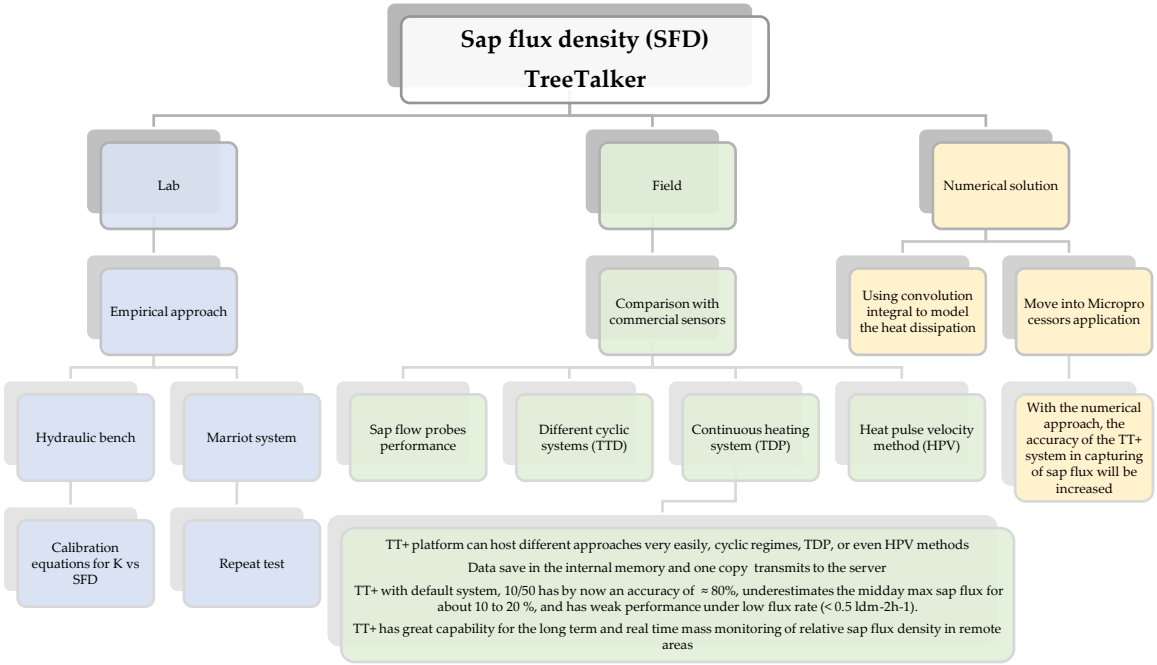

Figure 1. a flowchart of the study process for treetalker principles and applicability toward sap flow measurement

Materials and Methods

Sensor design

The TT+ sap flow measurement technique is based on the temperature difference between a pair of probes, the reference probe and the heater probe, which are inserted radially in the tree trunk

with a vertical separation of 10 cm, facing north and covered by a reflective shield to avoid direct solar heating which may impact registered temperatures (GRANIER, 1985). One of the probes is heated with a power input of 0.2 watts while the other is used to measure the stem temperature, and stem water content using a thermistor and capacitance sensor (Asgharinia et al; 2022). TT+ sap flow measurement by default is set on the transient thermal dissipation (TTD) technique with a cyclic heating system (10 minutes of heating/50 minutes of cooling) to measure sap flux density (Do et al., 2018, 2011; Isarangkool Na Ayutthaya et al., 2010; Masmoudi et al., 2012; Nhean et al., 2019a). The length and diameter of sap flow probes are 20 and 3 mm, respectively.

Lab experiment

Sap flux density measurements are a key feature and focus of the Treetalker technology and thus require correct calibration of the system. Therefore, three explicit yet separate laboratory experiments were designed to obtain a calibration equation to convert flow index outputs from Treetalker to sap flux. The three experiments included a.) A hydraulic bench filled with sawdust and b.) Using a stem segment of a felled beech tree. Each experiment utilizes the gravimetric water method as reference data where digital balance is used to collect water mass data, continuously.

Experiment using an artificial sapwood column

TreeTalker sensor testing to quantify water transport in woody species was conducted under controlled laboratory conditions applying the calibration experiment method (Lubczynski et al., 2012; Wiedemann et al., 2016) in the laboratories of Tuscia University, Viterbo. For this purpose, two sap flow probe pairs of TreeTalkers are inserted into a plastic pipe with a horizontal separation of 10 cm (fig 2). The plastic pipe with a diameter of 3.2 cm and length of 65 cm, was filled with pine sawdust (fig 2). The pipe is supported by a 5 liters water tank in the head to pass the water through the plastic tubing (fig 2), and a pressure gauge, water container, and digital balance in the tail (fig 2). To provide constant water pressure, the main tank feeds water continuously from the bottom overflow tank by way of a mini pump which pumps water into the head tank (fig 2). A pressure gauge and 2 valves at either end of the poly plastic tubing are utilized to set the hydraulic bench on different levels of flux rates, essentially controlling the flow rate. In this experiment, under different flux rates, TT+ is programmed to provide high-frequency temperature records (every second) from Ref and Heater probes to capture the heating and cooling phases before and after the current switches off in each cycle. Capturing this high-frequency data in this investigation aims to a.) Using different time windows from the temperature evolution records to provide calibration equations between different flow indices in the lab using hydraulic bench b.) To see the performance of the Ref probe and heater probes under different duration and amounts of heat input. In this experiment, the flux density rate was measured and collected via a digital balance. The digital balance specifically is utilized to facilitate the gravitational lab experiment where the calculation of stem water transport from the change in liquid mass on the balance to conduct non-species-specific calibration equations to convert the flow index of the TT+. This experiment covers sap flux density range between 0 to 8 (l dm-2 h-1).

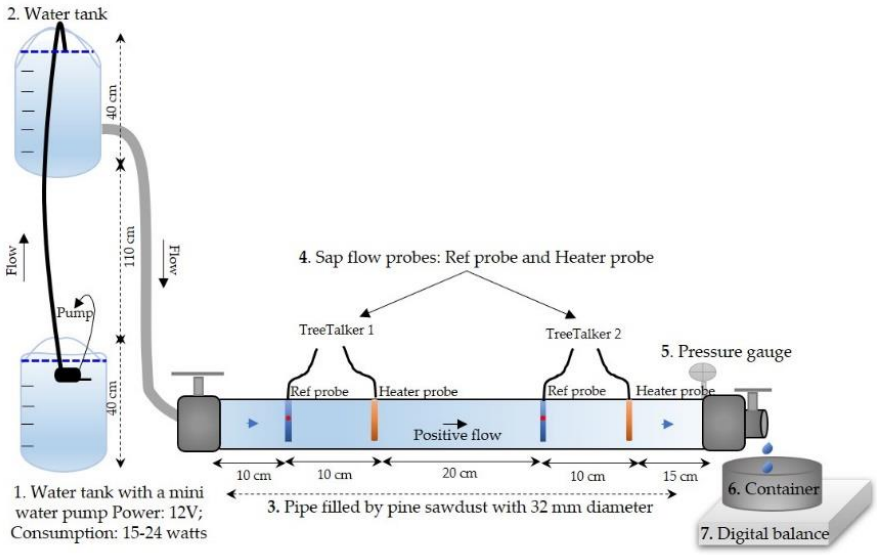

Figure 2. Hydraulic bench filled with pine sawdust for empirical calibration of TT+ regarding the sap flow measurement.

Experiment using a stem segment

Three European beech trees (*Fagus sylvatica* L.), beech 1, beech 2 and beech 3 were harvested at the experimental forest of Ghent University (Gontrode, Belgium) to retrieve cut stem segments with a length and diameter of approximately 22 and 14 cm, respectively. Each segment was stored in the fridge while wrapped with plastic film to retain its physiological integrity (avoid physiological deterioration) in preparation for hydraulic experiments. The first segment, beech 1 was installed as per the Mariotte-based verification system (Steppe et al. (2010). Firstly, a blade is used to remove the first layer of damaged vessels from the sample caused by destructively harvesting the stem. Secondly, a 2 cm collar of bark on one end of the segment is removed to attach and seal the plastic tubing column filled with water to avoid leakage. To improve the seal, a water-proof silicone glue is applied to fix the segment inside the tube where the bark was removed (fig 3.a). TT + sap flow sensors (Ref and Heater probes) were installed on the cut stem segment with a vertical separation of 10 cm, considering upstream and downstream directions in the segment (fig 3.b). In this experiment, the cycling mode of the TT+ was set to 10 minutes of heating and 50 minutes of cooling. Once sealed, probes inserted and TT+ ready to log the data, the segment and Mariotte system are placed in a climate chamber with a fixed temperature and humidity of 20° C and 70 %, respectively (fig 3.b). The Mariotte system with a principle of constant water pressure (McCharty, 1934), can provide different levels of water flow in the segment by changing the height of the Erlenmeyer flask (Steppe et al. (2010). Parallel measurements of the temperature difference between the TT+ probes are taken on an hourly scale, while water throughflow via the stem segment is recorded by a digital balance, every 2 minutes. Given our 5-hour time window, 5 data points were collected for this experiment. To control and check TT+ probe depth is correctly aligned with sapwood depth, dye in the form of food coloring is applied (fig 3.c). In this particular case, the sapwood depth of 3.5 cm is recorded and was sufficient to obtain both the correct installation of the probes and their functioning.

Beech 2 and beech 3 segments are used for detecting the capability of TT+ for measuring zero-flux. In this experiment, mounting two TT+ including the pair of sap flow probes (Ref and Heater probes), the hourly transient signal was measured in fresh-cut stem segments for approximately 2 days.

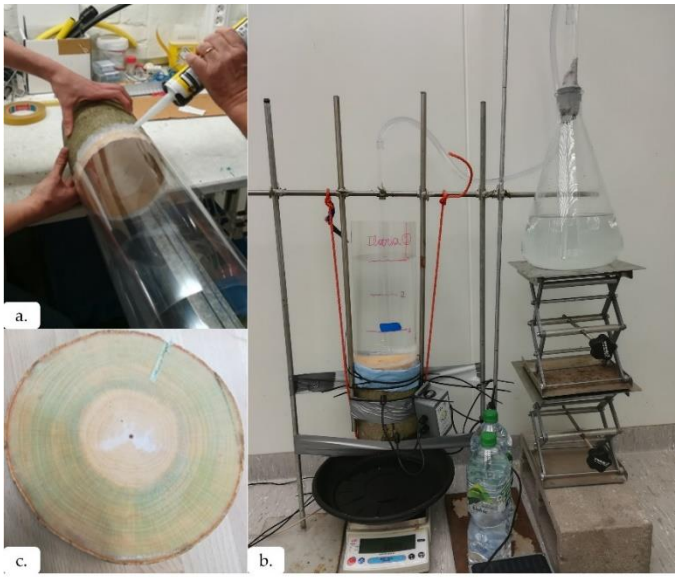

Figure 3. a. preparation of the harvested stem cut for Marriot system, b. Marriot system with fresh-cut beech stem segment for TT sap flow sensor calibration and c. detecting the sapwood depth with coloring technic.

Sap flux density measurements: field experiment

Time curves of temperature evolution for different cyclic regimes

To analyze the Ref and Heater probes responses under different flux rates with different heating duration, four TreeTalkers (TT+) were installed on two selected P. nigra trees at the experimental site of Tuscia University. TreeTalkers are installed vertically toward the north at DBH height. On each tree, two pairs of Ref and heater probes were placed on the vertical axis with 10 cm of spacing. In this experiment, TT+ was programmed to collect high-frequency records (every 2 sec) of heat dissipation data under different heating/cooling cycles in the living trees.

Figure 4. Installation of two pairs of TT+'s sap flow probes on *P. nigra*, recording high frequency data of heat dissipation, Unitus, Italy.

Effect of heating duration on sap flux measurement in a living tree

A Pinus Pinea, native to the Mediterranean region, was chosen to apply 3 TreeTalkers with 3 different cyclic TTD systems in Campania, Italy. Heating/cooling cycles selected for each TreeTalker were 50/10, 10/50- and 10/10-minutes, respectively.

Comparison of TT+ with HPV and TDP system across different species in different locations

TreeTalker were installed on different species, at different locations across Europe spanning several yet not identical growing seasons. Investigations focus on the accuracy of sap flux density measurement methods in comparison with other commercially available sensors.

a. To evaluate the TT+ capability in terms of measuring the absolute value of sap flux rate, two TT+ were installed on European beech trees (*Fagus sylvatica* L.) at the experimental forest of Ghent University (Gontrode, Belgium). On the same trees, TreeWatch sensors were installed which are performed based on the heat pulse velocity (HPV) system. The DBH of the selected trees, beech

1 and beech 2 were 26 and 63 cm, respectively. Moreover, the sapwood areas for the above-mentioned trees are equal to 130.5 and 710.6 cm2.

Figure 5. TT+ and TreeWatch installation on a beech tree, UGent, Belgium.

b. *Picea abies* as a native large pyramidal evergreen conifer in the alpine region of Switzerland was selected to apply commercial the UP Sap Flow-System (TDP based) and TreeTalker. The UPS sensor operates on a continuous heating technique and applies 0.2 watts of power consumption. The sensor includes the Granier-type probe with a total length of 33 mm and a heating zone of 20 mm. TT+ functions with the same characteristics, approximately. The heater probe of TreeTalker has a length of about 20 mm with heat across its entire surface area. In this study, TreeTalker was set on a non-steady heating regime with 10 minutes of heating and 20 minutes of cooling cycle. Sap flux density (SFD, l dm-2 h-1) was measured and compared in 5 randomly selected *P. abies* using TT+ and UPS sensors mounted at diameter at breast height and both facing south.

c. *Fagus sylvatica* L and *Qercus rubra* L were chosen to continue the investigation of TT+ sap flow sensor capability in capturing sap flux density in comparison with the TDP system in different locations with the collaboration of Technische Universität München (TUM) and Philipps-Universität Marburg. Mounting TT+ and TDP system, beech, and oak with DBH of 30.4 and 20.7 cm are monitored from mid-June to the end of July 2021. and oak in Technische Universität München. In addition, for two consecutive years (2020 and 2021), TT+ and TDP systems are installed on a beech tree with DBH of 52 cm at MOF study area with the collaboration of Philipps-Universität Marburg.

Results and discussion

Temperature gradient under different heating/cooling durations in hydraulic bench

One of the benefits obtained via the TT+ platform is its flexibility and user-specified firmware capabilities allowing the capture of a high frequency of heat flow data (fig 6). Benefiting from these capabilities and using tailored firmware, we demonstrate the capture of temperature evolution during the cyclic heating and cooling phases of the heater and reference probes under different flux rates and with several possible cyclic regimes in the lab with a hydraulic bench (fig 6). The aim of recording the full curve of heat dissipation was to extract temperature gradient data of different time windows and thus giving rise to different flow index evaluations. For instance, in the heating phase, using initial ΔT, ΔTmin and ΔTmax can fulfill evaluating K1, while using ΔT at 30 and 300 seconds provided a different flow index, K2 introduced by (Nhean et al., 2019a). In addition, in the cooling phase, getting ΔT at the initial point after turning off the heater current and 20 seconds after, we can apply K3 flow index.

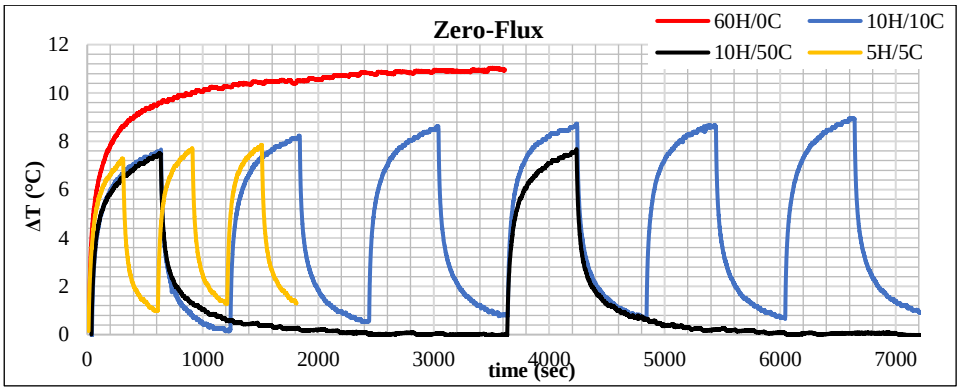

Figure 6. TT+ performance in recording heat dissipation data using different heating/cooling durations, e.g., 60/0, 5/5, 10/10, and 10/50.

Comparing the classic cyclic system 10/10 proposed by (Do and Rocheteau, 2002b, 2002a) to the 10/50 cycle which is the default of TT+ for the sake of low power consumption, shows that under low and fast-flux rate, irrespective of cooling duration, both of the cycles, 10/10 and 10/50 are reaching the steady-state as well as converging to each other within 600 sec, whereas, under the zero-flux condition, neither of the two stated conditions can be satisfied (fig 7). Moreover, cycle 10/50 in comparison with cycle 10/10 is underestimating the ΔTmax by about 1 °C (fig 7).

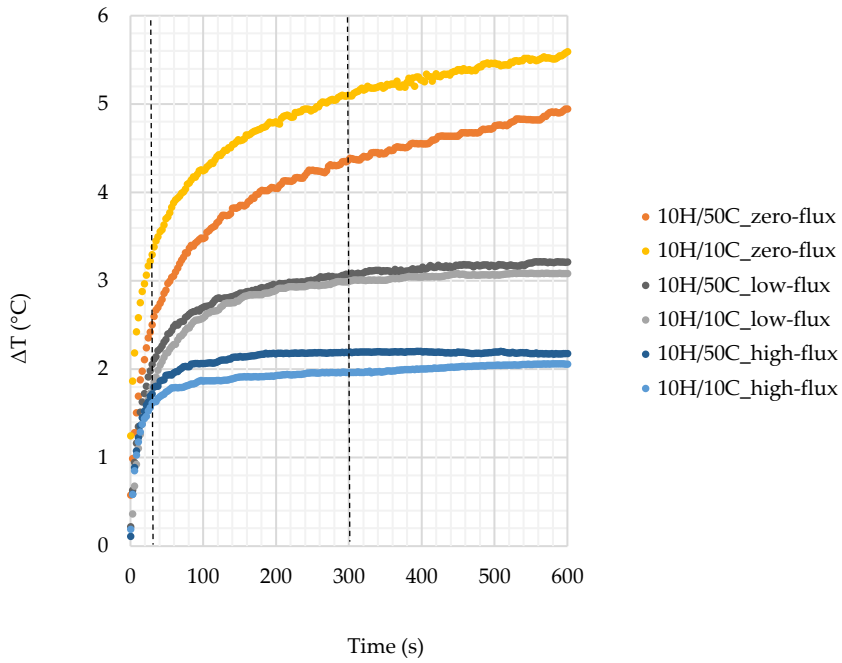

Figure 7. Comparison of the classic cyclic regime, 10/10 to TT+ default with 10/50 system under zero, medium (1.7 l dm-2 h-1), and fast-flux (5.6 l dm-2 h-1) rate.

Figure fig 8.a & 8.b captures changes in ΔT according to different flux rates from hydraulic bench experiments of heating and cooling phases using TT+ set on a 10/50 cycle with tailored firmware. In fig 8, time windows are highlighted by the red vertical lines to separate time windows as a reference to curves, in the heating phase 30, 300, and 600 seconds and in the cooling phase 20 seconds.

Focusing on time to reach a steady-state in the heating phase, where the plateau of the curve is, we see that under higher flux rates (SFD=1.7, 4.1, 5.6), a steady-state is achieved within the 600 seconds heating regime. On the contrary, however, for low and near null flux (SFD =0 and 0.36) the 600 seconds heating regime is not enough to reach a steady-state implying modification of heat duration input. As such, problems may arise when using this heating regime with 600 seconds to estimate ΔTmax for empirical approaches. Regarding the cooling phase, the heat dissipation curves for all SFD vary in exponential form, and the slope of each curve and respective ΔTmax change according to each SFD. Considering the empirical method of (Mahjoub et al., 2009), which is independent of ΔTmax under zero-flux conditions as well as heating duration, using the cooling phase data can lead to a more accurate estimation of the flow rate. Importantly for both heating and cooling phases, the magnitude of ΔT is distinguishable at the end of the heating phase and the start of the cooling phase for different flux rates.

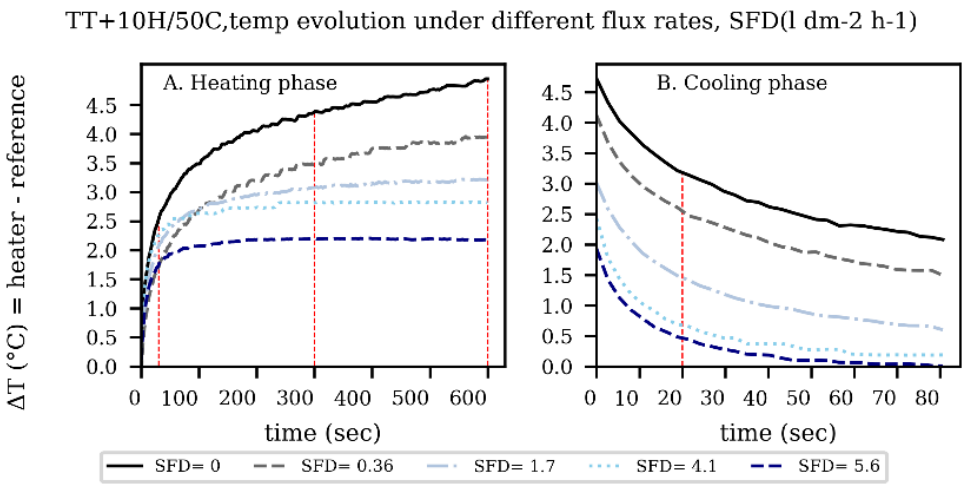

Figure 8. The temperature gradient in heating and cooling phases under different flux rates, data captured by TT+ set on 10/50 cyclic regime

Sap flux density vs flow indexes

Captured data for heat dissipation in the heating phase and cooling by using two sets of the Heater and Ref probes allowed the estimation of different flow indices K1 (K_Heating phase), K2 for the time window of 30 to 300 sec (K: 30 to 300 sec_Heating phase) and K3 (K: 0 to 20 sec_Cooling phase) to find calibration equations between flow indices and gravimetric SFD. Calibration involved the y variable as SFD captured by digital balance and the x-axis the different flow indices (fig 9). The different heating and cooling phases and durations are presented for each scenario. The results from this set of graphs demonstrate respectable correlations between the K1 and SFD under all scenarios with variations in intercepts and R2 values (table 1). Fig 9.a shows the relationship between K1 and SFD, where K1 is derived as the initial ΔT at 0 seconds and ΔTmax from the heat dissipation curves in the heating phase and r-value ranging 0.88-0.95 and slope ranging from 2.93 and 7.13 respectively. Here heat input consequently has a significant influence according to different flux. For example, the blue line or continuous heating approach, the TDP method, has a slope of 2.93, whereas the 15/45 TTD approach is 7.13. In fig 9.b, K2 and SFD, where K2, is still in the heating phase, applies the subsequent derivatives of ΔT from a range of 30-300 seconds as introduced for the transient regime (Nhean et al., 2019b). Again, we report similar linear forms, however, r-values differ in magnitude between 0.81 and 0.94 and intercepts between 7.33 and 10.07. In fig 9.c, K3 and SFD, where ΔT derivates are taken from the cooling phase rather than the heating phase and not surprisingly similar regarding slope given the natural behavior of heat loss over time and increased SFD. The poorest correlation between 5/10 may be explained by the lack of sufficient heat input of substrate volume not receiving a large enough heat pulse to be influential. Both Fig 9.a and 9.b show that the derivatives of flow indexes are highly varied under different heating/cooling durations whereas the cooling phase, 9.c is irrespective of heating duration. In general, the linear regression model is not the best form to represent the relation between flow indexes and SFD, polynomial models or sigmoid functions are recommended to capture the K behavior vs SFD (Do and Rocheteau, 2002a)(Do and Rocheteau, 2002b). However,

the table1 was the preliminary analysis to evaluate and compare the results in terms of different K, and different heating/cooling durations under different flux rates.

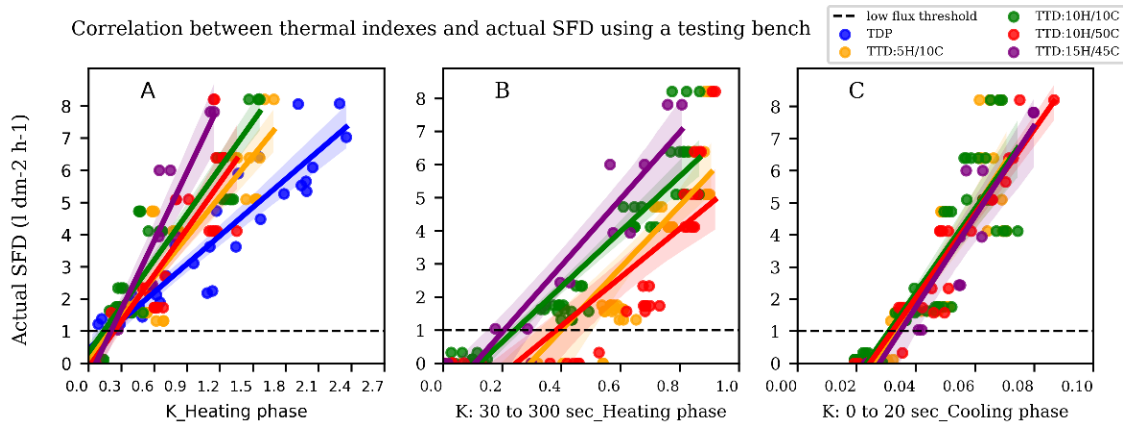

Figure 9. Linear correlation between flow indexes driven from TreeTalker vs gravimetric sap flux density a. K_Heating phase (K1), b. K: 30 to 300 sec_Haeting phase (K2), and c. K: 0 to 20 sec_Cooling phase (K3), and Y-axis: actual SFD measured by digital balance.

Table 1. regression analysis between flow indices and gravimetric SFD for different scenarios in linear standard form (SFD=aK+b)

Var.	K_Heating phase					K_30 to 300 sec_Heating phase				K3_Cooling phase			
	TDP	*5H/10C*	*10H/10C*	*10H/50C*	*15H/45C*	*5H/10C*	*10H/10C*	*10H/50C*	*15H/45C*	*5H/10C*	*10H/10C*	*10H/50C*	*15H/45C*
slope	2.93	4.18	4.79	4.79	7.13	9.40	8.34	7.33	10.07	143.36	131.08	130.91	141.44
intercept	0.45	0.16	0.33	-0.13	-0.47	-2.76	-1.03	-1.81	-1.09	-3.81	-3.06	-3.20	-3.91
rvalue	0.93	0.92	0.95	0.88	0.95	0.84	0.94	0.81	0.93	0.89	0.91	0.97	0.94
pvalue	7.1E-14	2.0E-17	1.4E-26	1.2E-10	7.38E-07	1.77E-12	4.42E-25	1.53E-08	4.63E-06	9.72E-19	1.5E-26	1.3E-27	2.5E-06
stderr	0.22	0.29	0.23	0.49	0.71	0.95	0.43	0.97	1.21	10.45	7.47	5.01	15.98
n	30	41	53	31	13	43	53	33	13	53	68	44	13.000

For the default mode of TT+, 10/50, the regression analysis for the hydraulic bench data, K_Heating phase, K: 30 to 300 sec_Heating phase, and K: 0 to 20 sec_Cooling phase were represented in the following section applying the polynomial model, as well (fig 10, table 2). A second-order polynomial function in the standard form of $SFD = a + bK + cK^2$ was applied to the data. In comparison to the offered linear regression forms (table 1), for K1, R-squared slightly degraded from 0.77 to 0.73, while K2 and K3 improved from 0.66 to 0.91, and 0.94 to 0.96, respectively (table 2). Applying polynomial function, with respect to RMSE and R-squared, in the heating phase K2, and in the cooling phase K3, offers the best empirical estimation of SFD (table 2). However, using the preferred flow index in the heating phase (K2) is limited for the low flux rate (< 1 l dm-2 h-1) and the flow index driven from the cooling phase is only applicable for the positive flow.

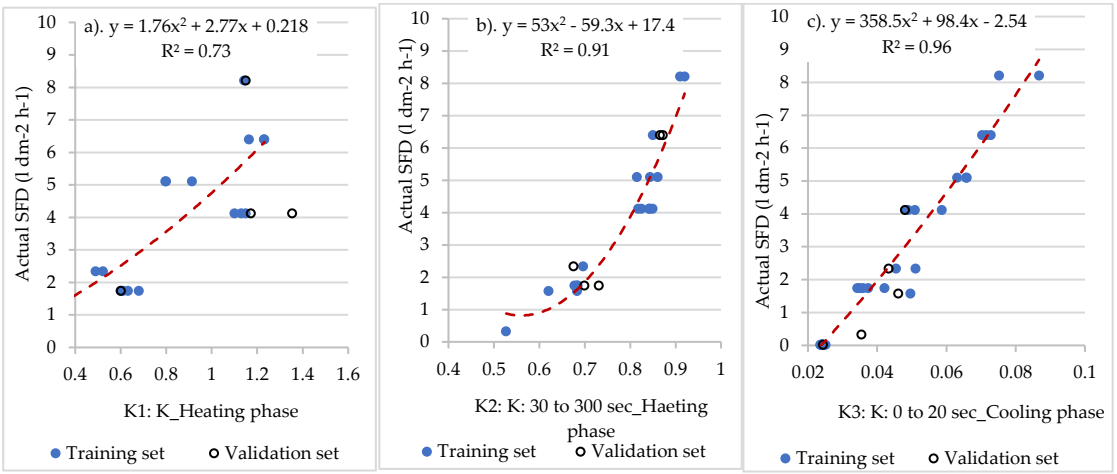

Figure 10. Quadratic polynomial model between flow indexes driven from TreeTalker (10/50) vs gravimetric sap flux density, a. K_Heating phase, b. K: 30 to 300 sec_Haeting phase, and c. K: 0 to 20 sec_Cooling phase.

Table 2. Regression analysis between flow indices and gravimetric SFD for different scenarios in second-order polynomial form ($SFD = a + bK + cK^2$)

non-linear regression for 10/50 regime	Parameters	Value	Standard error	Lower bound (95%)	Upper bound (95%)	MSE	RMSE	R-squared	Observations	restriction
SFD vs K_Heating phase	a	0.218	1.180	-2.298	2.734	1.508	1.228	0.73	25	-
	b	2.772	3.442	-4.564	10.109					
	c	1.766	2.308	-3.154	6.685					
SFD vs K: 30 to 300 sec_Haeting phase	a	17.414	7.967	0.433	34.395	0.503	0.709	0.91	25	K> 0.55
	b	-59.301	21.842	-105.857	-12.746					
	c	52.971	14.728	21.579	84.362					
SFD vs K: 0 to 20 sec_Cooling phase	a	-2.544	0.653	-3.876	-1.212	0.319	0.565	0.96	40	K> 0.025
	b	98.380	30.805	35.552	161.207					
	c	358.486	314.050	-282.023	998.995					

Stem segment results

Fig 11.a is representative of calibration equations for TT+ with 10/50 regime mounted on a stem segment, beech 1 placed in the climatic chamber using the Marriot system. The results of the Marriot system experiment provide a calibration equation between flow index, K1 (derived from TT output) and SFD (balance data). The resulting linear equation gives a slope of 3.5 which is quasi-close to the value achieved using sawdust in a hydraulic bench (4.79) for the mentioned cyclic system. The differences between the two may be explained by the lack of sufficient data from the Marriot system. Therefore, the Marriot system experiment should be repeated to obtain more data points to cover a greater range of SFD.

Fig 11.b instead, is a comparison of TT+ performance using the 10/50 regime aiming to detect zero flux. Here, two freshly cut stem segments, beech 2 and beech 3 were placed in a climatic chamber with independent TT+ mounted to record changes in SFD. As the results demonstrate, the TT+ is detecting a very low SFD up to 0.2 l dm-2 h-1for the first 18 hours. The expected zero-flux was achieved after this period. Indeed, this is considered as the relative error in SFD measurement

under zero flux conditions and may be attributed to fluctuations in the stem water content of freshly cut stems. Furthermore, these results confirm the overestimation of the SFD near null flux by applying empirical thermal approaches which is reported by several studies, as well (Čermák et al., 2007; Vandegehuchte and Steppe, 2013; Vergeynst et al., 2014).

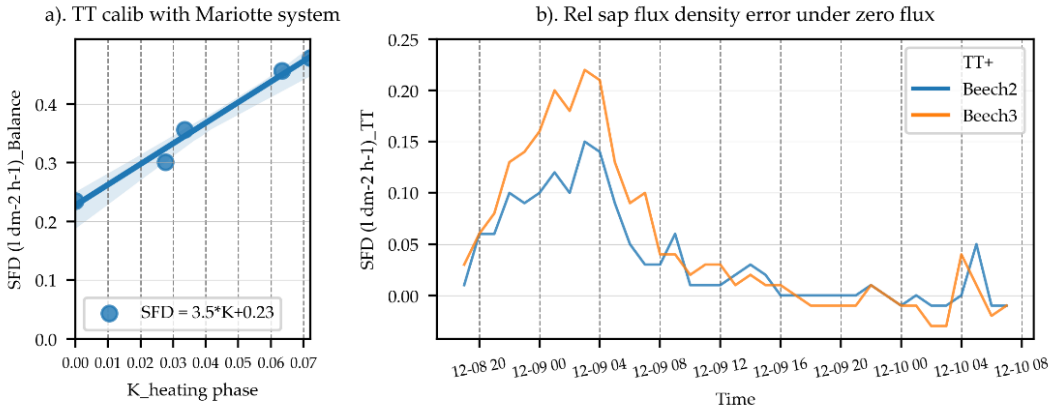

Figure 11. a. correlation between flow index (K1: K_Heating phase) and gravimetric SFD using stem segment of fresh-cut beech mounted in Marriot system, b. SFD data are recorded with two TT+ installed on two stem segments of fresh-cut beech to analyze the capability of the sensor in zero-flux measurement.

Reference and heater Probes' performance in living trees

Fig 12 displays the results of temperature fluctuation derived from the heater and reference probes with different cycling regimes (10H/50C and 10H/10C) applied to a living tree, P. nigra from 07:00 am 25th of May to 07:00 am 26th of May. The highlighted sections denoted as a and b were randomly chosen from the data set to reflect day and nighttime to discuss in detail such observations in the following section. The reference probe provides stem temperature data which is shown by the grey line in fig 12 and displays a max stem temperature at 18:00. The temperature oscillation of both heat probes (Black dashed and Blue solid lines) is closely aligned since both methods have 10 minutes of heat input, however, the cyclic 10/10 approach better responds to the maximum transpiration rate in this tree (occurring at 6 pm) This is also reflected in fig 12 by the respective ΔT.

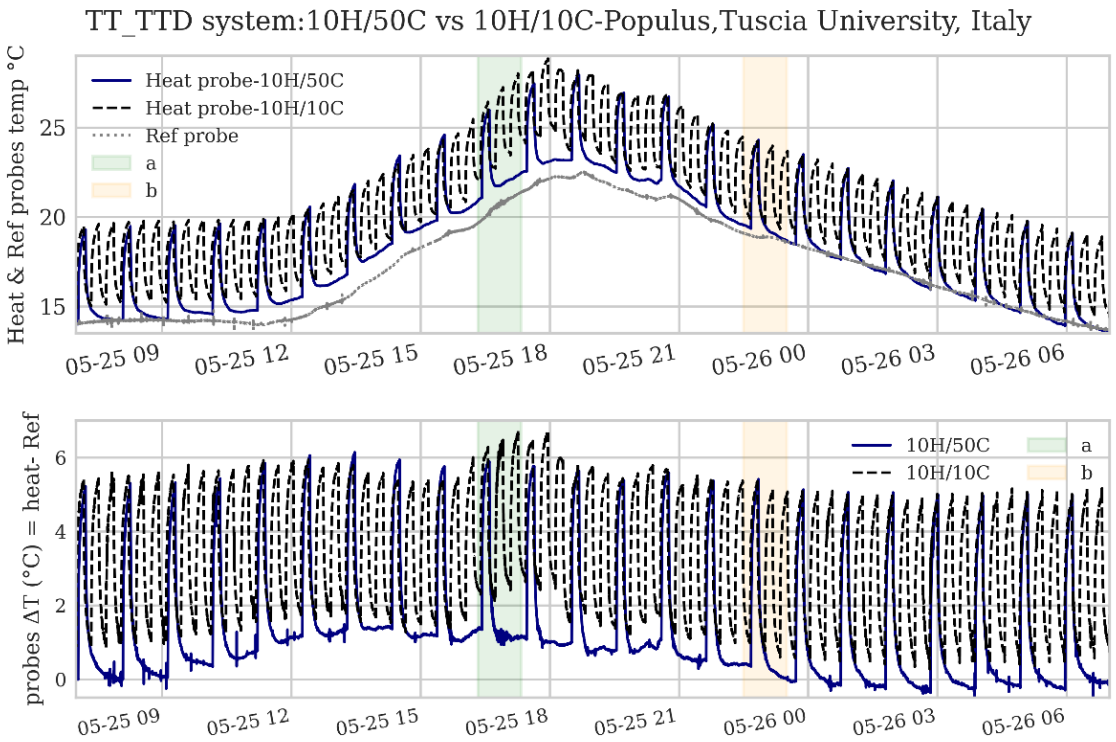

Figure 12. temperature evolution data for 10/10 and 10/50 regimes recorded by TT+ on P. nigra, Unitus, Italy.

Using the highlighted a and b sections from the above experiment, figs 13.a and 13.b provide a snapshot to see the impact of differing cycling regimes on the performance of the heater and reference probes during the day and night. Of note, fig 13.a demonstrates that recorded daily ΔT with the 10/10 approach (4.2 °C) is smaller than the same data provided by 10/50 approach (4.4 °C). This is further highlighted by the respective SFD estimations for both cycle regimes which show midday underestimation of about 20% and nighttime over estimation of flux rates with 10/50 system (fig 13.c). To estimate SFD, derivatives of ΔT contributed to the flow index equation (K2_Heating phase) and eventually provided SFD results based on the calibration equations for each cyclic system (fig 13.c). Overestimation of SFD may occur under very low flux rates (here ≈< 10 g m-2 s-1/ 0.36 l dm-2 h-1) and higher fluctuation of stem water storage (Vergeynst et al., 2014).

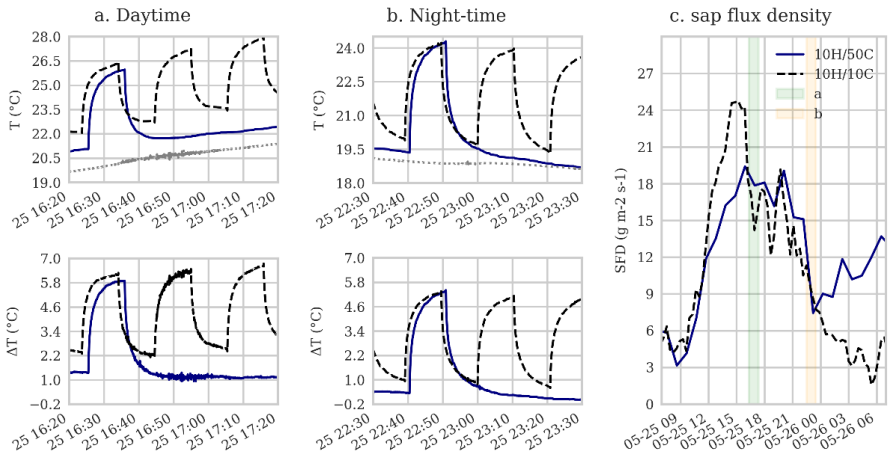

Figure 13. a. heat dissipation curve by 10/10 and 10/50 regimes in the daytime, b. heat dissipation curve by 10/10 and 10/50 regimes in the nighttime, c. estimated sap flux based on flow index of heating phase for both cyclic systems, *Populus nigra*, Unitus, Italy

Heating/cooling duration effect on SFD data in *P. pinea*

In this section, a comparison of different heating/cooling durations and their impact or effect on flow index and SFD are presented. To examine the variation of the measured sap flux by different cyclic systems, 3 TreeTalkers with heating/cooling regimes of 10/50, 50/10 and 10/10 minutes were mounted at diameter at breast height DBH on a *P. pinea* in Campania, Italy. As the 10/10 regime represents the original formulation established by (Do and Rocheteau, 2002a), in fig 14 we have considered it as a reference and thus the independent variable on the x-axis. The result of flow indexes of 10/50 and 50/10 modes are sat on the y-axis. The flow indices for all cyclic regimes are estimated based on eq.4, K1 and then applied in the SFD calibration equations provided in table 1. As we don't have calibrations for 50/10, we assume the TDP method to derive SDF for this particular cyclic regime.

Having data for 7 days, from 12th to 18th April 2020, it is apparent that TreeTalker set on 50H/10C mode overestimates the flow index and subsequently SFD by ≈ 2.3 and 1.5 times, respectively. In contrast, the average results associated with 10/50 suggest a plausible underestimation of the flow index and subsequently also SFD by ≈ 0.65 and 0.8 times compared with 10/10 method. In addition to capturing SFD using various heating/cooling regimes, we confirm that the max SFD occurs around midday irrespective of the regime applied to see fig 15. In fig 15, the Gustafsson noise filtering method (Gustafsson, 1996) slightly is applied to sap flux density results to smooth the curves while keeping the shape and magnitude of the SFD rate unchanged.

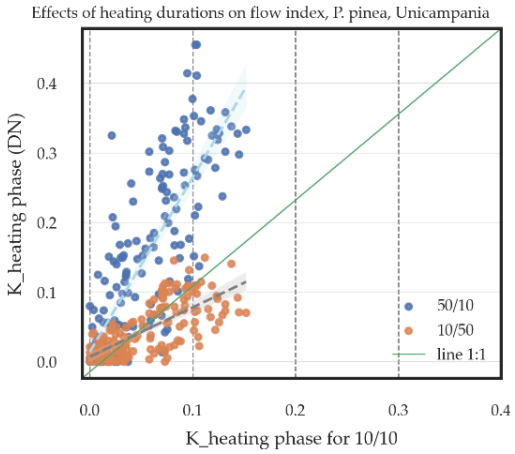

Figure 14. Comparison of flow indexes (K1) of TreeTalkers in 10/10 mode with 50H/10C and 10H/50C modes.

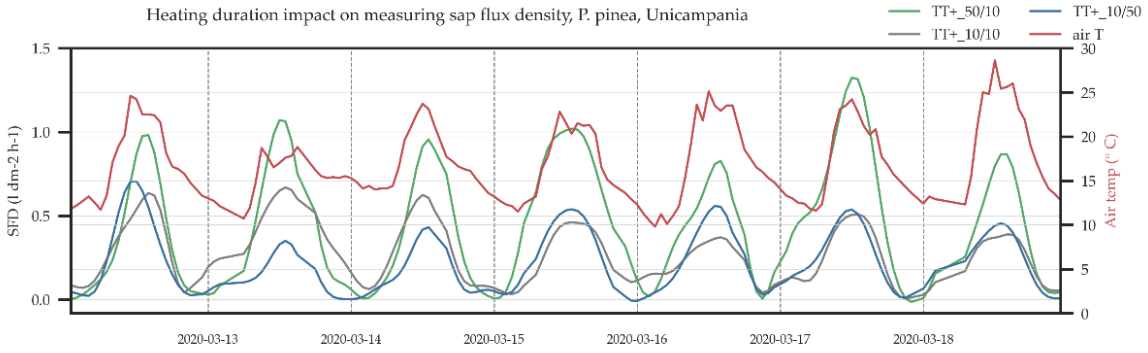

Figure 15. Results of hourly sap flux density and air temperature in a P. Pinea measured by TreeTalker with 3 different sets of heating/cooling durations (50/10, 10/50, and 10/10)

Comparison of TT+ with Heat pulse velocity method

As the heat pulse velocity method (HPV) is a non-empirical method where SFD is based on thermal dissipation from theoretical ideas of conduction (material substrate wood) and convection (water velocity sap) offering an absolute measurement of SFD in living trees. The result of this investigation between TT+ with 10/50 regime (grey solid line) and the HPV method (orange solid line) yields similar patterns regarding SFD measurements (fig 16). Interestingly, toward the end of the growing season when beech transpiration undergoes a reduction as they enter the dormancy phase for winter, the TT+ demonstrates a good capacity (≈80 %) for capturing the SFD in comparison with the HPV method (fig 16). However, TT+ again underestimates max daily SFD by approximately 20%. Furthermore, near null fluxes are difficult to detect accurate flux patterns utilizing TT+ as well as HPV method (fig 16). It should be considered that HPV method is overestimating the SFD rate under low flux conditions (fig 16) (Ren et al., 2020). In fig 16, applying the Gustafsson noise filtering method, the smoothed curve for TT+ is presented as a blue solid line with the label of TT+/ Gustafsson, as well.

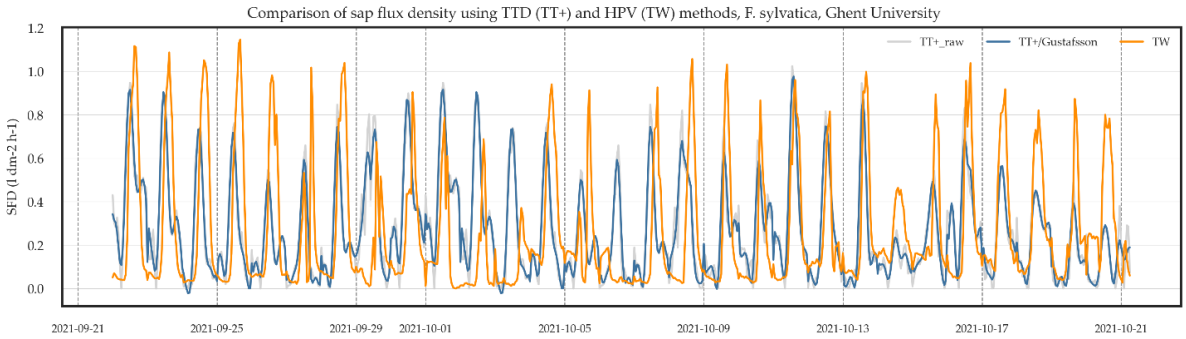

Figure 16. SFD measurement with Transient regime (TT+ with 10/50 mode) vs HPV method using TreeWatch (TW) in beech, UGent, Belgium.

Comparison of TT+ with 10/50 mode to the continuous heating system (TDP)

In the comparison of TT+ and HPV systems, the next phase involved a comparison of another well-established method, the continuous heating technique (TDP).

The total measurements of TT+ and TDP on a living beech tree for two consecutive growing seasons, 2020 and 2021 from the MOF study area, Philipps-Universität Marburg are displayed in fig 17.a and 17.b. The result of this experiment between hourly SFD data of TT+ (10/50) (muted blue solid line) vs TDP (muted green solid line) as well as daily max SFD of TT+ (10/50) (orange solid line) vs TDP (red solid line) are presented in fig 17.a and 17.b for two growing seasons, from July to mid-October, 2020 and 2021. In addition, fig 17.a and 17.b show the variations in average daily air temperature (black solid line) at the sampling site. When the annual average of SFD measured by TDP system is < 1 l dm-2 h-1, the relative error of SFD measurement with TT+ utilizing the 10/50 system is higher (fig 17.a), whereas, for the annual average flux rate > 1 l dm-2 h-1, TT+ (10/50) shows better performance in capturing SFD (fig 17.b). However, for the cyclic system with short heat input (10 min heating), a relative error of SFD measurements, about 41% is anticipated under a low flux rate (< ≈0.5 l dm−2 h−1) (Isarangkool Na Ayutthaya et al., 2010).

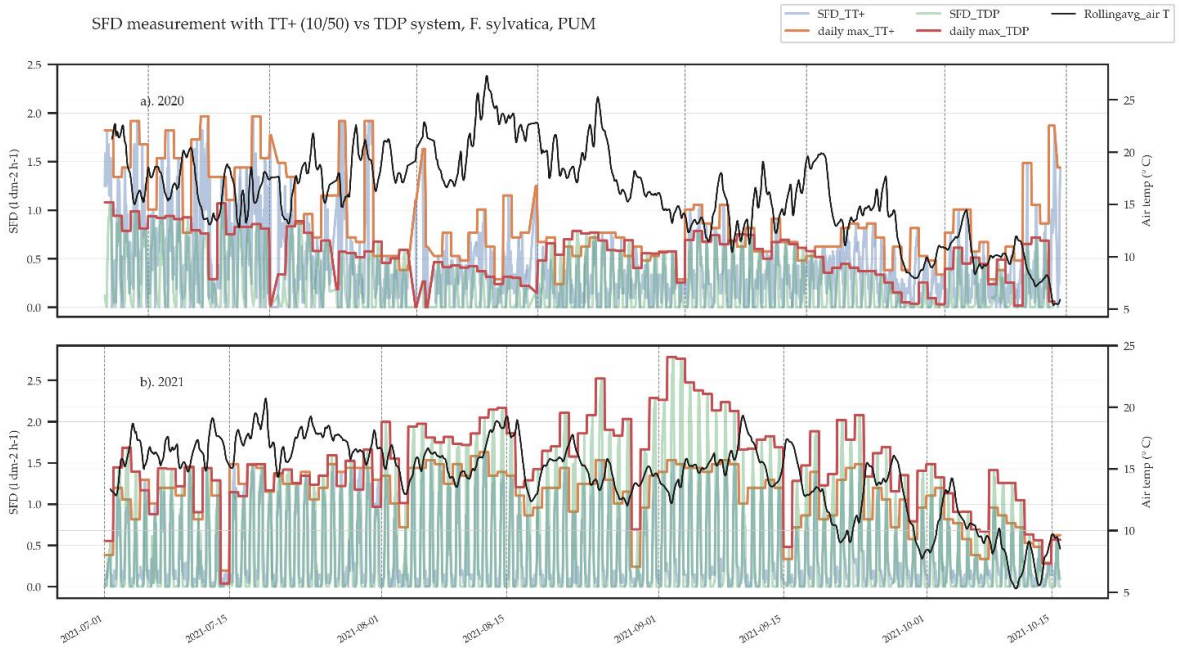

Figure 17. comparison of TT+ with the transient regime (10/50) with TDP method on beech, MOF study area, Philipps-Universität Marburg.

To compare the results of the two methods, the error of SFD is estimated using the following equation (Nourtier et al., 2011).

9. $$\boldsymbol{SFD_{Error} = (SFD_{max-24h} - SFD_i)_{TT+\left(\frac{10}{50}\right)} - (SFD_{max-24h} - SFD_i)_{TDP}}$$

When capturing data for the growing period with a heat wave in 2020 in comparison with 2021 records, TT+ and TDP systems, both are similarly aligned in terms of recorded data for low SFD whereas TT+ error of SFD measurement rises to +1.8 while in the growing season 2021, the SFD error measured by TT+ is equal to -1.6 (fig 18). The rate of occurred divergence between the two methods is remarkable. The continuous heating system (TDP) has the capability of capturing the SFD rate and pattern near null fluxes since the amount of heat input is sufficient to reach a steady state, yet, this method rise wound impact due to the non-stop heat input and thus, underestimates the SFD rate. Using thermal approaches dependent on ΔTmax, especially TTD method with shorter heat input, generally introduces some error in SFD measurement since detecting accurately the magnitude and time of ΔTmax occurrence are very difficult. Controlling the time of ΔTmax occurrence in collected data for two consecutive growing seasons with 10 min heat input revealed the possibility of occurrence of the event at any time within 24 hours (fig 18). Daytime ΔTmax might cause significant uncertainties in SFD estimation.

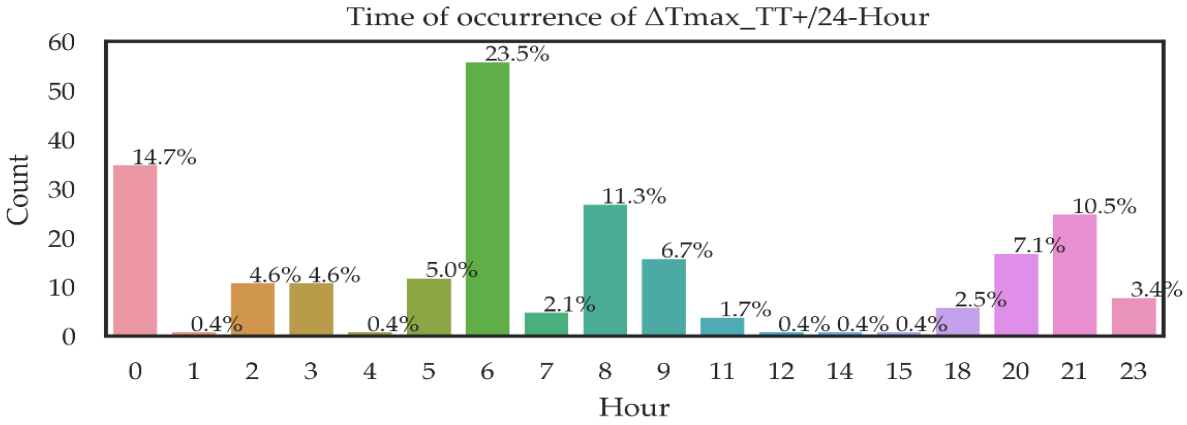

Figure 18. Frequency of the maximal ΔT occurrence time for two growing season (2020 and 2021), Fagus. sylvatica, MOF study area, Philipps-Universität Marburg.

Multiple ΔTmax approaches are now in use to detect correctly the zero-flow conditions including the daily predawn (PD; Lu etal., 2004), maximum moving window (MW; Rabbel etal., 2016), double regression (DR; Lu etal., 2004) and environmental dependent method (ED; Oishi etal., 2016). Here we applied PD and MW methods to see if the error of SFD measurement decreases (fig 19). Even though different approaches were utilized to detect the reasonable time and amount of ΔTmax, SFD estimates remain imprecise because of the empirical as well as strong dependency on the ΔTmax event. Improvement in SFD measurement using PD and MW approaches in comparison with the TDP system was about 3% which is negligible.

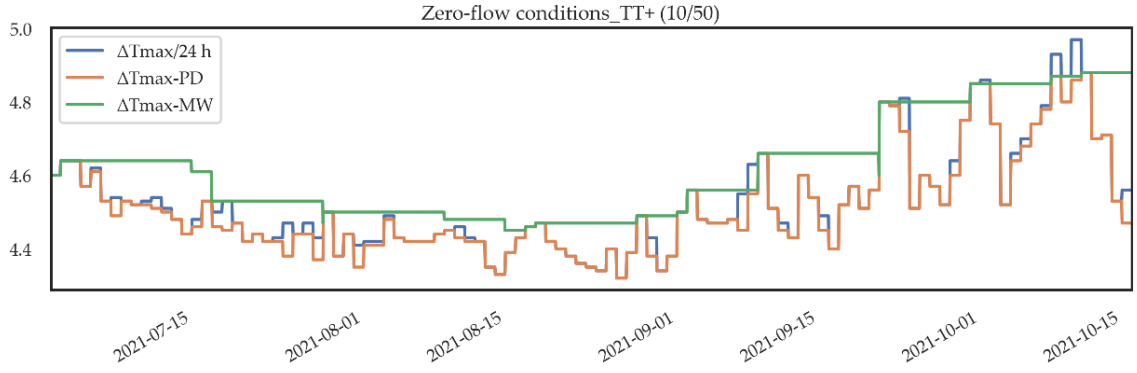

Figure 19. Multiple ΔTmax approaches under zero-flux conditions, daily ΔTmax (ΔTmax/24 h), the daily predawn ΔTmax (ΔTmax-PD), and maximum moving window ΔTmax (ΔTmax-MW)

Comparison of SFD output between TDP and TT+ (10/50) for *P. abies*, *Q. rubra*, and *F. sylvatica*

The last series of graphs below (fig 20) is a synthesis of the most used thermal approaches (TDP) versus the TT+ (10/50). Fig 20 represents three separate wood anatomical features important

for the transport of water via the stem and are separated as such according to their anatomical porosity. In fig 20, starting from the left side, *P. abies* being non-porous, *Q. rubra* being ring-porous, and *F. sylvatica* being a diffuse-porous medium. This is an important distinction for both thermal dissipation and bound water in the stem.

Although the SFD rate in fig 20 for *P. abies* vs *Q. rubra* is in the same range for the TT+ SFD records (≈ 0 to 1 l dm-2 h-1), the standard variation for *P. abies* is very high (r-value = 0.56 and p-value < 0.001) in compared to *Q. rubra* (r-value = 0.82 and p-value < 0.001). This may be explained by the different wood anatomy for both species where the small vessels of the *P. abies* trap and bind water which causes an underestimation of ΔT under zero-flux with 10 min heat input. Indeed, the stem water content may cause inaccurate estimation of ΔTmax, in terms of magnitude and the time of occurrence using empirical thermal approaches. Consequently, this causes a false evaluation of SFD. As displayed in fig 20 for *P. abies*, SFD data has a higher standard variation according to the TDP outcomes, the TDP system can overcome the stem water impact with non-stope heat and can neglect the stem water impacts. However, in oak, the vessels are larger, therefore TT+ with 10 min heating can capture a clear pattern yet the estimation is greater for the SFD amount rather than the TDP. Interestingly, the TDP system is known for underestimating the SFD rate (Vandegehuchte and Steppe, 2013). Therefore, it may be possible that the TT+ is capturing the SFD due to considering the natural temperature gradient. Fig 20: *F. sylvatica* is showing a very good correlation with TDP system (r-value = 0.89 and p-value < 0.001) since the flux rate is higher than the low flux threshold. In particular, this represents the functionality of the TT+ system to detect SFD using a heating/cooling regime of 10 minutes heating and 50 minutes cooling for different species confirming a low-cost IoT alternative for measuring SFD. In the empirical thermal approaches, TDP and TTD provide relative amounts of SFD rather than absolute (HPV), and consequently comparing these two systems remains a difficult task to summarise.

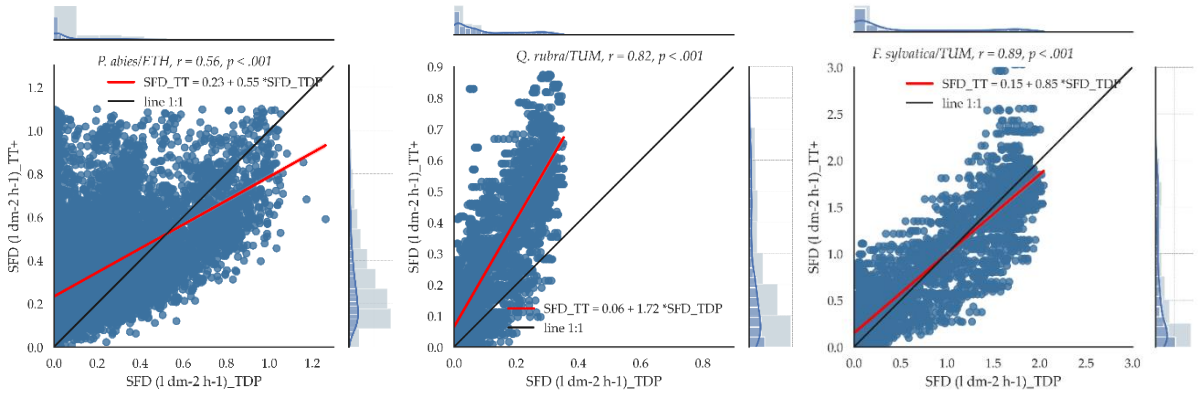

Figure 20. Comparison of SFD output between TDP and TT+ (10/50) for P. abies, Q. rubra, and F. sylvatica from left to the right

Predicting the sap flux density using climatic data

As discussed above, from the different application combinations and scenarios, the empirical thermal approaches did not demonstrate the full capability of measuring SFD. As such, an investigation into other possible factors and approaches affecting SFD prediction was pursued.

Therefore, an analysis of the impact of climatic variables on SFD is discussed below. Climatic variables should naturally impact SFD given the processes of photosynthesis and respiration. Data was obtained from *Fagus sylvatica* for one growing season with the collaboration of Technische Universität München (TUM), Germany. Exploiting air temperature, relative humidity and global radiation, a multivariate linear model approach was used to find the correlation between SFD and these potentially explanatory variables. A statistical description of the variables can be found in Table 3. The statistical approach considers a training set that uses 90% of the datum captured, with a random validation set of 10%.

Table 3: Statistical description for SFD and climatic variables

	Variable	Observations	Minimum	Maximum	Mean	Std. deviation
Training set	SFD (l dm-2 h-1)	3518	0.0	2.0	0.6	0.7
	Air T (°C)	3518	9.8	29.9	18.0	4.1
	RH %	3518	38.7	100.0	89.9	17.2
	global radiation (W/m2)	3518	6.6	1122.0	193.0	238.4
Validation set	SFD (l dm-2 h-1)	500	0.000	2.019	0.613	0.687
	Air T (°C)	500	10.2	29.0	18.0	4.3
	RH %	500	40.5	100.0	88.8	17.4
	global radiation (W/m2)	500	7.8	1049.8	203.3	247.4

The multivariate linear models report respectable explanations between the independent and dependant variables where SFD prediction is positively correlated with Air T (°C) (R2= 0.83) and global radiation (W/m2) (R2= 0.77), and negatively with RH% (R2= - 0.77). To further validate the impact of the abiotic variables described in Table 3, an ANOVA using Type III error was also performed. Results from the ANOVA suggest that global radiation (W/m2) has the highest weighted impact on sap flux density prediction in comparison with air temperature and RH%. This is supported by the stated F statistic and P values reported in Table 4. However, each variable is statistically significant for the prediction of SFD in its own right.

Here we have demonstrated the impact of climatic data on SFD by applying Eq. 10 and as such, we suggest that future analysis apply the same approach for further elaboration and validation of abiotic variables on SFD prediction, including longer-term data sets and a broader representation of species. The results for predicted SFD based on Eq 10. Versus SFD applying TDP system are displayed in figure 21 including the training and validation set.

10. FD (L DM-2 H-1) = 0.31 + 5.63E-02 * AIR T (°C) - 0.011 * RH % + 1.103E-03 * GLOBAL RADIATION (W/M2)

Table 4. Statistical results from ANOVA

Source	DF	Sum of squares	Mean squares	F	Pr > F
Air T (°C)	1.000	55.660	55.660	**707.842**	**<0.0001**
RH %	1.000	47.700	47.700	**606.605**	**<0.0001**
global radiation (W/m2)	1.000	139.668	139.668	**1776.185**	**<0.0001**

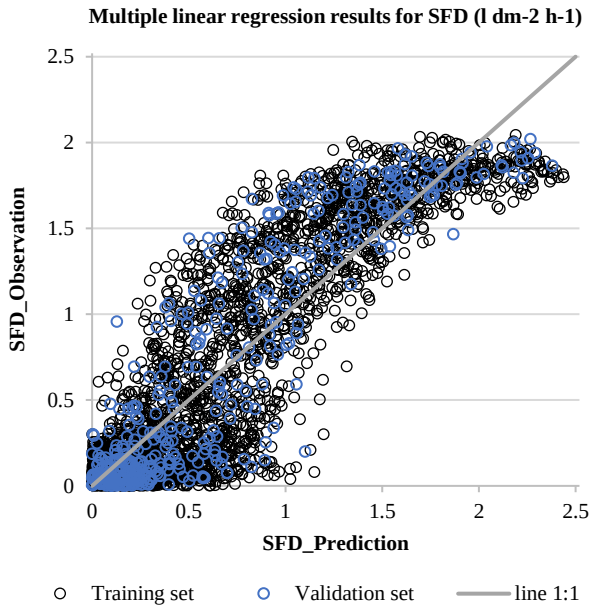

Figure 21. Results from predicted SFD based on abiotic variables versus measured SFD by TDP system.

Conclusion

Taking advantage of tailored firmware, TT+ platform can easily perform as continuous heating, or a cyclic system with customizable measurement time intervals. Empirical calibration equations were provided for different flow indices using a hydraulic bench filled with pine sawdust in the lab. Using thermal approaches and comparing different sensors and approaches is difficult where limitations arise according to precision limitations for sensors and the subsequent impacts from the surrounding environment and within the trees themselves e.g. physical processes of water transport in stress, climatic events and sensor failure. Nonetheless, comparing TT+ set on the transient regime (10H/50C) performance across different species Norway Spruce, European Beech and Oak in situ with well know thermal approaches (TDP: Conintous Heating and HPV: Heat Pulse Velocity method) proved that the tree talker is capable to measure sap flow with reasonable accuracy (80%) for network-based mass monitoring in remote areas with low power consumption. TreeTalker underestimates approximately 20% midday max sap flow rate and has a weak performance under low flux (<0.5 l dm-2 h-1), however, the latter weakness is reported across most thermal approaches. This common weakness may be negated where a TDP approach (Granier) is applied at a higher energy consumption cost. The role of stem water content is not banal and is highly

important for capturing accurate temperature differences between the heater and reference probes, ΔT.

Using cooling phase data of temperature gradient, ΔT, provides better results of the sap flux density estimation, irrespective of the duration of heating/cooling. Flow index based on cooling phase data is independent of ΔTmax under zero-flux conditions. However, it is limited under the low flux rate. We found that if we can program a tailored firmware, we can capture the full curve of heat dissipation in a living tree with a customizable power input and as such, we can apply the different available equations to evaluate SFD in living trees. Also having the full curve of heat dissipation allows us to apply heat partial differential equations at the microprocessor level to directly provide an output of thermal diffusivity (an indicator of stem water storage) and heat velocity (a direct indicator of sap velocity). TreeTalker, a low-cost IoT-based technology, allows testing and examining different methodologies under different conditions and is emerging as a solution for mass monitoring networks for forests.

Article 3: Sap Flow-Part II: Semi-analytical solution

An Automated Platform For Real Time Sap Velocity Detection Applying A Semi-analytical Solution

Shahla Asgharinia [1*], Mazda Kompanizare [2], Francesco Renzi [1], Nicolas Friess [3], and Riccardo Valentini [1]

1. Department for Innovation in Biological, Agro-food and Forest Systems (DIBAF), Tuscia University, Via San Camillo de Lellis snc 01100 Viterbo (VT), Italy

2. Global Institute in Water Security, University of Saskatchewan, 11 Innovation Blvd, Saskatoon, SK S7N 3H5, Canada

3. Department of Biology, Philipps-Universität Marburg, Karl-von-Frisch-Straße 1, 35043 Marburg, Germany

* Correspondence: asgharinia@unitus.it

In preparation

An Automated Platform For Real Time Sap Velocity Detection Applying A Semi-analytical Solution

Abstract

The simplest and most widely used method for measuring water transport in plants is the thermal dissipation probe (TDP) and the transient thermal dissipation method (TTD) which is essentially derived from the TDP system. Because of the low-cost, non-destructive, multifunctional nature of the IoT-based TreeTalker (TT+), both TDP and TTD systems have become more accessible and interchangeable. Using this advance in technology, and its application, we aim to assess the applicability and thus merit of the TreeTalker toward sap flux density measurement and computation. So far, the above-mentioned thermal dissipation approaches use empirical equations to estimate sap flow and although robust, by nature, are limited by their accuracy. Here, a semi-analytical method was developed to exploit the convolution integral of the heat flow equation driven by the mechanisms of conduction/convection for the TTD approach with heating/cooling cycles. The capability of the semi analytical solution was approved by comparing their results with gravimetric data in the lab. The obtained solution method and approach was constructively applied at the microprocessor level hosted by the TreeTalker platform to mathematically evaluate the amount of sap velocity for trees in a quasi-real-time for collecting precision-based big data from forests. Introducing a further novelty, this study also proposes the development of an automated platform based on the thermal approach to achieve a steady state for each species in real-time, where the amount of heat input is determined by the tree via involved ecophysiological and abiotic parameters. An essential feature of the platform, therefore, is to capture the full heat flow curve at the microprocessor level and integrate a semi/analytical approach to mathematically evaluate the amount of sap velocity and thermal diffusivity at a large scale and in real-time.

***Keywords**: IoT, TreeTalker, thermal dissipation probe, transient thermal dissipation, semi-analytical solution, thermal diffusivity, sap velocity, convolution integral, microprocessor*

Introduction

In the previous chapter, the family of heat dissipation methods for sap flow measurement was discussed. Within the thermal approaches, the cyclic system (Do and Rocheteau, 2002b) with 10 min heating and 50 minutes cooling is set as the default program in TreeTalker (TT+) to reduce the sensitivity to the natural thermal gradients. The cyclic system thermal approach is based on the constant heating method developed by (GRANIER, 1985). Furthermore, the cyclic thermal approach reduces the power consumption which is extremely important in long-term mass monitoring networks. A schematic illustration of the heat dissipation during midday and midnight applied by TT+ is shown in Figure 1. As it can be seen in this figure the sap flow happens within the sap wood part or outer part of the stem (Figure 1a). Also, the red parts in Figures 1 b and c shows the areas with higher temperature and blue shows the areas with lower or background temperatures. During midnight when there is zero-flux (Figure 1b) the heated parts are concentrated around the heat probe. However, during midday with max flux the heated (red) parts were dissipated outward from the probe and more in upward direction and that is because the sap flow direction is upward. The measured temperature by the lower probe and its change over time is related to the sap flux density and rate of thermal dissipation. The estimations of sap flux density under the thermal dissipation approaches have so far been based on empirical calibrations, whose uncertainty is difficult to be accurately analyzed (Flo et al., 2019). Empirical equations based on regression between flow index (K) and sap flux density (SFD) introduce some percentages of errors in prediction of SFD. For instance, RMSE for TT+'s default setting varies from 0.5 to 1.8 l dm-2 h-1. Considering the approximate range of SFD values in European forests, of 0 to 3 l dm-2 h-1, the minimum error in our regression analysis is ≈17 %. Additionally, many factors such as wood thermal properties, wound impact of probe insertion, and the dependency to ΔTmax, have a compounding effect on the total error.

Heat dissipation in trees is typically governed by heat partial differential equations (Aumann and David Ford, 2002a; Burgess et al., 2001; Chuang et al., 2006; COHEN et al., 1981; Janbek and Stockie, 2017; Marshall, 1958; Ren et al., 2020; Swanson and Whitfield, 1981; Vandegehuchte and Steppe, 2012b) in them the stem is assumed as a homogeneous and isotropic medium. The heat partial differential equation was solved analytically by Marshall (1958), for the thermal dissipation around a heat probe in a tree stem, considering the input heat as a linear source and the stem's wood as an isotropic medium. The analytical approach was introduced for an instantaneous heat pulse, optimally for 2 to 6 seconds pulse duration with a power input of 500 to 900 j m^{-1}. Moreover, some studies introduced complex mathematical 1D, 2D and 3D models, using Fourier-Bessel series, or semi analytical based models to simulate water flow in the trees (Aumann and David Ford, 2002b; Chuang et al., 2006; Janbek and Stockie, 2017; Theses and Ray Ballard, 2011).

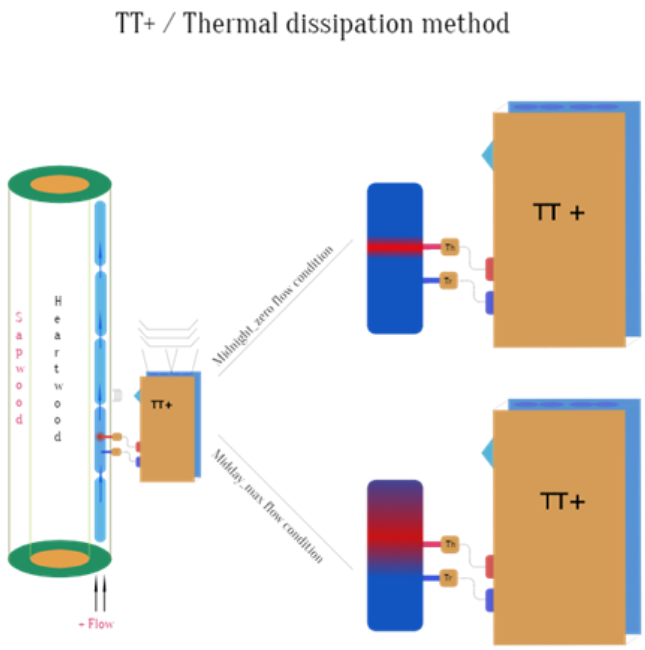

Figure 1. Schematic illustration of TreeTalker (TT+) measuring the heat dissipation through the sapwood (a), under midnight zero-flux(b) and midday max-flux (maximum-flux). The red parts are warmer, and the blue parts are colder.

Although these models are complex and consider both direct (i.e. thermal diffusivity of the matrix), and indirect (i.e. wind speed and factors influencing heat flow in trees), they are not suited to long-term monitoring applications. Based on our knowledge, only a few studies were focused on mathematical solutions for transient regime with a cyclic system of heating/cooling periods (Mahjoub et al., 2009; Masmoudi et al., 2012; Sousa et al., 2020). For instance, (Sousa et al., 2020) applied Fourier analysis of temperature variations in a cyclic heat pulse system for a very short heating/cooling periods with maximum of 120 sec heating to introduce a new convection index. (Mahjoub et al., 2009; Masmoudi et al., 2012) applied Darcy's law (Darcy, 1856). (Whitaker, 1986) developed a one-dimensional flow equation in porous media to propose a new flow index, involved in the estimation of SFD rate in trees. Their work has had a significant impact on SFD estimation by introducing an analytical flow index in addition to Granier's empirical flow index. Although their breakthroughs are substantial, the direct solution of heat flow equation in trees and extraction of sap velocity when heat input is non-instantaneous still remained under investigation.

The apparent lack of information or research in this field for tree sciences is compelling. Having a general knowledge about the role of various factors impacting the heat flow inside woody tissues is important in unraveling water transport in trees. Heat flow inside trees is driven by two main mechanisms of conduction and convection. Conduction, is by considering that the trees are as the anisotropic materials having vascular tissues (Nobel, 2009), and convection is due to the movement of sap inside the tissues. Thermal diffusivity and sap velocity, the two main parameters involved in the heat equation change with variations in porosity and stem water content along x, y, and z directions. The change in water content is associated with variation in relative proportions of wood-liquid-air, subsequent complex hydrophysical interactions, anisotropic nature of trees due to the vertical orientation of tracheids and the effect of boundary conditions coming from the surrounding

environment (Figure 2). These two main parameters, sap velocity and thermal diffusivity, vary across space and time (Janbek and Stockie, 2018, 2017; Steppe, 2004).

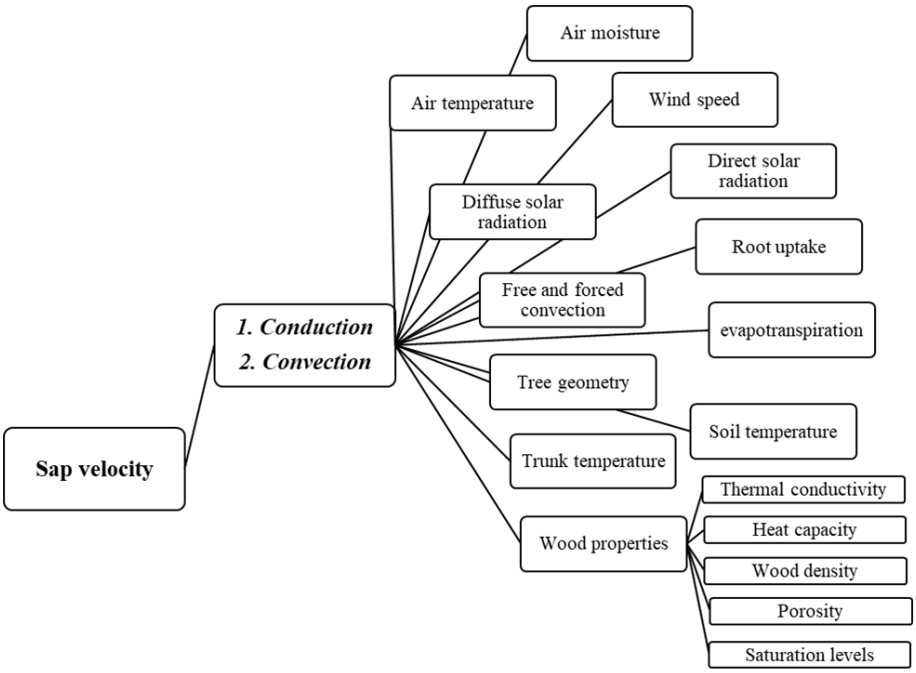

Figure 2. Key factors involved with the mechanics of conduction and convection driving sap velocity in woody plants.

In this study, we developed a multiparameter semi-analytical solution to solve the heat partial differential equation in a cyclic system. We used this solution in trees to estimate heat velocity which is directly proportional to sap flux density. The multiparameter semi-analytical model was implemented to extract the optimal D and V from a predefined range, when the minimum weighted sum of errors occurred between the measured data by TT+ and the simulated results. Here we consider the two main heat transfer mechanisms, conduction and convection, by applying (Marshall, 1958)equation (Marshall, 1958). Unlike Marshall's equation who was developed through assumption of instantaneous heat pulse, in this study, we proposed a new approach in solution of heat transfer equation through using a non-instantaneous heat input. An initial attempt was made by integrating Marshall's equation for a longer time window of > 300 sec and developing a mathematical method for the transient regime (TTD). We realized, however, that it is not easily possible to find an antiderivative to the heat flow equation of Eq. 1, using non-instantaneous heat input seizing at $\int \ln(f)$. This finding compelled the investigation of a semi-analytical solution (Atkinson, 1989; Kurimoto et al., 2007; Potter and Andresen, 2002; Shah, 2020; Swanson, 1983; Swanson and Whitfield, 1981) to integrate the heat flow equation by applying a convolution integral for a longer time window. This solution addressed the non-instantaneous nature of the TTD system.

Materials and Methods

Theory

In this solution it was assumed that the heating duration in the TTD system was divided into heat propagation elements with infinitely small-time steps. These heat elements are equivalent to very short heat pulses (Figure 3). This approach is assumed as a non-instantaneous heat propagation, as it is a combination of many instantaneous heat pulses (Figure 3). In Figure 3 the heat duration from $\tau 1$ to $\tau 2$ is divided to 8 heat propagation elements. The heat duration could be divided to larger number of element (i.e. n elements) with shorter time steps. The higher the number of elements be, for a certain time interval, the resultant outputs from numerical integration of temperature anomalies they create will be more accurate. As such n-number is the step size of the semi analytical analysis, i.e. with a higher-order integration scheme, the output results are thus more accurate.

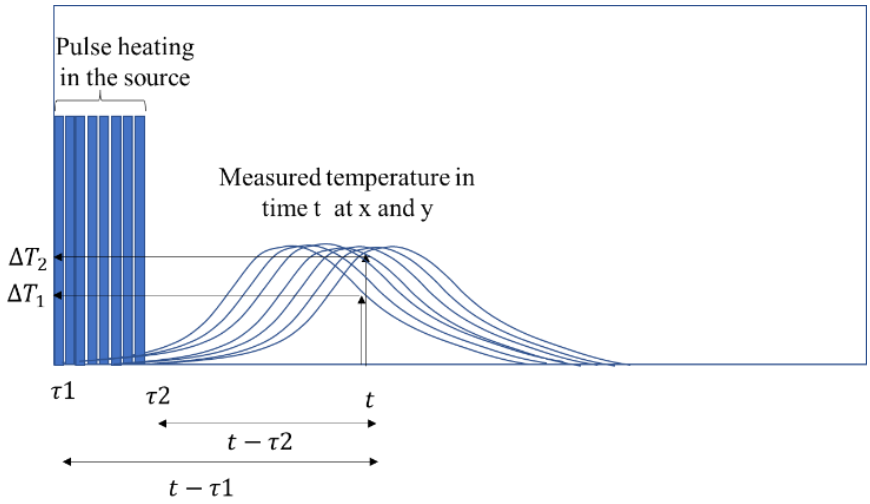

Figure 3. assuming propagation of heat pulses driven by heating

Each heat element or heat pulse results in a temperature rise following Eq. 1.

$$\mathbf{1.} \qquad \Delta \boldsymbol{T} = \boldsymbol{f}(\boldsymbol{D},\boldsymbol{V}) = \int_{\tau}^{t} \frac{\boldsymbol{Q}}{\boldsymbol{4\pi D(t-\tau)}} \boldsymbol{exp}\left(-\frac{\boldsymbol{(x-V(t-\tau))^2+y^2}}{\boldsymbol{4D(t-\tau)}}\right) \boldsymbol{dt}$$

The subsequent temperature rises are the function of thermal diffusivity (D) and heat velocity (V) as ($f(D,V)$). Q with unit of $\frac{K}{m^2}$ defined as the temperature to which the amount of heat liberated per unit length of the line would raise a unit volume of the substance. As the summation of heat pulses provides the total heating implementation curve, the summation of temperature rise curve for each heat pulse provides the total temperature rise curve (Figure 4, solid orange line). Solid orange line in Figure 4 shows the temperature rise curve when the ending time (600 sec) of the heat curve approach infinity. To end the heating curve at time 600 sec, we need to add a cooling pulse started from 600 sec and end to infinity. Adding the heating and cooling impulses will result is a limited heating curve started from 0 and ended to 600 sec time. It represents the heating duration that started from 0 and end to 600 sec. The cooling started when the heating source is off and sum of negative and positive heating pulses will be zero. Cooling phase is represented by the negative

form of the Marshall equation (Eq. 1) and correspondingly the summation curve for the temperature drop result from cooling phase will be obtained from integration of negative form of Eq.1 (Figure 4, solid blue line). Finally, the temperature change curve is obtained by adding the summation heating and summation cooling temperature change curves as follow,

$$2. \qquad \Delta \boldsymbol{T} = \Delta \boldsymbol{T_{Heating}} \left(\int_{\tau 1}^{t} \boldsymbol{f(D,V)}\, \boldsymbol{dt} \right) + \Delta \boldsymbol{T_{Cooling}} \left(- \int_{\tau 2}^{t} \boldsymbol{f(D,V)}\, \boldsymbol{dt} \right)$$

Where ΔT with unit of K is the amount of temperature rise at the distance of $r = \sqrt{(x^2 + y^2)}$ at time t (s) from the line heater after application of heat pulse with the duration time of $\tau 1$ to $\tau 2$. The plot of Eq. 2 is in form of black dashed line in Figure 4. V the heat pulse velocity in unit of $\frac{m}{s}$, and D the thermal diffusivity with unit of $\frac{m^2}{s}$ which is defined by:

$$311. \qquad D = \frac{\lambda}{\rho_s c_s}$$

Where, λ with unit of $\frac{W}{mK}$ is the thermal conductivity, ρ_s in $\frac{kg}{m^3}$ is the sap density which is assumed to be equal to the density of water (1000 $\frac{kg}{m^3}$), and c_s in $\frac{J}{kgK}$ is the sap heat capacity which is also assumed to be equal to water heat capacity (4186 $\frac{J}{kgK} at$ 20 ℃) (Becker and Edwards, 1999).

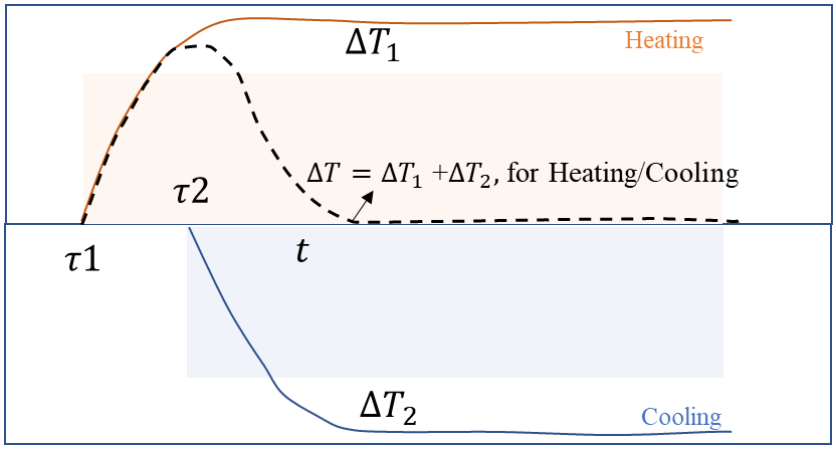

Figure 4. Summation heating (orange curve) and summation cooling curves (Blue curve) and summation curve of the heating and cooling curves (black dashed line), using Eq.1.

Although heat velocity is a direct indicator of sap flux density in the tree, to evaluate the amount of true transpiration rate, a conversion of heat velocity to sap flux density (SFD) must be considered. Therefore, it is recommended to compute SFD $\left(\frac{m^3}{m^2}s\right)$ by Eq. 4.

$$SFD = \frac{\rho_w}{\rho_s}\left(MC + \frac{c_w}{c_s}\right)V \quad (4)$$

Where V $\left(\frac{m}{s}\right)$ is the heat velocity, MC $\left(\frac{Kg}{Kg}\right)$ is the gravimetric stem water content; ρ_w $\left(\frac{kg}{m^3}\right)$, the dry wood density; and c_w $\left(\frac{J}{Kg\ K}\right)$ is the specific heat capacity of dry wood (1200 $\frac{J}{Kg\ K}$ at 20 °C) (Becker and Edwards, 1999).

According to Eq. 4, SFD is a function of V and MC, where both vary temporally and spatially. However, many studies often ignore the variation of stem water content (MC), and measure MC once using the wood core sampling technique. MC is important in accurate estimation of SFD rate and therefore should be monitored continuously by non-destructive methods such as time and frequency domain reflectometry (Constantz and Murphy, 1990; Fares and Polyakov, 2006; He et al., 2021; Nadler and Tyree, 2008; Asgharinia et al., 2022; Zhou et al., 2015). (Swanson, 1983) introduced Eq. 5 to determine MC in situ, for the conditions that the volumetric heat capacity ρc $\left(\frac{J}{m^3\ K}\right)$ of the sapwood is known.

$$MC = \frac{1}{c_s}\left(\frac{\rho c}{\rho_w} - c_w\right) \quad (5)$$

They provided a multiparameter semi analytical solution method to solve Eq. 1 based on the following steps.

1. Finding the optimum integration step sizes.

2. Defining initial values, and constant variables as well as giving a range of predefined values to D and V.

3. Running the model for both positive (heating) and negative (cooling) forms of Eq. 1 considering step sizes and range of D and V.

4. Evaluating simulated ΔT by summation of heating and cooling data.

5. Minimizing the sum of errors between measured (using TT+) and simulated values by applying the theory introduced by (Nelder and Mead, 1965).

To forge an optimization process between multiparametric numerical model and TT+ observations, here we utilized a hydraulic bench with a sawdust filled medium and a specifically tailored firmware allowing high frequency measurements, as described in chapter 2.

Results and Discussion

Integration step size and its influence on analysis quality

The major algorithmic parameter of the numerical model is the integration step size as its influence on numerical model stability, accuracy, and computational cost and time is unavoidable. To increase the stability and accuracy of the numerical model, the integration time step should be decreased to follow the general rule of "smaller integration steps lead to more accuracy" (Atkinson, 1989; Kurimoto et al., 2007; Shah, 2020). On the contrary, however, computation cost and time increase with decrease in integration time step. The phenomenon of deriving optimum step size is known as stiffness and the solution will be achieved when the numerical result straightens out to approach a line with a slope of nearly zero (Hairer and Wanner, 1996). To find the optimum step size of the convolution integral, given some constant values to all parameters in Eq. 1, ΔT is estimated for different integration step sizes from 0.2 – 3 seconds. In Figure 5 for the step sizes smaller than 1 sec the resulted $\Delta \boldsymbol{T}$s converge to a constant value of ~6.518. So, 1 sec should be a reasonable integration step size. However, the ideal step size is closer to ≈ 0.6 sec if more accurate values should be reached. We considered 0.6 sec as an optimum integration step size and assumed it to be constant for the sake of simplicity. For instance, if we are working on 3600 seconds (10 minutes heating /50 minutes cooling-TT+ default) the total number of integration steps is equal to 6000.

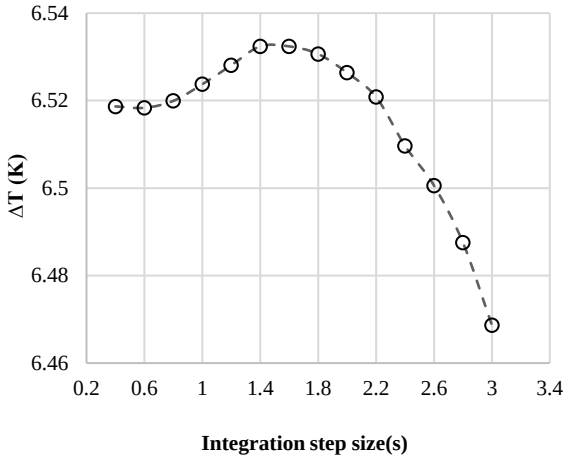

Figure 5. Calculated $\Delta \boldsymbol{T}$ varies with change in integration step size. The optimum integration step size is when $\Delta \boldsymbol{T}$ converges to the constant value, in step sizes of less than 0.6 sec.

The effect of integration step size, on numerical stability of Eq. 1 is shown in Figure 6. Specifically, near the peak of the ΔT time series (Figure 6a), the effect of step sizes are more crucial, however for smaller ΔT values this effect is smaller. as under low flow or small SFD rate there is an associated small variation in ΔT value. As you can see in Figure 6, in all curves all variables and conditions were the same and the only differences between them are their integration step sizes. It can be seen how the resultant ΔT can vary for different step sizes.

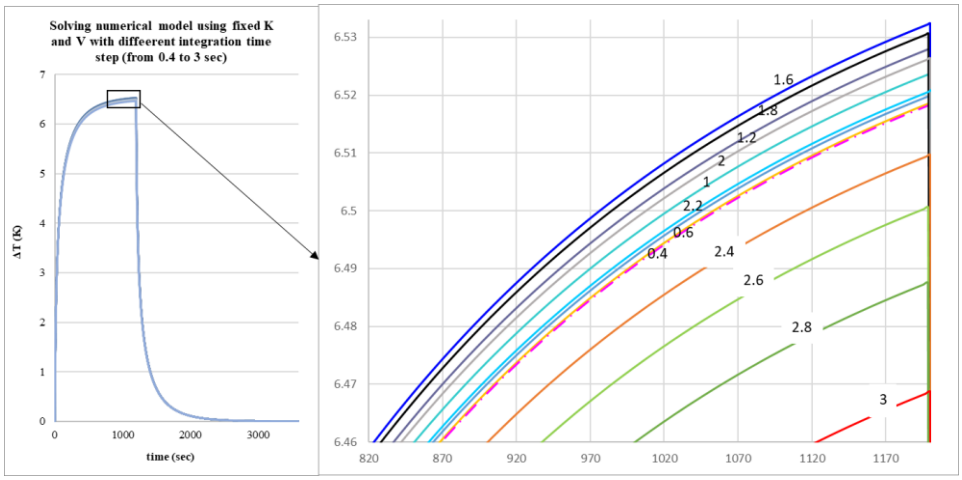

Figure 6. Effect of change in integration step sizes on the stability and accuracy of the simulated ΔT by numerical integration of Eq. 1

Computation over the repeated integrals

Advances in computational power mean that technical analysis tends toward solving their nonlinear differential equations of higher order with numerical approaches, especially when the antiderivative of the equation is difficult to obtain (Tvrdá and Minárová, 2018). These problems often solve through taking multiple integration repeatedly over a definite function as below,

$$6. \qquad \int_{\tau}^{t_0} \int_{\tau}^{t_1} \int_{\tau}^{t_2} \dots \int_{\tau}^{t_i} \boldsymbol{f(D,V)}\ \boldsymbol{dt_i} \dots \boldsymbol{dt_2 dt_1 dt_0}$$

Integrations in Eq.6 has a positive and a negative term which were for heating and cooling phases. Each of the positive or negative integration terms can be calculated by numerical approach (Adeyi et al., 2020). In the numerical approach instead of calculating one integral analytically and continuous over time, it is done by dividing the heat duration to n parts, calculating the resultant change in temperature time series for each part. Then sum up the resultant temperature change time series to each other by considering the lag times between the ΔT time series. Eq. 1 enables the decomposition of a definite integral on the interval $\langle \tau, t \rangle$ over an n-time repeated integral into two phases. Phase 1 is the positive form of Eq. 1 (heating curve) and phase 2 is the negative form

of Eq. 1 (cooling curve) with delay time of 600 sec. This results in two matrices, 1 for the heating curve and the other for the cooling curve with 6000 columns (n-time = 6000) in each matrix, considering step size of 0.6 sec. Each column is set for a time interval of 0.6 sec, so, the delay between each column is also 0.6 sec. The summation of the two matrices provides the heat dissipation curve resulted from the cyclic TTD system.

time	0	1	2	…	n	Sum of elements
t_0	ΔT(t0)	0	0		0	$\sum_{0}^{n} \Delta T_{t0}$
t_1	ΔT(t1)	ΔT(t0)	0		0	$\sum_{0}^{n} \Delta T_{t1}$
t_2	ΔT(t2)	ΔT(t1)	ΔT(t0)		0	...
⋮	⋱	ΔT(t2)	ΔT(t1)		0	...
		⋱	ΔT(t2)		ΔT(t0)	...
			⋱		ΔT(t1)	...
				⋱	ΔT(t2)	...
					⋱	...
t_i	ΔT(ti)	ΔT(ti-1)	ΔT1(ti-2)		ΔT(ti-(n-1))	$\sum_{0}^{n} \Delta T_{ti}$

Figure 7. Matrix of n-times-repeated integrals of temperature changes due to implementation of heat dissipation pulses. Each column shows the resultant changes in temperature for one step of 0.6 sec of heat dissipation. Each row is one time step of 0.6 sec.

Optimization of the numerical simulation results by comparing with TreeTalker measurements

In this step the numerical integration results were optimized by matching the simulated temperature changes with the recorded ΔT time series, by TT+. In principle, the optimum solution is where the simulated ΔT values converge with the recorded values. The multiparametric numerical model runs for all possible combinations of given D and V and ceases when Eq. 7 is satisfied. For instance, as shown in Figure 8, the summation of the total heating curve (Figure 8. solid purple line) with the total cooling curve (Figure 8. solid blue line) which was a result of the heat flow equations described earlier, gives the heat dissipation curve by numerical simulation (Figure 8. solid red line). By selecting some points along the observed ΔT time series (Figure 8. solid black line), we conducted such an optimization. Note that the selected points should be representative of the turning points along the ΔT time series curve since the amplitude of the ΔT curve is principally dependent on thermal diffusivity (D) and its shape depends on the amount of heat velocity (V). Considering $\Delta Tmin$ and $\Delta Tmax$ as the representative observation points, the numerical model was runs as

described above and optimization error was calculated. The optimization error for different values of D and V are visualized in a 3D diagram of Figure 9.

$$7. \qquad \sum_{i}^{n} \left| \frac{\Delta T_{obs} - \Delta T_{sim}}{\Delta T_{obs}} \right| \rightarrow 0$$

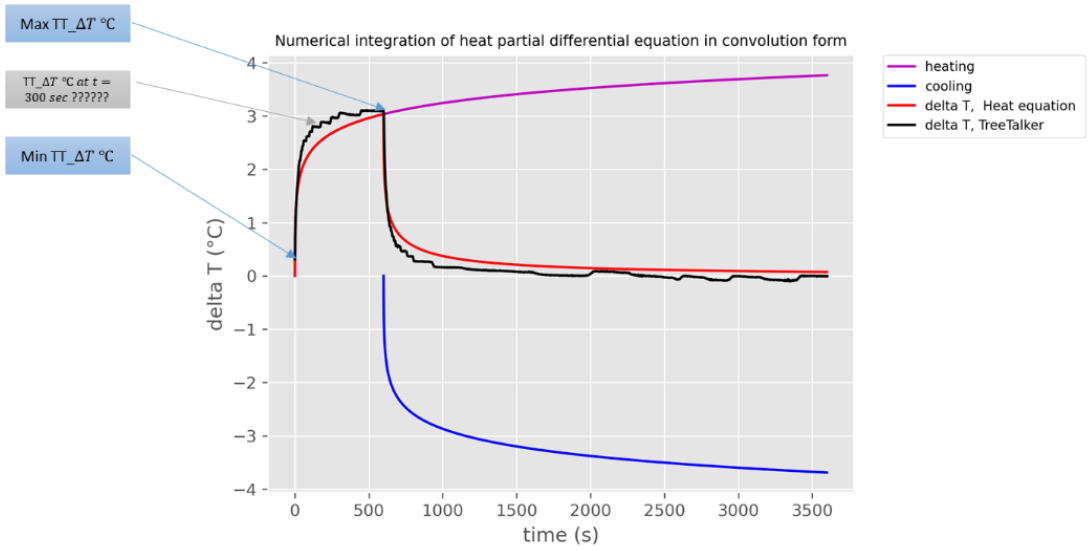

Figure 8. Simulated heating, cooling, and resultant **ΔT** time series curves versus observed **ΔT** time series, recorded by TT+

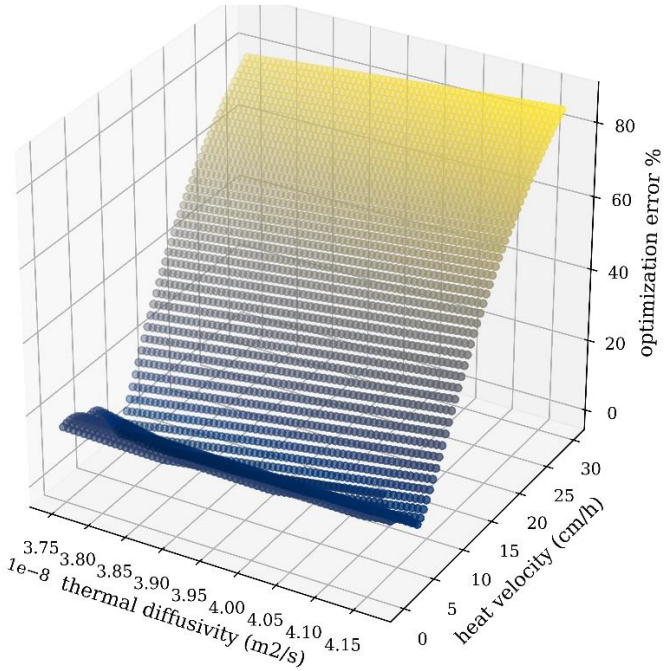

Figure 9. 3D plot of calculated optimization error percentage for the predefined ranges of thermal diffusivity and heat velocity.

Feeding the model with more observation data expectedly leads to more accurate estimations. Besides the tailored firmware of TT+, which allows recording high-frequency data, in situ TT+, by default, records and transmits only $\Delta Tmin$ and $\Delta Tmax$ every hour through applying 10 min heating/50 min cooling cycles. Whereas for forging the optimization process, we suggest recording more data along the heat flow curve, during the heating phase, including $\Delta Tmin$, ΔT at 30 sec, ΔT at 300 sec, and $\Delta Tmax$, as well as in the cooling phase after switching off the current, at ΔTs of 0, 20, and 100 sec (Figure 10).

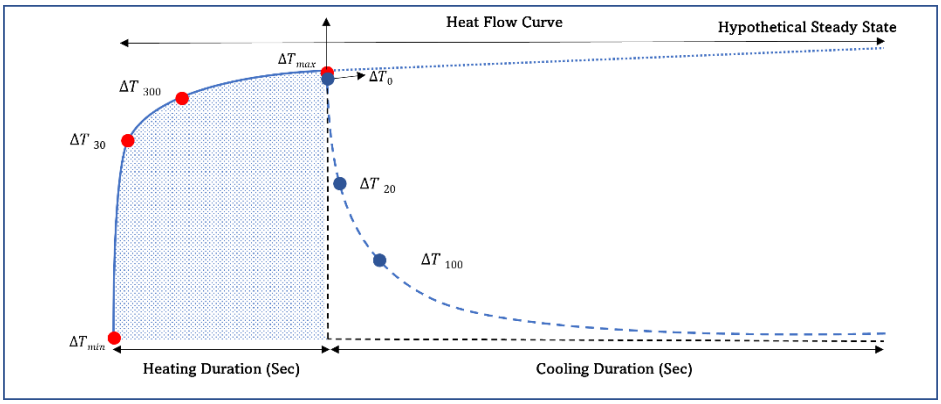

Figure 10. Suggested observation points recorded in situ by TT+ to forge the optimization process.

Results of the multiparametric semi-analytical model for different D and V

Figure 11 demonstrates the results of optimization processes using $\Delta Tmin$ and $\Delta Tmax$ in the heating phase as the observation points. $\Delta Tmin$ and $\Delta Tmax$ were derived from TT+ records, following all steps described in section 2.1. The results show how the simulated heat curves can be match with the observed values by using the multiparametric numerical solution and adjustment of thermal diffusivity and heat velocity values. The adjustment of the parameters was done under three conditions of zero, medium, and fast flow rates. The optimization errors for each condition are listed in Table 1. As shown in Figure 10, the optimization errors are smaller for faster heat velocity and higher thermal diffusivity.

To validate the multiparametric semi-analytical solution the model adjustment performances were shown by four statistic indices of MAE (mean absolute error), R^2 (R_squared coefficient of determination), NSE (Nash-Sutcliffe Efficiency) and KGE (2012) (Kling–Gupta efficiency) (Knoben et al., 2019). The performance indices were calculated for all observed point along the recorded values by TT+ and their corresponding simulated values under different flux rates (Table 1).

Table 1. Validation of numerical model using statistical indices for different flux rates.

Actual SFD (g.m-2.s-1)	***Simulation vs Observation***			
	MAE	*R2*	*NSE*	*KGE*
0	*0.23*	*0.95*	*0.94*	*0.88*
10	*0.34*	*0.90*	*0.87*	*0.84*
48	*0.15*	*0.99*	*0.98*	*0.83*

114	*0.16*	*0.97*	*0.96*	*0.87*
157	*0.07*	*0.98*	*0.98*	*0.95*

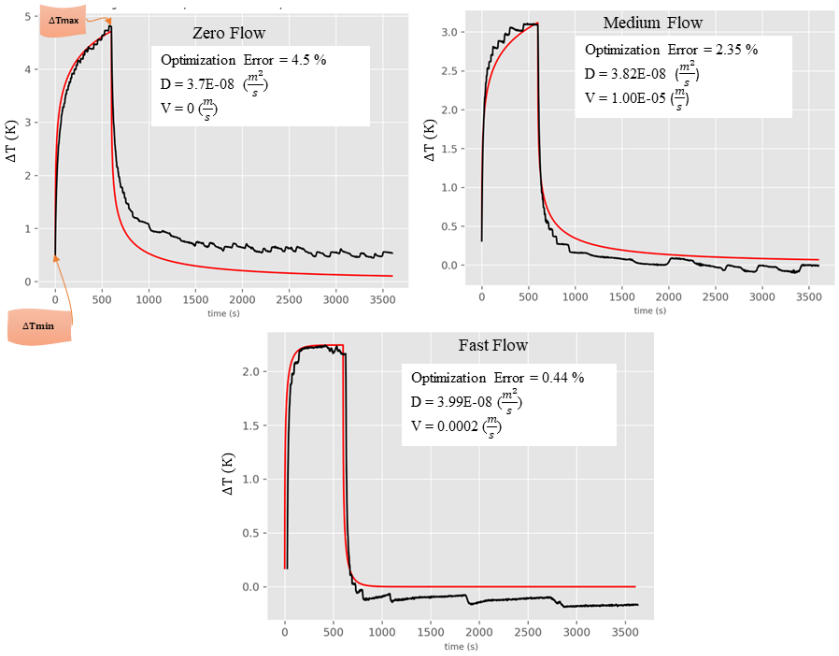

Figure 11. Optimized simulated heat flow curves versus TT+ observations for zero, medium and fast flow rates.

To have a more accurate evaluation and a clearer understanding about the model performance, for both heating and cooling phases, the heat curve was divided into the heating phase (rising limb) and cooling phase (falling limb), respectively. Figure 12 shows a snapshot of the full heat curve (Figure 12a), the plot of simulated versus temperature changes for heating phase (Figure 12b) and cooling phase (Figure 12c). The heating and cooling sections were statistically assessed independently. For example, for the full curve, R^2 is 0.966, where in heating section (Figure 12b) R^2 for the simulated heat curve and the TT+ observations are 0.98 and for the cooling section (Figure 12c) is 0.96. The better model performance in the heating phase was due to use of ΔTmin and ΔTmax derived from the heating phase to forge the optimization process, however, we anticipated a better result by feeding the optimization process with more observation points as discussed in section 3.3. In general, the statistical indices for the full heat curve display a satisfactory to a very good level of performance (Knoben et al., 2019).

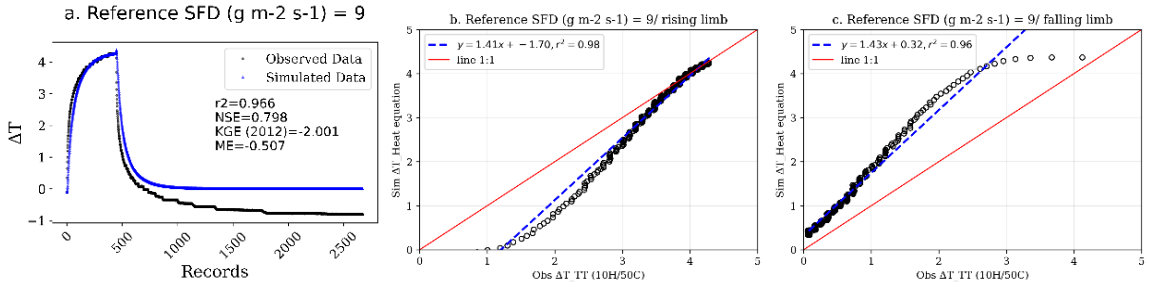

Figure 12. Full heating curve (a) and the simulated versus observed (by TT+) temperature changes for the heating section (b), and cooling section (c).

Using Eq. 3, the computed heat velocity data from the semi-analytical model was converted to sap flux density, assuming constant MC. This was an approach taken to compare the available empirical equations reported by (Do and Rocheteau, 2002a; Mahjoub et al., 2009) with semi-analytical model results, given actual sap flux density measured by a digital balance in the hydraulic bench experiment. The results for different methods are presented in Table 2. Available empirical approaches, mentioned above, as well as empirical calibration of TT+, were discussed comprehensively in chapter 2. Each method has its advantages and drawbacks. For instance, as demonstrated in Mahjoub's results, when $K3 < 0.05$, it is impossible to compute SFD. Also, Do and Rocheteau's equation underestimates the low flux rates and overestimates the high flux rates. For instance, when the actual flux rates were 10 and 48 the rates that calculated by our semi analytical model were 13.7 and 38.7 Respectively. The empirical calibration equation of TT+ has better performance in the estimation of SFD overall. The semi-analytical model can compute SFD rate for any given heat flow data, however, results should improve by increasing the model's accuracy and stability.

Table 2. A comparison between simulated versus empirical approaches for SFD estimation using actual gravimetric SFD

Flow indices		***Actual SFD (g m-2 s-1)***	***Do and Rocheteau, 2002b based on K1***	***Mahjoub et al, 2009 based on K3***	***TT calibration by K1***	***TT calibration by K3***	***semi analytical model***
K_Heating phase(K1)	*K_Cooling phase(K3)*						
0.000	0.020	0	0.0	-	0.0	-	0.0
0.001	0.023	10	0.3	-	0.1	-	13.7
0.570	0.037	48	189	-	75.8	47.4	38.7
0.905	0.051	114	301	12.7	120.5	96	72.3

Numerical integrations are heavy by nature as is the case here and require substantial computing power when running for the optimal n-number of step sizes. Therefore, to facilitate this, an R code was developed and applied, using the DIBAF supercomputer with parallel computation and a customizable number of cores to complete the convolution integral.

Conclusion

This study is devoted to the task of simulation of the heat flow curve using the partial differential equation of conduction and convection through computation of definite integral over repeated integrals. Here our primary idea was to present the concept of bringing a mathematical solution, rather than an empirical solution, to measure transpiration rate. Therefore, the main contribution to this field is offering a multiparametric semi-analytical model for computing thermal diffusivity and heat velocity for a porous medium, in this case, trees. The semi-analytical solution,

although limited by computational cost and time may be improved in terms of accuracy and stability by decreasing the integration step size and increasing the predefined range of D and V. In addition, by considering more observation points to run the optimization process, the model performance was improved. Therefore, future studies should aim to derive more observations from platforms such as the TreeTalker and integrate them into a semi-analytical solution as described in this study. The future preceptive, as such, is to find the optimum range of D and V, optimization points to find microprocessor level solutions for in situ real-time mathematical measurement of D and V.

Article 4: Forest digitalization

TreeTalker Applicability for Individual Mass Monitoring in Alpine Region

Shahla Asgharinia [1*], Jim Yates [1], Damiano Gianelle [2], Luca Belelli Marchesini [2], and Riccardo Valentini [1]

1. Department for Innovation in Biological, Agro-food and Forest Systems (DIBAF), Tuscia University, Via San Camillo de Lellis snc 01100 Viterbo (VT), Italy

2. Research and Innovation Centre, Sustainable Ecosystems and Bioresources Department, Fondazione Edmund Mach, Via E. Mach 1, 38098 San Michele all'Adige, TN, Italy

* Correspondence: asgharinia@unitus.it

In preparation

TreeTalker Applicability for Individual Mass Monitoring in Alpine Region

Abstract

The science of forest digitalization via technological innovation offers an opportunity to develop new methods for mass monitoring forest resources. A key constraint for both has been cost restraints constraining the mobilization and collection of big data to efficiently capture, store, and analyze retrieved data. The Internet of Things and advances in micro processing is steadily changing this. The TreeTalker® is a multisensory IoT-driven platform designed to detect and collect information on individual trees, where its nested sensor approach, captures several key ecophysiological parameters autonomously and in quasi real time at a relatively low cost. In this investigation, TreeTalkers are deployed across two sites (Molveno and Val Canali) totaling 84 TreeTalkers® in the Alpine zone, Northern Italy. The Italian Alps are important ecosystems supporting rich landscapes and biodiversity with their forests maintaining several key ecosystem services. Thus, monitoring these forest ecosystems is of critical importance especially as anthropogenic and more significantly, climate change threatens their said function. We focus on two of the most dominant tree species across Central Europe, *Fagus Sylvatica* and *Picea Abies*, to evaluate the 'TreeTalker' as a novel biosensing platform for mass monitoring. Furthermore, we explore the relationships between site characteristics and abiotic factors using collected TreeTalkers data. Our results suggest that the 'TreeTalker' is a suitable device for tree and forest mass monitoring providing hourly information on ecophysiological factors over 2 consecutive growing seasons. Data gathered from the devices and evaluated via machine learning algorithms demonstrate statistically significant relationships between species, site characteristics, and selected abiotic parameters. Statistical inference suggests that each species maintains specific strategies across the growing season supporting the predominating literature on this species and forest ecosystems.

Although not a complete substitute for field data collection, platforms such as the TreeTalker can enhance established methods for mass monitoring, offering big data solutions on individual trees, and furthering the pursuit of forest digitalization. Yet, as with any new technology challenges remain related to obstacles such as sensor green character, durability, flexible design, maintenance, precision, and accuracy.

***Keywords**: Alpine region, beech, Norway spruce, digitalization, mass monitoring, machine learning algorithms, ecophysiological parameter, climatic data*

Introduction

Forest monitoring is increasingly integrating innovative technologies offering greater insight into the behaviours of trees and forest ecosystems (Henry et al., 2015). Technologies such as UAVs, lidar base stations, and remote sensing using satellite imagery drive frontiers in forest monitoring (Camarretta et al., 2019; Ghazali et al., 2021; Hsu et al., 2020; Senf, 2022; Xue and Su, 2017). Despite these approaches, a single tree in situ ecological monitoring is still limited to relatively expensive sap flow sensors, dendrometers, and leaf surface spectrometers (Matasov et al., 2020) and is usually installed as single sensors rather than a combined sensing platform. Until recently a single device integrating a suite of different ecophysiological sensors in one linked and the integrated system did not exist (Asgharinia et al., 2022). However, as new technologies emerge, costs often reduce, thus facilitating novel approaches and insights to ensuing conundrums. Once such conundrum is the ability to monitor tree and stand behaviour in real or quasi real time across multiple ecophysiological variables. The TreeTalker, a novel IoT based multifunctional biosensing platform aims to contribute to forest monitoring by bridging the gap between spatial-temporal limitations of existing high precision instruments. As the technology is relatively new, an exploration into the opportunities and challenges applied as a mass monitoring network is required. Mass monitoring networks are typically applied to improve system processes and functions delivering optimization based solutions via big data and in situ communication (Torresan et al., 2021). Usually focused on system processes, functions and optimization, their application has been predominantly devoted to commercial spheres such as project management or supply chain optimization (Bzai et al., 2022). This is indeed apparent in applications where the 4th industrial revolution or industry 4.0 has emerged (Valentini et al., 2019). Spurred on by connectivity via protocols such as LoRa and wireless (Mousavi et al., 2022; Singh et al., 2022), mass monitoring networks via the inherent technological advances in sensors, cloud computing, AI and connectivity are achieving cost effective solutions across industrial spheres predominantly (Ang et al., 2022; Bzai et al., 2022). As such, it is somewhat inevitable that this technology or similar would offer applications to environmental sciences. Indeed, the 4th chapter of this thesis will focus on individual tree mass monitoring networks principally, with demonstrations of such technological applications at the forest plot level. The importance of advancing tree and forest monitoring, how individual tees respond to climatic impacts for example, via the detection of ecophysiological response to climatic and site is a key topic among forest ecologists (Illés and Móricz, 2022). As introduced throughout this dissertation, the novel IoT platform, the TreeTalker harnesses the evolution in 'Nature4.0' offering real time insight into tree ecological responses via its nested sensors and LoRa capability (Valentini et al., 2019).

Until now, sensor calibration, numerical solutions, and data processing have been presented in the previous sections and as such will not be detailed here.

The overall objective for this study, a proof of concept for a TreeTalker-based observational network is settled in two high-ecological-value Alpine natural forests in Molveno and Val Canali belonging to the Dolomites UNESCO World Heritage. Selected species for monitoring include Norway spruce and European beech as the dominant species sub categorized as representatives of coniferous and broadleaved trees respectively. In detail, the following sub objectives are pursued **a.)** the demonstration of an innovative in-situ mass forest monitoring network applied to two alpine forests under climatic and site constraints in the Trentino Region in Northern Italy providing a

substantial attempt toward forest digitization **b.)** examining the capability of TreeTalker toward measurement of specifically sap flux density and stem water content for each tree and therefore allowing scaling to stand level for two different species across two different sites **c.)** quality control of TT+ data toward different collected variables **d.)** the exploitation of retrieved TreeTalker, henceforth (TT+), data continuously collected to determine if each species in the network can be characterized by ecophysiological variables and site using machine learning algorithms: Principal Component Analysis (PCA) and Linear Discriminant Analysis (LDA) (Lotte et al., 2018; Saranya et al., 2020; Stewart et al., 2014).

Materials and Methods

Brief Technological description

The TreeTalker® technology was developed by our team, and subsequently already deployed and initial results and applications are discussed by (Asgharinia et al., 2022; Matasov et al., 2020; Tomelleri et al., 2022; Valentini et al., 2019; Zorzi et al., 2021) with the patent process for the device in progress. Each TT+ communicates wirelessly (using a new LoRa low power chipset) to a node, TTCloud, designed as a gateway serving a cluster of individual TT devices of the plot (typically 30 trees per node). The TTCloud contains a modem/router enabling connectivity to a cellular network giving internet capabilities which transmit data to a web server. Pooling of data and interfacing including commands are directly forwarded from the internet to the node which communicates commands to each device at tree level using our own in-house protocol. In fact, firmware for each device, including the node run on protocols and firmware developed by us. In a normal daily rotation cycle, the data are collected every 60 minutes for each TT+ and transmitted to the server database. For the TT+ version 2.0, the battery system supports such operation mode for about 100 days. Raw sensor signals are collected by each TT+ and refer to the string types of “45” and “49” forming the raw data found on the TTCloud and Server (Table 1). TTCloud also reports the site status with string types of “4B” and “4C” (Table 1). Details about data strings (45, 49, 4B, and 4C) and conversions of digital numbers to physical units are reported in TreeTalker’s user manual (TT+manual ver. 2.0) in an open platform of “https://osf.io/7vgbm”.

In General, raw signals of TT devices carry the following key parameters:

1) Radial growth as a physical increment of stem girth
2) Sap flux density, as an indicator of tree transpiration and xylem functionality
3) Stem water content
4) light transmission in 12 spectral bands to infer the quantity and quality of the canopy
5) The tree stability through a gyroscopic sensor (accuracy ± 0.01 degrees)
6) Microclimate parameters (air and relative humidity)

Given the large volumes of TT+ data, in this study, predominantly, Python (Belcastro et al., 2022) is exploited for retrieving data from the server, data analysis and interactive, exploratory computing, basic quality assurance procedures, machine learning algorithms, and data visualization. Moreover, JMP® Statistical Software (Jones and Sall, 2011) is deployed for clustering analysis. Big data processing is followed by the conversions from digital numbers to

physical units, which are conducted according to TreeTalker's user manual (TT+manual ver. 2.0) and the sensor calibrations conducted under controlled laboratory conditions. For further processing, we applied the prior investigations reported in previous chapters in this study as well as published reports about TT technology (Matasov et al., 2020; Tomelleri et al., 2022; Valentini et al., 2019; Zorzi et al., 2021).

On a stand scale, each TT+ is hosted by a TTCloud. While each single device stores the records in the internal memory level, two other storage points occur where the data is transmitted to the TTCloud and then to the web server in quasi-real-time at the following addresses:

1. *P. abies* in Molveno: http://ittn.altervista.org/C19A0073/ttcloud.txt
2. *F. sylvatica* in Molveno: ittn.altervista.org/C1990072/ttcloud.txt
3. *P. abies* in Val Canali: ittn.altervista.org/C1990069/ttcloud.txt
4. *F. sylvatica* in Val Canali: ittn.altervista.org/C1990068/ttcloud.txt

Table 1. Data string sample from cloud no. C1990068 for both cloud (string types 4B and 4C) and TT+ (string types 45 and 49)

24.04.21 03:59:34;C1990068;51238;4B;1619229600;245751;0;222;88;1;14;4044;rel.5.0d
24.04.21 03:59:51;C1990068;51239;4C;1619229600;1;0;-59;-78;-78;-72;-77;-62;-68;-66;-83;-80;-82;-62;-79;-64;-74
24.04.21 04:10:15;21990659;5123C;45;1619028000;50;51;48131;41775;17;92;11;-3958;0;5;0;-730;0;50;49;8610
24.04.21 04:10:33;21990659;5123D;49;1619028000;179;241;201;174;205;186;671;697;358;304;288;350;50;3

Site Description

General site descriptions for Molveno and Val Canali are presented in table and figure These forest ecosystems are predominantly mixed forests characterized by *Fagus sylvatica* L. (European beech), *and Picea abies* L. (Norway spruce) with some Abies Alba (Silver Fir) on which our monitoring will be focused the former two species spruce and beech. Based on the closest meteo stations data, annual precipitation varies across sites where Val Canali typically receives 327.8 mm more rainfall than Molveno and the average annual temperature of Val Canali is 1.8 °C less than Molveno (Table 2 and Figure 1).

For each experimental site, Molveno and Val Canali, we established two rectangular plots of 10,000 m^2 (1ha) for each site avoiding locations close to roads, buildings (at least 1000 m) and steep slopes. Within the plots, a randomly distributed set of 20 to 21 mature trees (diameter at breast height (DBH) ≈> 30 cm) across 4 plots were equipped with a TreeTalker having a unique identifier code (Table 3 and Figure 2). In total we installed 82 TreeTalkers version TT+2.0 and 2 TTRadiation (TTR) for both species and sites (Table 3 and Figure 2).

Table 2. General information about 2 selected sites in Alpine Forest, Molveno and Val Canali

Location	Species	Zone	UTMx	UTMy	Elev (m)	ave DBH (cm)	ave precipitation (mm)	ave Tair (°C)	Cloud No.
Molveno	F. sylvatica	32	649115.51	5114073.81	1420	56	2076	9.7	C1990072
	P. abies	32	649108.44	5114624.49	1410	59			C19A0073
Val Canali	F. sylvatica	32	720350.66	5123463.17	1590	37	2404	7.9	C1990068
	P. abies	32	720496.24	5123605.97	1560	51			C1990069

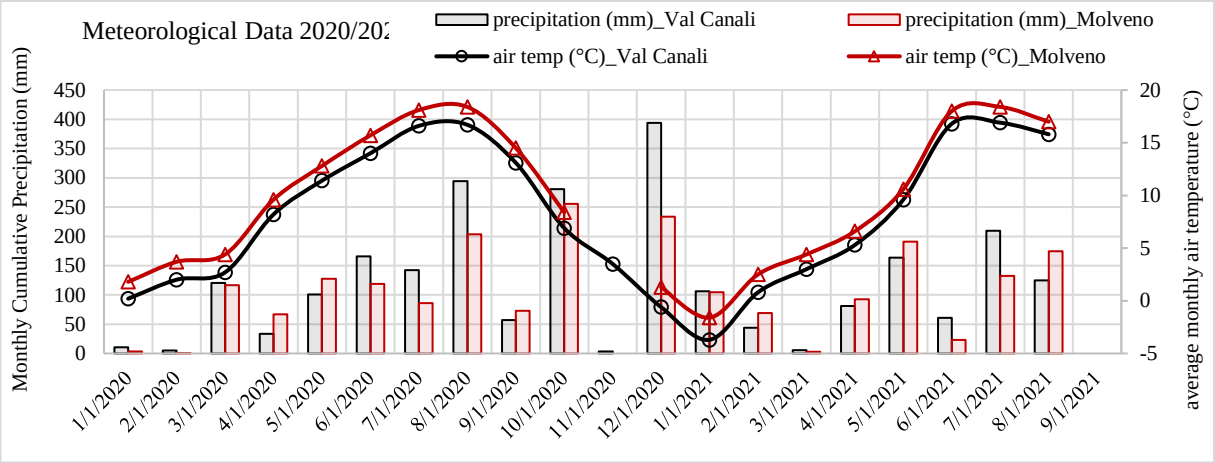

Figure 1. Meteorological data, average monthly air temperature, and monthly cumulative rainfall for both sites, Molveno and Val Canali

Table 3. List of TreeTalkers for each site including diameter at breast height at installation day

IoT Devices	Molveno						Val Canali					
	P. Abies	*DBH (cm)*	*installation date*	*F. sylvatica*	*DBH (cm)*	*installation date*	*P. Abies*	*DBH (cm)*	*installation date*	*F. sylvatica*	*DBH (cm)*	*installation date*
Cloud ID	C19A0073			C1990072			C1990069	25,0	6/30/2020	C1990068	25,0	7/1/2020
TT1	21990733		5/31/2021	21990709	45,0	8/10/2020	21990684	54,5	6/30/2020	21990659	24,0	7/1/2020
TT2	21990734	49,5	8/6/2020	21990710	52,0	8/10/2020	21990685	52,0	6/30/2020	21990660	32,0	7/1/2020
TT3	21990735	36,5	8/6/2020	21990711	57,0	8/10/2020	21990686	30,0	6/30/2020	21990661	54,5	7/1/2020
TT4	21990736	61,5	8/6/2020	21990712	57,0	8/10/2020	21990687	54,0	6/30/2020	21990662	40,0	7/1/2020
TT5	21990737	44,5	8/6/2020	21990713	52,5	8/10/2020	21990688	49,0	6/30/2020	21990663	49,5	7/1/2020
TT6	21990738	53,5	8/6/2020	21990714	45,5	8/10/2020	21990689	65,0	6/30/2020	21990664	43,5	7/1/2020
TT7	21990739	50,0	8/6/2020	21990715	62,5	8/10/2020	21990690	61,0	6/30/2020	21990665	33,5	7/1/2020
TT8	21990740	71,5	8/6/2020	21990716	44,0	8/10/2020	21990691	46,0	6/30/2020	21990666	30,0	7/1/2020
TT9	21990741	53,5	8/6/2020	21990717	56,5	8/10/2020	21990692	54,5	6/30/2020	21990667	49,5	7/1/2020
TT10	21990742	65,0	8/6/2020	21990718	49,5	8/10/2020	21990693	24,5	6/30/2020	21990668	38,0	7/1/2020
TT11	21990743	65,5	8/6/2020	21990719	47,0	8/10/2020	21990694	50,0	6/30/2020	21990669	38,0	7/1/2020
TT12	21990744	54,5	8/6/2020	21990720	75,0	8/10/2020	21990695	55,5	6/30/2020	21990670	27,0	7/1/2020
TT13	21990745	62,5	8/6/2020	21990721	61,0	8/10/2020	21990696	63,5	6/30/2020	21990671	31,5	7/1/2020
TT14	21990746	61,0	8/6/2020	21990722	53,0	8/10/2020	21990697	55,0	6/30/2020	21990672	36,5	7/1/2020
TT15	21990747	68,0	8/6/2020	21990723	54,0	8/10/2020	21990698	54,5	6/30/2020	21990673	24,5	7/1/2020
TT16	21990748	80,5	8/6/2020	21990724	65,5	8/10/2020	21990699	63,0	6/30/2020	21990674	33,0	7/1/2020
TT17	21990749	74,0	8/6/2020	21990725	68,0	8/10/2020	21990700	53,5	6/30/2020	21990675	66,5	7/1/2020
TT18	21990750	62,0	8/6/2020	21990726	48,5	8/10/2020	21990701	53,0	6/30/2020	21990676	22,0	7/1/2020
TT19	21990751	63,5	8/6/2020	21990727	67,5	8/10/2020	21990702	59,0	6/30/2020	21990677	33,0	7/1/2020
TT20	21990752	49,5	8/6/2020	21990728	64,0	8/10/2020	21990703	38,0	6/30/2020	21990678	36,5	7/1/2020
TT21	21990753	54,0	8/6/2020	21990729		5/31/2021						
TTR	55210006		6/30/2021							55200001	30,0	7/1/2020

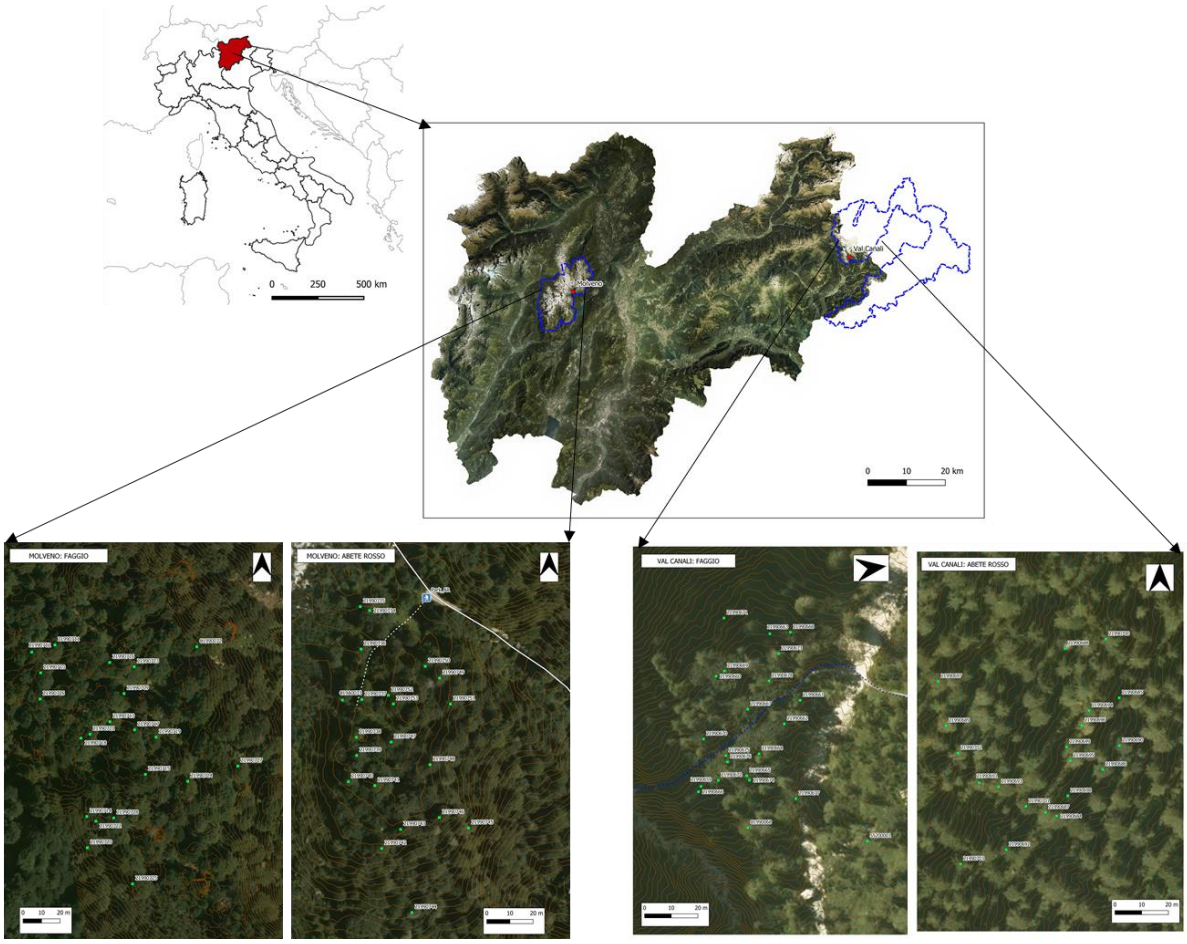

Figure 2. Map of the study area, Molveno and Val Canali in Trentino region, showing the location of the mounted TreeTalkers on beech and spruce trees.

The Molveno and Val Canali forest ecosystems include the fertile Beech forests of the soils with neutral reaction (or almost), with sweet humus of the mull type, pure or mixed with conifers (especially in the higher mountain range). They are distributed in Central and Atlantic Europe and are characterized by a species-rich herbaceous layer. The dominant tree species include *Abies alba*, *Fagus sylvatica, Picea abies.* The species selected for this study are Fagus Sylvatica and Picea abies with each species and site coded as *P. abies* in Molveno: PA-M, *P. abies* in Val Canali: PA-V, *F. sylvatica* in Molveno: FS-M and *F. Sylvatica* in Val Canali: FS-V, naturally (Figure 3).

Figure 3. Sample of TreeTalker (TT+) installation on beech and spruce trees

All sites chosen for the TT+ installations demonstrate different site characteristics including changes in soil types, annual rainfall and temperature. The soil types broadly vary between Phaeozems, Leptosols and Cambisols for both sites (Costantini et al., 2014). Average rainfall can vary between 1000 mm to as high as 1750 mm with localized higher rainfall according to geomorphological features (Pasqualetto et al., 2019). The actual annual average temperature for both sites ranges between 2.5 to 10 °C, with local maxima and minima varying seasonally (Antonacci and Todeschini, 2013).

Site 1. P. abies in Molveno: PA-M

The site is located in the Val delle Seghe, not far from the village of Molveno, near the Croz Dell' Altissimo Refuge at an altitude of about 1410 meters. The established plots are located on a gently sloping hill facing south in an area with a prevalent presence of spruce. The TreeTalkers sensors were installed on mature spruce plants, whose average diameter is 59 cm.

TT+ devices from serial numbers 21990733 to 21990753 and one TTRadiation: 55210006, Cloud Id: C19A0073 are installed in this area.

Site 2. F. Sylvatica- Molveno: FS-M

The site is located in Val delle Seghe, not far from the village of Molveno, in an area of large columnar beeches called "Busa del formai", at about 1420 meters of altitude. The study area is located on an almost flat terrace on a slope with North-East exposure, in an area with almost exclusive presence of beech: The TreeTalkers sensors were installed on beech trees whose average diameter is 56 cm. TT+ from 21990709 to 21990729 and, Cloud Id: C1990072

Site 3. P. abies-Val Canali: PA-V

The site is located in Val Canali in Primiero, at an altitude of 1560 meters on an east-facing slope. The study area is in the mid-slope, in an area with a slope of about 20°, where spruce is almost exclusively present: TreeTalkers sensors were installed on mature or overripe spruce plants, whose average diameter is 51 cm. TT+ from 21990684 to 21990703 and, Cloud Id: C1990069

Site 4. F. sylvatica-Val Canali: FS-V

The site is located in Val Canali in Primiero, at an altitude of 1590 meters on a slope facing east. The study area is located in a strip of beech forest between two gullies in the middle slope, in an area with a slope of about 20°, where the beech is present in a mixed forest with Spruce and larch: the TreeTalkers sensors were installed on beech plants of different ages, including some very old ones. The average diameter of the plants is 36 cm. TT+ from 21990659 to 21990678 and one TTRadiation: 55200001, Cloud Id: C1990068

Results and Discussions

We have created a unique digital infrastructure and quasi real time mass monitoring system for two Alpine mixed-species forest ecosystems. By monitoring 82 individuals in two locations, Molveno and Val Canali, with two different species, Norway spruce (*P. abies*) and beech (*F. sylvatica*), we established a big data series to study tree functionality based on ecophysiological parameters collected by TreeTalker® in the Dolomites Park UNESCO heritage site. The results here within highlight both the functional capacity of the TreeTalker to produce high fidelity ecophysiological mass monitoring and reveal some preliminary stand responses for species across all forest sites. As the focus of this study is not to provide an in-depth synthesis of forest ecosystem behavior, a focused look at each variable is demonstrated. Some of the more striking features of data gathered are discussed in the discussion section.

Size distribution

Both sites follow different DBH size distributions according to manual measurements using DBH Tapes, however as stated previously, stems are generally greater than 30 cm indicating that these forests are in secondary successional stage (Buchholz and Pickering, 1978; Reyer et al., 2020). As displayed in Figure 4, DBH differs by species and by site. This observation is possibly a function of the associated climatic characteristics of each sites including soil type, elevation, climatic data, slope etc. Indeed, the Molveno and Val Canali sites have elevation differences that cause climatic gradients. The Molveno forest at 1410-1420 MASL elevation experience 1.7 °C more warming than the Val Canali site at 1560-1590 MASL elevation and furthermore, the warmer site shows 328 mm of annual precipitation less than the high elevation site. This difference impacts growing periods and as such tree ecological functionality (Bréda et al., 2006; Gazol et al., 2018; Iii et al., 1993). In high elevation sites, the growing season starts in May and ends in October, while in Molveno it starts earlier in mid-April. However, this is more tangible in beech forests rather than spruce since spruce is slightly physiologically active during the dormant period (HEIDE, 1974). There are many factors dictating mean diameter and as such it is difficult to assert one singular or a suit of attributes that describe diameter distribution without prior information which was not pursed in great detail given the focus of the research.

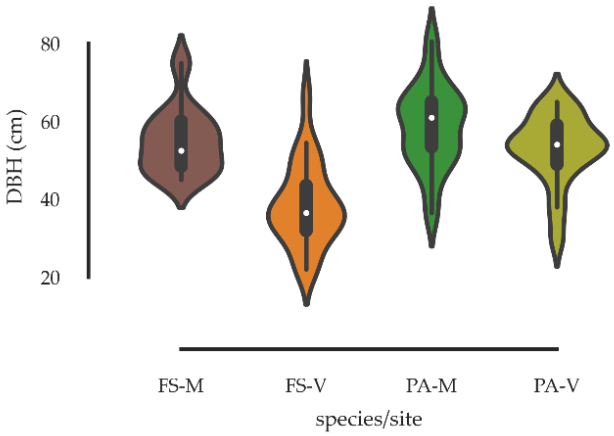

Figure 4. Size distribution for beech and spruce in Molveno and Val Canali

Outlier Identification

The detection of outliers as exogenous phenomena is intuitive given prior knowledge on the TreeTalker and its sensors. Two strategies were adopted to detect outliers within the big data sets for each variable and TreeTalker. The first approach considers sensor failure and the second consider abrupt fluctuations without explanation. Each sensor has an operational range measured and validated via extensive lab calibration and testing. Therefore, outliers outside of these ranges may be excluded. Moreover, abrupt changes that are not explained by climate, occur on a short time scale are considered outliers, too. Therefore, conducting any post hoc analysis requires outliers' detection for all sensor raw signals recorded by the TreeTalker. The size of the data collected as such requires Python prepossessing applications which were pursued here.

To detect outliers, different statistical tests may be performed, from the interquartile rule (IQR) to the standard deviation rule (Jones, 2019). Figure 5 is an example of outlier detection for transient signals (dT) based on IQR method in the two sites considering all TreeTalkers in the beech and spruce forests. While in Figure 6 with dT for beech in Val Canali site, those observations which lie outside of two standard deviations of the mean are highlighted as outliers.

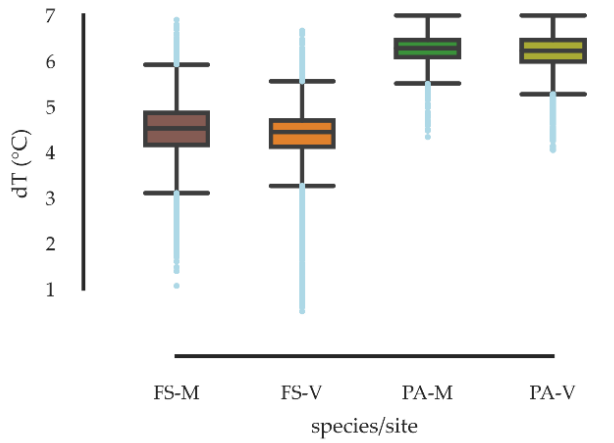

Figure 5. Distribution of transient signal data in 2 growing seasons in beech and spruce at population scale

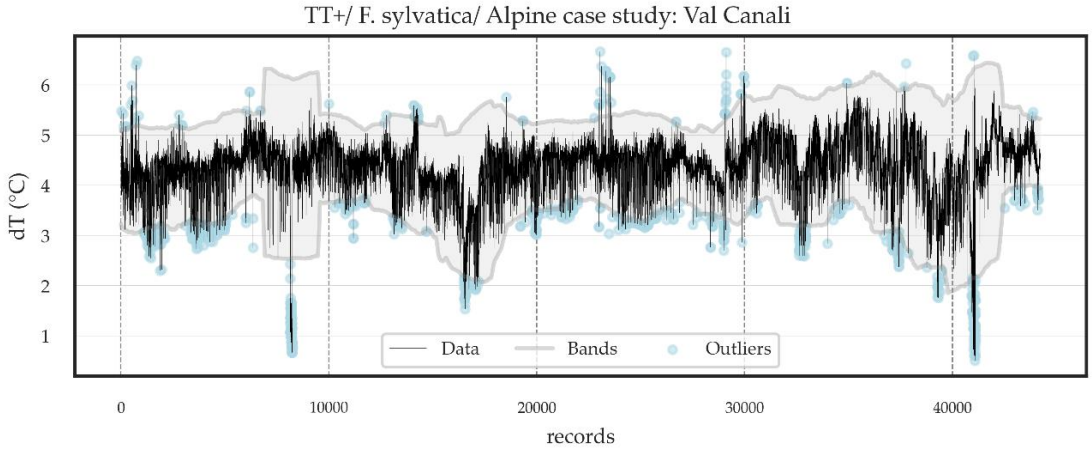

Figure 6. standard deviation rule for detecting outliers in dT data for beech in Val Canali

Data summary

Considering the outlier detection process and irrespective of ancillary data limitations, the analysis here within was carried out based on collected data by TreeTalkers nonetheless and significant. Also, I note that there are more interval-wise missing data in Molveno compared to Val Canali site, which may affect all type of presented analysis in this study.

To summarize key parameters, here we start with a statistical descriptive table (Table 4) on transient signal, sap flux density, stem capacitance sensor frequency, relative saturation index, stem temperature and air temperature for both sites and both species. Descriptive statistics for each variable are displayed in Table 4.

Sap flux density (SFD)

The data used for evaluating sap flux density was the transient signal (dT) measured by the TreeTalker sap flow probes based on transient regime with 10 minutes heating and 50 minutes cooling (Do and Rocheteau, 2002a). Therefore, in the descriptive table above we start with the values for transient signal. Transient signals in the spruce plots were in average 2 degrees greater than those in the Beech sites. A higher transient signal is associated with a lower facilitation of sap flux (see chapter 2 in this study). Utilizing dT and applying equation in Chapter 2: Table 2 sap flux densities are realized across individuals and summarized for stands (Table 4). Considering species, the results from individuals in the beech sites from both experiments show an average of approximately 50% more SFD than the Spruce forests for both sites. While considering location, the beech and spruce forests in Val Canali demonstrate slight mean differences in sap flux density, however the average of max daily SFD in Val Canali are 12% and 21% higher than the Molveno sites when comparing species. These results may be driven by the species specific ecophysiological responses to abiotic parameters. The latter result may correspond to water availability, which is the strongest climatic driver for hydrological functionality driver among the climatic conditions (Toledo et al., 2011). As observed the Val Canali site has higher annual precipitation than the other sites. The assumption that this phenomenon is driven solely by water availability is however inconclusive given tree size distribution and forest successional phase. Figure 7 displays annual and seasonal trends of SFD for both sites and species.

Table 4. descriptive statistical data on key ecophysiological parameters based on all TT records for both beech and spruce in Molveno and Val Canali

Molveno	FS-M: *F. sylvatica*_Molveno (since Jul 2020)								PA-M: *P. abies*_Molveno (since Jul 2020)							
Ave of all TT	dT (°C)	SFD (l dm-2 h-1)	ECF (Hz)	rel sat index %	Tstem (°C)	Growth (mm)	Tair (°C)	VPD (Kpa)	dT (°C)	SFD (l dm-2 h-1)	ECF (Hz)	rel sat index %	Tstem (°C)	Growth (mm)	Tair (°C)	VPD (Kpa)
mean	4.6	0.5	8614	77	11	10.2	10	0.7	6.3	0.3	12427	81	9	7.6	9	0.5
std	0.4	0.5	1128	14	4	4.2	5	0.3	0.4	0.2	930	11	5	2.6	5	0.3
min	2.5	0.0	6470	50	-1	7.2	-5	0.0	4.6	0.0	10234	66	-2	5.2	-5	0.0
Q1	4.4	0.2	7887	67	8	7.7	7	0.4	6.0	0.1	11776	77	5	6	5	0.2
Q2	4.6	0.4	8500	79	11	9.3	10	0.7	6.3	0.2	12336	83	9	7.1	9	0.4
Q3	4.8	0.7	9223	87	14	10.4	13	0.9	6.5	0.4	13021	88	13	7.9	13	0.6
max	6.2	3.4	12565	99	20	23.9	23	2.0	7.0	1.8	14571	100	19	17.2	23	1.7
Val Canali	FS-V: *F. sylvatica*_Val Canali (since Oct 2020)								PA-V: *P. abies*_Val Canali (since Oct 2020)							
Ave of all TT	dT (°C)	SFD (l dm-2 h-1)	ECF (Hz)	rel sat index %	Tstem (°C)	Growth (mm)	Tair (°C)	VPD (Kpa)	dT (°C)	SFD (l dm-2 h-1)	ECF (Hz)	rel sat index %	Tstem (°C)	Growth (mm)	Tair (°C)	VPD (Kpa)
mean	4.3	0.6	7480	88	13	8.6	12	0.6	6.3	0.3	10993	67	12	14.2	11	0.5
std	0.6	0.6	1287	9	5	1.9	5	0.3	0.3	0.3	979	13	4	13.3	5	0.3
min	1.3	0.0	6196	63	0	5.5	-2	0.0	4.4	0.0	8487	52	1	0.33	-1	0.0
Q1	4.1	0.2	7254	84	9	6.7	8	0.4	6.1	0.1	10377	68	8	5.1	8	0.3
Q2	4.4	0.4	7697	90	13	8.7	12	0.6	6.3	0.2	10998	77	12	9.1	11	0.5
Q3	4.7	0.8	8249	94	16	10.1	15	0.8	6.5	0.4	11595	85	15	17.3	15	0.7
max	6.2	3.9	11603	100	21	12.9	23	1.7	7.0	2.3	13332	99	21	48.2	25	1.7

The significance of the results achieved above will be discussed individually in the following sections.

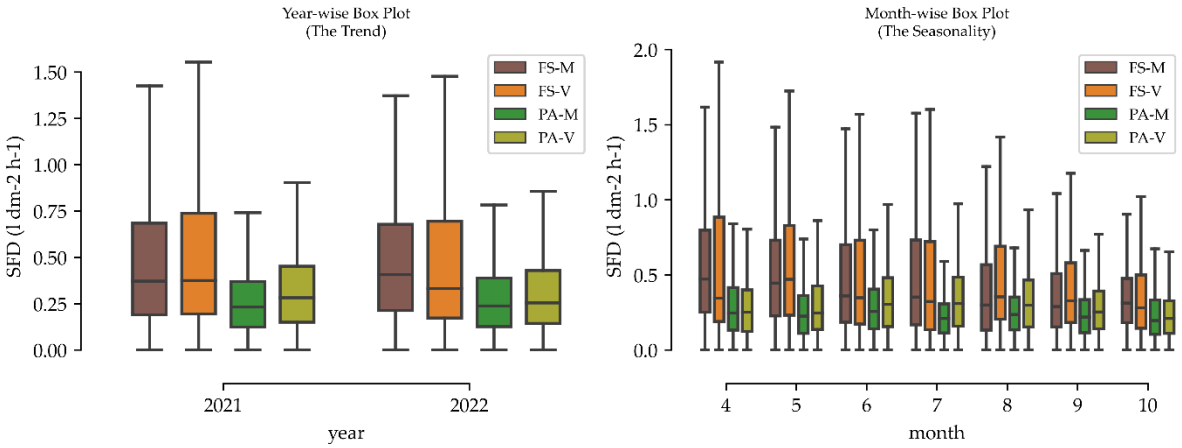

Figure 7. Annual and seasonal trend of sap flux density (SFD) for both population of beech and spruce in Molveno and Val Canali

In general, comparing sap flux density without considering the sapwood area may cause a significant error therefore it becomes prudent to compare the amount of sap flow. Sapwood area (SA) as a scaling factor for transpiration varies highly across species and forest ecosystems and it is difficult to measure incurring high costs given the destructive nature of sampling (Güney, 2018; Magh et al., 2019; Mitra et al., 2020). Having DBH data, an attempt to find sapwood area functions was made, however as reported by (Matyssek et al., 2009), the high variability of available functions

rendered them difficult to apply. The literature supports a general trend toward higher rates of sap flow for beech compared to spruce (Pretzsch et al., 2014a). As we lack sap wood area information we cannot convert our sap flux data to sap flow, however it is reasonable to assume that given the observed difference in SFD for both species from the long term data set as displayed in Figure 7, that this general trend is confirmed for this study. However, future investigations should focus on integrating SFD with sapwood area derived a site level. In the boxplots we demonstrate results for two seasons and the averages of both seasons at monthly resolution thus giving a snapshot at an annual timescale (Figure 7). Again, the results demonstrate a strong seasonality with beech showing considerably higher SFD compared with spruce. However, to provide insight into each species sap flux density rates specifically across the season a deeper analysis of the diurnal patterns of SFD versus air temperature is demonstrated in Figures 8. The first graph displays the mean stand sap flux oscillation for beech and spruce at the Val Canali site with mean values for the air temperatures below canopy. The second graph is a weekly resolution taken from the first graph and provides a clearer picture of the differences between each species sap flux. Interestingly, spruce maintains a steady SFD throughout the year irrespective of change in temperature, with small signals observed shortly after temperature drops. Beech on the other displays a stronger relationship with temperature where a general stand response is observed to increasing temperature. This result suggests that beech are opportunistic, maintaining high hydrological functionality during the growing season and such a result is in line with reported studies (Bužková and Pokorný, 2013; Gartner et al., 2003).

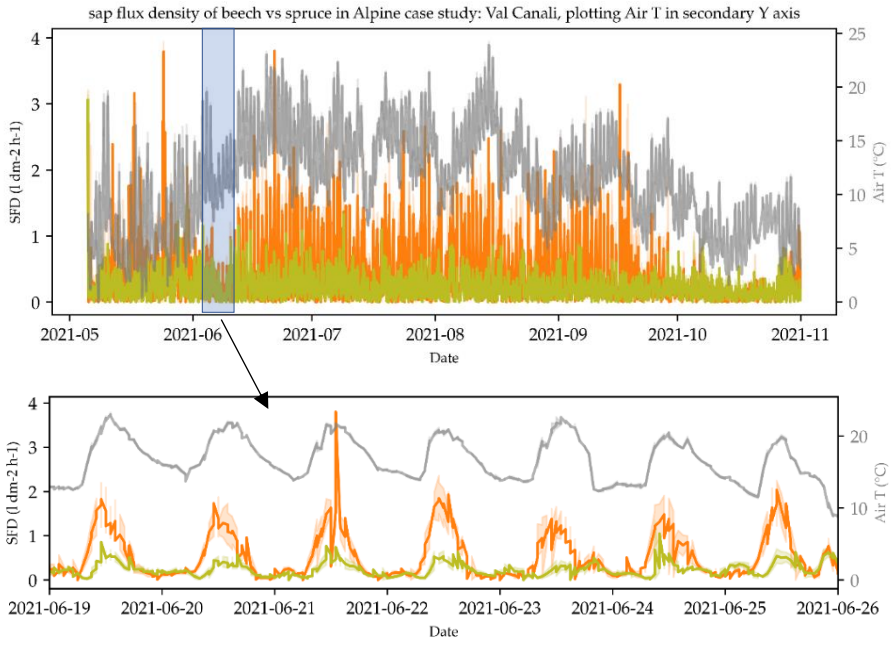

Figure 8. Sap flux density comparison between beech (orange solid line) and spruce (light green solid line) respect to air temperature (grey solid line) for one growing season, 2021 in Val Canali site

Focusing on the differences observed in SFD, the distinguishing features of spruce and beech, there isohydric and anisohydric characteristics (Rötzer et al., 2017) possibly explain a significant part of the data accuracy. Spruce is highly productive given its evergreen nature and maintains an opportunistic yet conservative use of available soil water (Pretzsch et al., 2014b). Whereas beech

demonstrates lower water use efficiency, continuing leaf gas exchange throughout periods of low soil water availability (Pretzsch et al., 2014a). In addition, the stomata closure behavior of spruce to water scarcity is another possible contributing factor to observed sensor signals of SFD with studies suggesting significant differences in seasonal evapotranspiration based on this behavior alone (Schume et al., 2004). Therefore, the lower average SFD results of the spruce stands compared with the beech stands confirm the general strategies of beech and spruce towards soil water availability. Furthermore, the waning of observed SFD is also in line with the phenological characteristics of each species where beech loses its leaves in the fall thus reducing hydrological functionality.

Stem water content

The TreeTalker, with its capacitance sensor, records frequency data (ECf (Hz) as an indicator of stem water content. Recalling the fact that ECf data has an inverse relationship with stem water content. As discussed compressively in chapter 1, conversion of ECf data to physical stem water content requires species and site specific calibrations. Therefore, we prefer to analyze raw signal output (Figure 9). Considering temperature impact on the raw signal we also use stem temperature data for further analysis. Average stem temperature annually and seasonally across both species and sites is approximately the same +/- 2 °C (Table 4 and Figure 9). Consequently, we may ignore Tstem influence on the signal for species-site ECf ranges. However, ECf varies exceptionally considering species alone with a somewhat marked difference between sites (Figure 9). The difference between ECf across species reports approximately 30% lower ECf values for beech forests which corresponds to 30 % more available stem water content. We can conclude that beech trees have more free water than bound water as a result. However, the influence of site characteristics and climate variables should not be undermined. For example, Val Canali, having more rainfall has slightly lower ECf ranges in both species in comparison to Molveno. Max ECf occurs in the first 15 days of October, Min ECf occurs in the first 15 days of July for individuals in both sites. In general, maximum stem water content (minimum ECf records) occurs in the first 15 days of October when the growing season is completed whereas the driest stem water condition is reported in the first 15 days of July corresponding to the highest physiological activity of the plant. This topic is comprehensively discussed in chapter 1.

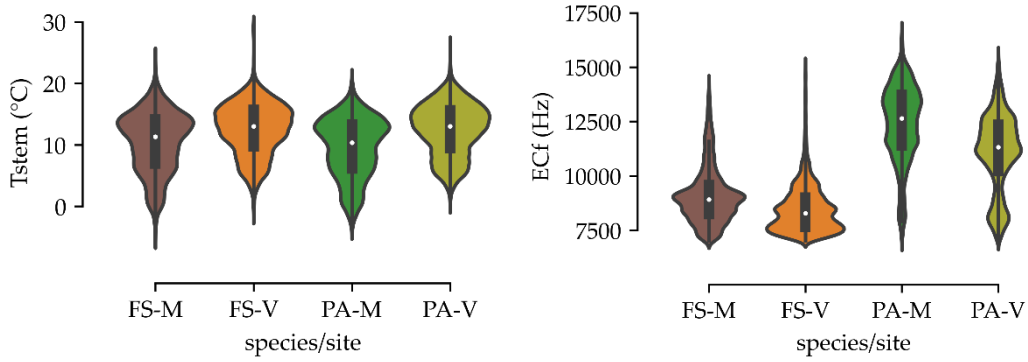

Figure 9. Distribution of stem temperature and ECf for beech and spruce in Molveno and Val Canali

Radial growth

Figures 10 is radial growth data captured from the TreeTalker automatic infrared dendrometer for an individual beech tree where Figure 11 is the mean growth for each individual tree across a 2-year period. The data gathered from these sensors underwent a process of outlier detection with the weekly median chosen as the best representation of observed trends. As demonstrated in Figure , beech growth shows strong seasonality in response to photosynthetic activity and canopy leaf out (Skomarkova et al., 2006). This trend is observed over consecutive years, 2021 and 2022. By applying a simple mathematical function where delta radial growth for each season was calculated as the summed sub section delta for each tree and averaged to give species specific and site radial growth. For example, at the Molveno site, the typical or median growth for Beech is between 3-4 mm per year and 8.7 mm per two and a half years period. This result is similar to the radial increments reported across Europe for European Beech (Pretzsch et al., 2021). The mass monitoring of stem growth is a novel entry in forest monitoring offering possible significant cost reductions when compared to traditional forest sampling.

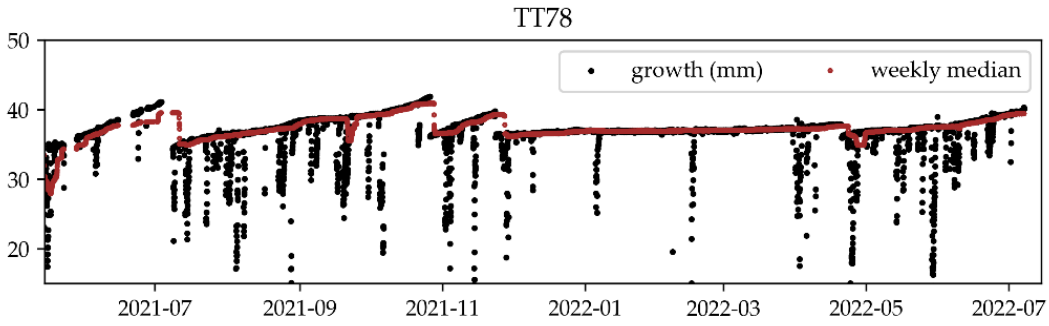

Figure 10. Individual growth trend for 2 growing seasons captured by TT+ sharp sensor for beech in Val Canali

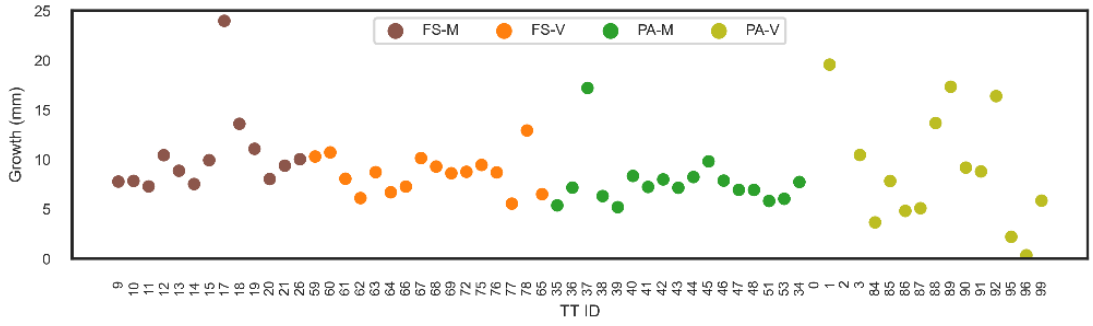

Figure 11. Total growth rate for each individual captured by TT+ for both beech and spruce in Molveno and Val Canali

Light transmitted radiance below the canopy

Utilizing the TreeTalker spectrometer, we have captured transmitted radiant light below the canopy across 12 bands, 6 in the Visible light (450, 500, 550, 570, 600, and 650 (±40 nm)) and 6 in the NIR range (610, 680, 730, 760, 810, 860 (±20 nm)). Figures 12 and 13 demonstrate two selected sample averages from the TreeTalkers onboard spectrometers for both species at each site. Preliminary analysis involved two steps. Firstly, for individual trees and each band, the exclusion

of data lying outside of the digital number ranges 0-65,000 was applied as this is considered sensor failure. Secondly, to avoid the direct exposure of the sensor to sunlight, often causing light saturation, we chose data for each site when the solar zenith was below 30 degrees. Therefore, data collected uses time windows between 8 and 10 AM to avoid this issue. Figures 12 and 13 are boxplots displaying the monthly trends of data captured using the above method for two selected bands, Visible: 550 nm and NIR: 760 nm for both sites and both species.

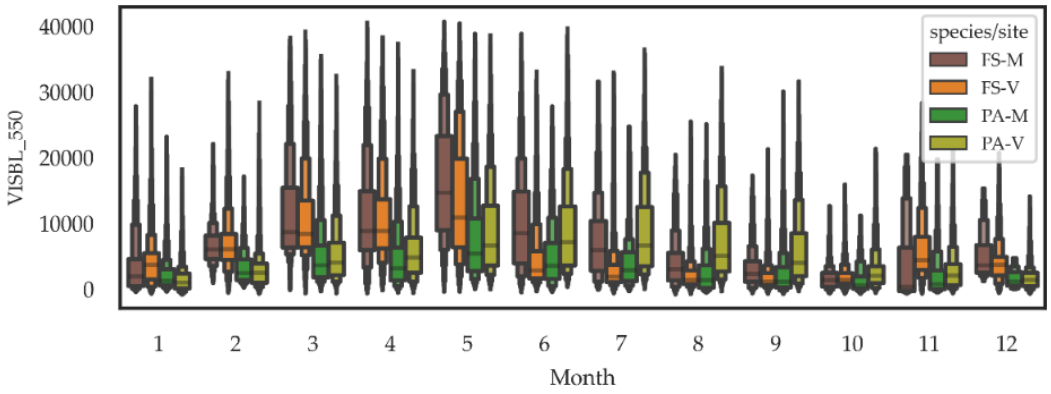

Figure 12. Monthly distribution of visible band 550 nm for both beech and spruce in Molveno and Val Canali

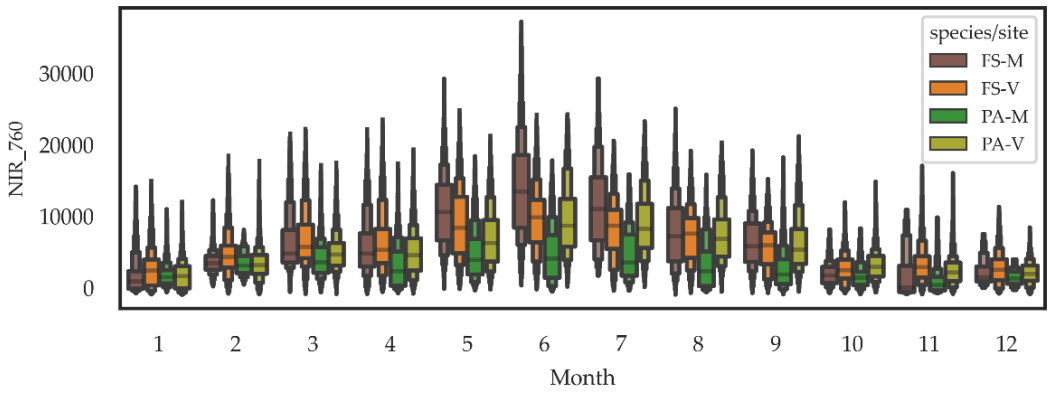

Figure 13. Monthly distribution of Near Infra-Red band 760 nm for both beech and spruce in Molveno and Val Canali

The extraction of this data for the inference and calculation of indices such as NDVI are not common given the nature of the spectrometric data which subsequently is transmitted light below the canopy. However, using monthly averages of TreeTalkers spectrometer data to feed NDVI (Normalized Difference Vegetation Index) formula (NIR-RED/NIR+RED) we present in figure 14 the seasonal dynamics of beech and spruce in Val Canali. Although we are in reality exploiting transmitted radiance below the canopy to estimate NDVI, the graphs clearly demonstrate the phenological response during the leaf out canopy development and leaf fall phases for beech with higher values reported around the early spring (May) to late autumn (October) as expected. Whereas spruce, also demonstrating a similar trend is lower in magnitude for spectrometric values.

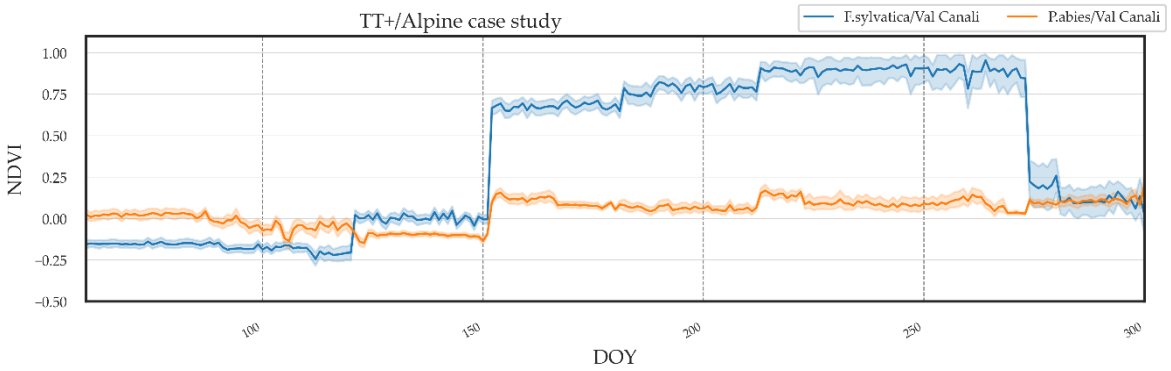

Figure 14. annual seasonal NDVI for beech and spruce in Val Canali

The data gathered were used to feed a machine learning algorithm for discriminative analysis as described in the following sections.

Preliminary ecological comparative analysis

To test the hypothesis that the two species, Beech, and Spruce are distinguishable based on ecophysiological parameters, we leveraged both Principal Components Analysis (PCA) and Linear Discriminant Analysis (LDA). For these analyses, we included 46 ecophysiological characters recorded by TreeTalkers. For each individual, the monthly values for the first quartile (Q1), the median (Q2), and the third quartile (Q3) of independent variables Tstem, SFD, ECf, 6 visible bands, and 6 NIR bands and radial growth were considered to provide the database for 46 characters. Our overall objective is to determine if beech and spruce are distinguishable at stand scale given retrieved ecophysiological data from the TreeTalkers in addition to site characteristics for the Molveno and Val Canali sites. Based on PCA analysis being unsupervised, a clear differentiation between spruce and beech was observed in Val Canali (Figure 15). However, beech and spruce in the Molvena sites were not (Figure 15). The reason behind this is associated with the continuation of the data given where inconstant battery replacement led to said gaps- Big gaps in data are a limiting factor for the analysis overall, yet as displayed in the Val Canali PCA results, the maintenance of the TreeTalkers with continued data capture is sufficient to discriminate and categories species.

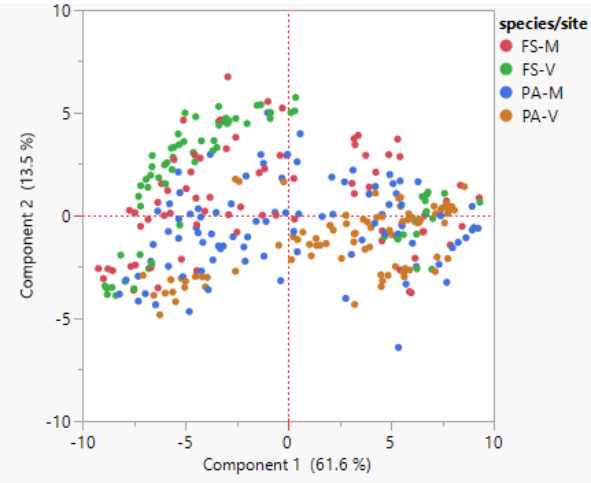

Figure 15. Unsupervised PCA analysis for species categorization applying TreeTalker ecophysiological variables.

This result allows the next step in the analyses iteration where we apply LDA to ascertain which dimensional constraints (site, species, site/species) to adopt. By applying such a protocol, our findings provide evidence that each individual, based on ecophysiological response is in fact distinguishable regarding species type and site at stand level. In addition, the results show that the role of ecophysiological data from individuals are less significant in location wise categorization (Figure 16). While species wise stand classification using ecophysiological showed a striking and strong result (Figure 17). Figure 18 demonstrates species-site supervision classification using the same ecophysiological results from the PCA. Table 5 reports the classification error for each scenario based on the training set demonstrating the clustering of each individual in different stands regarding the dimensional constraints, for site 26%, for species 4% and for species/site 19% misclassification error. Using the validation set, the predicted rate for the site supervision LDA demonstrates 83 %, and 82 % prediction rate for Molveno and Val Canali, for the species supervision LDA, beech 95 % and Spruce 97 % respectively. For the combination supervision (Site/Species), model prediction is > 82 %, with the best result of prediction belonging to spruce in Molveno (PA-M).

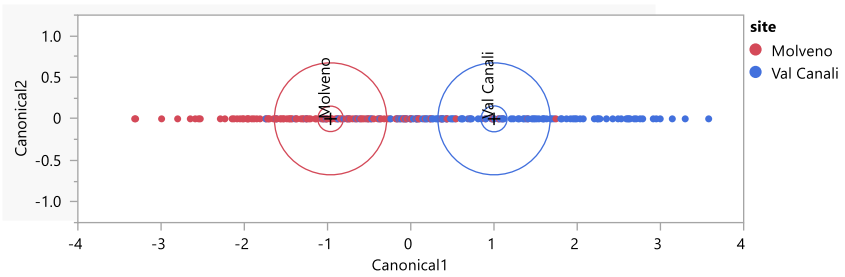

Figure 16. LDA analysis based on ecophysiological data from TreeTalkers under site supervision

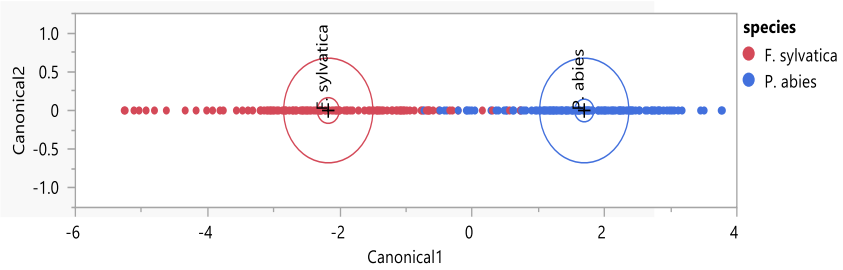

Figure 17. LDA analysis based on ecophysiological data from TreeTalkers under species supervision

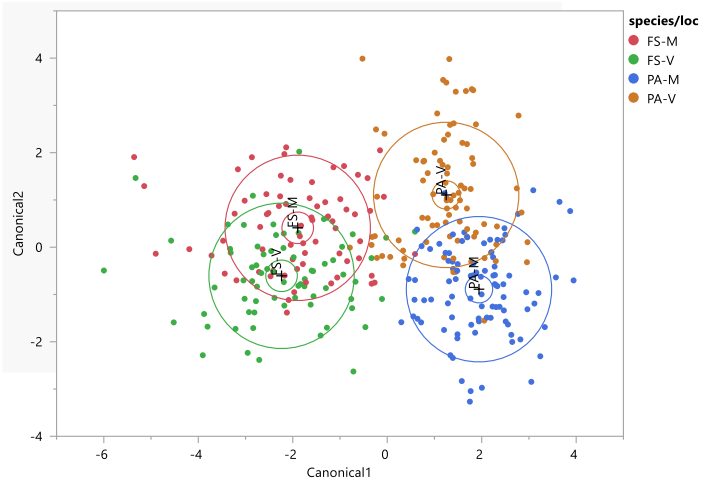

Figure 18. LDA analysis based on ecophysiological data from TreeTalkers under species/site supervision

Table 5. LDA model performance under each supervision criteria

Supervision criteria	Count	Number Misclassified	Percent Misclassified	Entropy RSquare	Log Likelihood
site	320	86	26.8750	0.24588	334.455
species	320	11	3.43750	0.87798	53.5194
site/species	320	63	19.6875	0.68357	279.093

Given the results achieved from the LDA for the dimensional constraints by species and site by ecophysiological parameters and site characteristics, we now move to an analysis by individual ecophysiological parameters to understand the impact of variables on species classification. The importance of variables in LDA classification is provided in Table 6 for site and species scenarios. In Table 6 each column is described as the variable with associated percentage weight, the total effect, and the proportion of the total effect of that variable in explaining the classification of species. Taking Table 6 we see that the main drivers of LDA vary for each scenario. For instance, site-wise analysis shows that the transmitted light radiance under the canopy takes the main role to predict individuals belonging in which location, Molveno or Val Canali. Whereas variable importance order changes under species scenario, having ECf and SFD in 3rd and 4th places as a driver of species-based classification.

Table 6. TreeTalker ecophysiological variable importance applied to supervised LDA

Variable Importance

LDA: Site		LDA: Species	
Variable	**Total Effect**	**Variable**	**Total Effect**
Q1-860	0.249	Q2-730	0.341
Q3-500	0.225	Q3-ecf	0.268
Q3-730	0.198	Q3-730	0.225
Q3-760	0.196	Q3-sfd	0.212
Q1-680	0.186	Q1-600	0.211
Q3-860	0.179	Q1-860	0.208
Q1-760	0.165	Q1-610	0.181
Q3-680	0.163	Q1-450	0.164
Q2-730	0.153	Q1-760	0.143
Q1-500	0.13	Q1-550	0.139
Q2-680	0.126	Q2-860	0.137
Q2-610	0.109	Q2-ecf	0.129
Q1-610	0.106	Q1-ecf	0.117
Q3-810	0.101	Q3-810	0.083
Q2-450	0.1	Q1-570	0.08
Q2-860	0.093	Q1-Tstem	0.074
Q3-600	0.091	Q2-810	0.072
Q1-550	0.082	Q2-760	0.068
Q2-Tstem	0.078	Q2-610	0.067
Q3-570	0.069	Q3-600	0.06
Q3-sfd	0.068	Q1-680	0.057
Q2-550	0.05	Q1-650	0.05

Conclusion

We have demonstrated:

- An innovative in-situ mass forest monitoring network toward forest digitalization: The TT+ and respective IoT capabilities have successfully been demonstrated here. Indeed preliminary applications of TreeTalker data are emerging (Asgharinia et al., 2022; Tomelleri et al., 2022). The capture of in situ digital tree ecophysiological parameters from a network of devices is novel and could possibly provide better information for forest ecosystem modeling and offer the necessary big data to feed a forest digital twin (Buonocore et al., 2022).
- Capability of TreeTalker toward ecophysiological parameters: The TT+ collects several ecophysiological variables, however, a higher fidelity toward SFD measurement when SFD > 0.5 l dm-2 h-1 as demonstrated in a previous chapter of this dissertation. The capture results from the two long term monitoring sites here revealed the differences in species hydrological functionality illustrating the generally accepted phenological and strategic growth behavior of beech and spruce. Stem Water Content, although explicitly linked to SFD, requires in situ calibration equations and as such should be the focus of further research. We can report that the capacitance sensor due to its surface contact limitations, not a feature of our sensor alone, true stem humidity given sensory integration with the wood matrix and wound impacts from sensor installation. Although not of a specific focus here, the spectrometric data applying preliminary analysis demonstrates the ability of the sensor to capture the seasonal canopy light interactions with the results used in the

classification analysis. This is also the case with the detected radial growth data. In summary, the TreeTalker's ability to capture such data, at a high temporal resolution drove the significant results achieved in the classification analysis.

- Disentangling PCA and LDA analysis: As highlighted in part by the PCA and more prominently by the LDA, which are a combination of the data retrieved from the TreeTalkers respectively, a relatively well defined species separation was achieved. The model results achieved in the PCA for Molveno illustrate the importance of TT+ device maintenance. The large gaps in data at this site reduce the model efficiency, however, in for the Val Canali site PCA was sufficient to explain the differences in species behavior. The LDA improves all analysis because of its supervised nature. In both the PCA and LDA, a prominent explanation for our results is a combination of species specific phenological and ecophysiological characteristics defining the different survival and growth strategies of beech and spruce. For the LDA supervised by species, the most important variables included SFD and ECf. For the LDA supervised by site, light, SFD ad ECf are significant.
- Overall, although not a complete substitute for field data collection, platforms such as the TreeTalker can enhance established methods for mass monitoring, offers big data solutions on individual trees, and further the pursuit of forest digitalization. Yet, as with any new technology challenges remain related to obstacles such as sensor green character, durability, flexible design, maintenance, precision, and accuracy.

Challenges and future research

- **Technological aspects:** The improvement of the sap flow sensor should be pursued. It currently captures 80 % of the total sap flux dynamic where the associated discrepancy can be attributed to poor capture of low flux rates. This problem is due to the 10 minutes heat input setting applied to save more battery which is considerably important for remote forest areas. However, if we choose to stay with the same methodology of thermal approach (Transient regime (Do and Rocheteau, 2002b)), a heat input increase appears to be one solution to improve the capability of the sensor at a cost to power consumption. A second solution for improving the data from the sap flow sensor is to capture the full heat flow curve at the microprocessor level and integrate a semi-analytical approach to mathematically evaluate the amount of sap velocity and thermal diffusivity at a large scale and in real-time. These solutions are indeed suggested through this PHD dissertation. Although the current version of the stem water content sensor shows potential for mass monitoring at an individual scale, deriving stand or population hydraulic behavior will require more fine tuning and conversion of the current capacitance sensor to a volume-sensing stem water content sensor. This future research preposition will be key in defining optimum installation time regarding tree hydrological activity and increasing sensor accuracy.

- **Ecophysiological aspects:** Long term big data collection is necessary to define normal ecophysiological operation of trees, that is defining a threshold for species based on their requirements and responses to abiotic stress. Tree ecophysiological responses to seasonality, extremes due to air temperature and water availability in different species under different site characteristics may reveal the individual hydrological strategies and these data may help to detect anomalies driving by legacy or pathogens. The continued fine tuning of the TreeTalker and its inherent nature to capture such large volumes of data will most likely improve process based deterministic modeling for growth under climate stress as well. We encourage this research using well defined installation, meat data, site and species specific protocols. Current standing and generally accepted ecological thought regarding the expansion of European beech into alpine areas and at higher altitudes for example often presumes temperature as the most significant factor in this range expansion (Fang and Lechowicz, 2006; Illés and Móricz, 2022), however as demonstrated by capture TreeTalker data, the hydrological implications regarding aggressive water use strategies whilst favoring distribution and expansion could be limiting under shifting long term seasonal precipitation along with changes to annual or period glaciation and subsequent melting in these zones. As such we suggest future long term monitoring applications to test a such hypothesis.

References

Adeyi, G.O., Adigun, A.I., Onyeocha, N.C., 2020. Unit Hydrograph: Concepts, Estimation Methods and Applications in Hydrological Sciences.

Alexandru Borz, S., Proto, A.R., Keefe, R., Nita, M., Viedma, O., Tomelleri, E., Belelli Marchesini, L., Yaroslavtsev, A., Asgharinia, S., Valentini, R., 2022. Toward a Unified TreeTalker Data Curation Process. For. 2022, Vol. 13, Page 855 13, 855.

Alizadeh, A., Toudeshki, A., Ehsani, R., Migliaccio, K., Wang, D., 2021. Detecting tree water stress using a trunk relative water content measurement sensor. Smart Agric. Technol. 1, 100003.

Ang, L.M., Seng, K.P., Wachowicz, M., 2022. Embedded intelligence and the data-driven future of application-specific Internet of Things for smart environments. Int. J. Distrib. Sens. Networks 18.

Antonacci, G., Todeschini, I., 2013. Derivation of meteorological reference year with hourly interval for Italy. Build. Simul. Appl. 2013-Janua, 49–57.

Araújo, G.P., Vellame, L.M., Costa, J.A., Costa, C.A.G., 2021. A low-cost monitoring system of stem water content: Development and application to Brazilian forest species. Smart Agric. Technol. 1, 100012.

Asgharinia, S., Leberecht, M., Belelli Marchesini, L., Friess, N., Gianelle, D., Nauss, T., Opgenoorth, L., Yates, J., Valentini, R., 2022. Towards Continuous Stem Water Content and Sap Flux Density Monitoring: IoT-Based Solution for Detecting Changes in Stem Water Dynamics. Forests 13, 1040.

Atkinson, K., 1989. Intro To Numerical Analysis 2e 712.

Aumann, C.A., David Ford, E., 2002a. Modeling Tree Water Flow as an Unsaturated Flow through a Porous Medium. J. Theor. Biol. 219, 415–429.

Aumann, C.A., David Ford, E., 2002b. Modeling tree water flow as an unsaturated flow through a porous medium. J. Theor. Biol. 219, 415–429.

Barbour, M.M., Whitehead, D., 2003. A demonstration of the theoretical prediction that sap velocity is related to wood density in the conifer Dacrydium cupressinum. New Phytol. 158, 477–488.

Becker, P., Edwards, W.R.N., 1999. Corrected heat capacity of wood for sap flow calculations. Tree Physiol. 19, 767–768.

Belcastro, L., Cantini, R., Marozzo, F., Orsino, A., Talia, D., Trunfio, P., 2022. Programming big data analysis: principles and solutions. J. Big Data 9, 1–50.

Boone, R.S.S., Wengert, E.M.M., 1998. Guide for Using the Oven-Dry Method for Determining the Moisture Content of Wood. For. Facts 89, 1–4.

Bowman, W.P.P., Barbour, M.M.M., Turnbull, M.H.H., Tissue, D.T.T., Whitehead, D., Griffin, K.L.L., 2005. Sap flow rates and sapwood density are critical factors in within- and between-tree variation in CO2 efflux from stems of mature Dacrydium cupressinum trees. New Phytol. 167, 815–828.

Bréda, N., Huc, R., Granier, A., Dreyer, E., 2006. Temperate forest trees and stands under severe drought: A review of ecophysiological responses, adaptation processes and long-term consequences. Ann. For. Sci.

Buchholz, K., Pickering, J.L., 1978. DBH-Distribution Analysis: An Alternative to Stand-Age Analysis. Bull. Torrey Bot. Club 105, 282.

Buonocore, L., Yates, J., Valentini, R., 2022. A Proposal for a Forest Digital Twin Framework and Its Perspectives. Forests 13, 1–19.

Burgess, S.S.O., Adams, M.A., Turner, N.C., Beverly, C.R., Ong, C.K., Khan, A.A.H., Bleby, T.M., 2001. An improved heat pulse method to measure low and reverse rates of sap flow in woody plants. Tree Physiol.

Bužková, R., Pokorný, R., 2013. Biomass allocation and transpiration of Picea abies and Fagus sylvatica cultivated under ambient and elevated [CO2] concentration. Acta Hortic. 991, 157–162.

Byrne, G.F., Fenn, M.D., Burgar, M.I., 1986. Nuclear magnetic resonance studies of water in tree sections. Agric. For. Meteorol.

Bzai, J., Alam, F., Dhafer, A., Bojović, M., Altowaijri, S.M., Niazi, I.K., Mehmood, R., 2022. Machine Learning-Enabled Internet of Things (IoT): Data, Applications, and Industry Perspective. Electron. 2022, Vol. 11, Page 2676 11, 2676.

Camarretta, N., Harrison, P.A., Bailey, T., Potts, B., Lucieer, A., Davidson, N., Hunt, M., 2019. Monitoring forest structure to guide adaptive management of forest restoration: a review of remote sensing approaches. New For. 2019 514 51, 573–596.

Cermák, J., Deml, M., Penka, M., 1973. A New Method of Sap Flow Rate Determination in Trees. Biol. Plant.

Čermák, J., Kučera, J., 1981. The compensation of natural temperature gradient at the measuring point during the sap flow rate determination in trees. Biol. Plant.

Čermák, J., Kučera, J., Bauerle, W.L., Phillips, N., Hinckley, T.M., 2007. Tree water storage and its diurnal dynamics related to sap flow and changes in stem volume in old-growth Douglas-fir trees. Tree Physiol. 27, 181–198.

Cheng, X., Yan, X., Grantz, D.A., Xiang, Y., de Oliveira, R.F., Huang, L., Wang, Z., Du, T., Cheng, Q., 2021. In-situ and non-invasive measurement of stem water content of trees using an innovative interdigitated-electrodes dielectric sensor less susceptible to stem diameter variation. Agric. For. Meteorol. 307, 108473.

Chetpattananondh, P., Thongpull, K., Chetpattananondh, K., 2017. Interdigital capacitance sensing of moisture content in rubber wood. Comput. Electron. Agric. 142, 545–551.

Chuang, Y.L., Oren, R., Bertozzi, A.L., Phillips, N., Katul, G.G., 2006. The porous media model for the hydraulic system of a conifer tree: Linking sap flux data to transpiration rate. Ecol. Modell. 191, 447–468.

COHEN, Y., FUCHS, M., GREEN, G.C., 1981. Improvement of the heat pulse method for determining sap flow in trees. Plant. Cell Environ.

Constantz, J., Murphy, F., 1990. Monitoring moisture storage in trees using time domain reflectometry. J. Hydrol. 119, 31–42.

Costantini, E., Barbetti, R., Fantappiè, M., L'Abate, G., Lorenzetti, R., Napoli, R., Marchetti, A., Rivieccio, R., 2014. The soil map of Italy. In: GlobalSoilMap. CRC Press, pp. 109–112.

Dean, T.J., Bell, J.P., Baty, A.J.B., 1987. Soil moisture measurement by an improved capacitance technique, Part I. Sensor design and performance. J. Hydrol. 93, 67–78.

Dietsch, P., Franke, S., Franke, B., Gamper, A., Winter, S., 2015. Methods to determine wood moisture content and their applicability in monitoring concepts. J. Civ. Struct. Heal. Monit. 5, 115–127.

Do, F., Rocheteau, A., 2002a. Influence of natural temperature gradients on measurements of xylem sap flow with thermal dissipation probes. 2. Advantages and calibration of a noncontinuous heating system. Tree Physiol.

Do, F., Rocheteau, A., 2002b. Influence of natural temperature gradients on measurements of xylem sap flow with thermal dissipation probes. 1. Field observations and possible remedies. Tree Physiol.

Do, F.C., Isarangkool Na Ayutthaya, S., Rocheteau, A., 2011. Transient thermal dissipation method for xylem sap flow measurement: Implementation with a single probe. Tree Physiol. 31, 369–380.

Do, F.C., Puangjumpa, N., Rocheteau, A., Duthoit, M., Nhean, S., Isarangkool Na Ayutthaya, S., 2018. Towards reduced heating duration in the transient thermal dissipation system of sap flow measurements. Acta Hortic. 1222, 229–235.

Dzikiti, S., Steppe, K., Lemeur, R., Milford, J.R., 2007. Whole-tree level water balance and its implications on stomatal oscillations in orange trees [Citrus sinensis (L.) Osbeck] under natural climatic conditions. J. Exp. Bot.

EDWARDS, W.R.N., JARVIS, P.G., 1983. A method for measuring radial differences in water content of intact tree stems by attenuation of gamma radiation. Plant. Cell Environ.

Ehrenberg, R., 2015. Global forest survey finds trillions of trees. Nature.

Fang, J., Lechowicz, M.J., 2006. Climatic limits for the present distribution of beech (Fagus L.) species in the world. J. Biogeogr. 33, 1804–1819.

Fares, A., Polyakov, V., 2006. Advances in Crop Water Management Using Capacitive Water Sensors. Adv. Agron.

Fares, A., Safeeq, M., Awal, R., Fares, S., Dogan, A., 2016. Temperature and Probe-to-Probe Variability Effects on the Performance of Capacitance Soil Moisture Sensors in an Oxisol. Vadose Zo. J. 15, vzj2015.07.0098.

Flo, V., Martinez-Vilalta, J., Steppe, K., Schuldt, B., Poyatos, R., 2019. A synthesis of bias and uncertainty in sap flow methods. Agric. For. Meteorol. 271, 362–374.

Friess, N., Bendix, J., Brändle, M., Brandl, R., Dahlke, S., Farwig, N., Freisleben, B., Holzmann, H., Meyer, H., Müller, T., Opgenoorth, L., Peter, C., Quillfeldt, P., Reudenbach, C., Seeger, B., Steinmetz, R., Nauss, T., 2019. Introducing Nature 4.0: A sensor network for environmental monitoring in the Marburg Open Forest. Biodivers. Inf. Sci. Stand. 3, 3–4.

Fuchs, A., J. Moser, M., Zangl, H., Bretterklieber, T., 2009. Using Capacitive Sensing To Determine the Moisture Content of Wood Pellets – Investigations and Application. Int. J. Smart Sens. Intell. Syst. 2, 293–308.

Gartner, Leitgeb, K., Nadezhdina, E., Cermak, 2003. Sap flow of birch and Norway spruce during the European heat and drought in summer 2003.

Gazol, A., Camarero, J.J., Vicente-Serrano, S.M., Sánchez-Salguero, R., Gutiérrez, E., de Luis, M., Sangüesa-Barreda, G., Novak, K., Rozas, V., Tíscar, P.A., Linares, J.C., Martín-Hernández, N., Martínez del Castillo, E., Ribas, M., García-González, I., Silla, F., Camisón, A., Génova, M., Olano, J.M., Longares, L.A., Hevia, A., Tomás-Burguera, M., Galván, J.D., 2018. Forest resilience to drought varies across biomes. Glob. Chang. Biol.

Gebauer, T., Horna, V., Leuschner, C., 2012. Canopy transpiration of pure and mixed forest stands with variable abundance of European beech. J. Hydrol. 442–443, 2–14.

Ghazali, M.H.M., Teoh, K., Rahiman, W., 2021. A Systematic Review of Real-Time Deployments of UAV-Based LoRa Communication Network. IEEE Access 9, 124817–124830.

Goldstein, G., Andrade, J.L., Meinzer, F.C., Holbrook, N.M., Cavelier, J., Jackson, P., Celis, A., 1998. Stem water storage and diurnal patterns of water use in tropical forest canopy trees. Plant, Cell Environ. 21, 397–406.

Granier, A., 1987. Evaluation of transpiration in a Douglas-fir stand by means of sap flow measurements. Tree Physiol.

GRANIER, A., 1985. Une nouvelle méthode pour la mesure du flux de sève brute dans le tronc des arbres.

Ann. des Sci. For.

Güney, A., 2018. Sapwood Area Related to Tree Size, Tree Age, and Leaf Area Index in Cedrus libani. Bilge Int. J. Sci. Technol. Res. 2, 83–91.

Gustafsson, F., 1996. Determining the initial states in forward-backward filtering. IEEE Trans. Signal Process. 44, 988–992.

Hafner, B.D., Tomasella, M., Häberle, K.H., Goebel, M., Matyssek, R., Grams, T.E.E., 2017. Hydraulic redistribution under moderate drought among English oak, European beech and Norway spruce determined by deuterium isotope labeling in a split-root experiment. Tree Physiol. 37, 950–960.

Hairer, E., Wanner, G., 1996. Examples of Stiff Equations 2–14.

Hao, G.Y., James, K.W., N. Michele Holbrook, Guillermo Goldstein, 2013. Investigating xylem embolism formation, refilling and water storage in tree trunks using frequency domain reflectometry. J. Exp. Bot.

Hardie, M., 2020. Review of Novel and Emerging Proximal Soil Moisture Sensors for Use in Agriculture. Sensors 2020, Vol. 20, Page 6934 20, 6934.

He, H., Turner, N.C., Aogu, K., Dyck, M., Feng, H., Si, B., Wang, J., Lv, J., 2021a. Time and frequency domain reflectometry for the measurement of tree stem water content: A review, evaluation, and future perspectives. Agric. For. Meteorol. 306, 108442.

He, H., Turner, N.C., Aogu, K., Dyck, M., Feng, H., Si, B., Wang, J., Lv, J., 2021b. Time and frequency domain reflectometry for the measurement of tree stem water content: A review, evaluation, and future perspectives. Agric. For. Meteorol. 306, 108442.

HEIDE, O.M., 1974. Growth and Dormancy in Norway Spruce Ecotypes (Picea abies) I. Interaction of Photoperiod and Temperature. Physiol. Plant. 30, 1–12.

Henry, M., Réjou-Méchain, M., Jara, M.C., Wayson, C., Piotto, D., Westfall, J., Fuentes, J.M.M., Guier, F.A., Lombis, H.C., López, E.C., Lara, R.C., Rojas, K.C., Del Águila Pasquel, J., Montoya, Á.D., Vega, J.F., Galo, A.J., López, O.R., Marklund, L.G., Milla, F., de Jesús Návar Cahidez, J., Malavassi, E.O., Pérez, J., Zea, C.R., García, L.R., Pons, R.R., Sanquetta, C., Scott, C., Zapata-Cuartas, M., Saint-André, L., 2015. An overview of existing and promising technologies for national forest monitoring. Ann. For. Sci. 72, 779–788.

Hernández-Santana, V., Martínez-Fernández, J., Morán, C., Cano, A., 2008. Response of Quercus pyrenaica (melojo oak) to soil water deficit: A case study in Spain. Eur. J. For. Res. 127, 369–378.

Hsu, A., Khoo, W., Goyal, N., Wainstein, M., 2020. Next-Generation Digital Ecosystem for Climate Data Mining and Knowledge Discovery: A Review of Digital Data Collection Technologies. Front. Big Data 3, 29.

Huber, B., 1932. Beobachtung und Messung pflanzlicher Saftstrome. Ber Deutsch Bot Ges.

Huber, B., Schmidt, E., 1937. Eine Kompensationsmethode zur thermoelektrischen Messung langsamer Saftströme. Ber. Dtsch. Bot. Ges.

Iii, F.S.C., Rincon, E., Huante, P., 1993. <Environmental responses of plants and ecosystem as predictors of global change.pdf> 18, 515–524.

Illés, G., Móricz, N., 2022. Climate envelope analyses suggests significant rearrangements in the distribution ranges of Central European tree species. Ann. For. Sci. 79.

Irvine, J., Grace, J., 1997. Non-destructive measurement of stem water content by time domain reflectometry using short probes. J. Exp. Bot.

Isarangkool Na Ayutthaya, S., Do, F.C., Pannengpetch, K., Junjittakarn, J., Maeght, J.L., Rocheteau, A.,

Cochard, H., 2010. Transient thermal dissipation method of xylem sap flow measurement: Multi-species calibration and field evaluation. Tree Physiol. 30, 139–148.

Janbek, B.M., Stockie, J.M., 2017. Asymptotic and numerical analysis of a porous medium model for transpiration-driven sap flow in trees.

Janbek, B.M., Stockie, J.M., 2018. Asymptotic and numerical analysis of a porous medium model for transpiration-driven sap flow in trees. SIAM J. Appl. Math. 78, 2028–2056.

Jones, B., Sall, J., 2011. JMP statistical discovery software. Wiley Interdiscip. Rev. Comput. Stat. 3, 188–194.

Jones, P.R., 2019. A note on detecting statistical outliers in psychophysical data. Attention, Perception, Psychophys. 81, 1189–1196.

Kizito, F., Campbell, C.S., Campbell, G.S., Cobos, D.R., Teare, B.L., Carter, B., Hopmans, J.W., 2008. Frequency, electrical conductivity and temperature analysis of a low-cost capacitance soil moisture sensor. J. Hydrol. 352, 367–378.

Knoben, W.J.M., Freer, J.E., Woods, R.A., 2019. Technical note: Inherent benchmark or not? Comparing Nash-Sutcliffe and Kling-Gupta efficiency scores. Hydrol. Earth Syst. Sci. Discuss. 1–7.

Korkua, S.K., Sakphrom, S., 2020. Low-cost capacitive sensor for detecting palm-wood moisture content in real-time. Heliyon 6, e04555.

Kurimoto, T., Nemoto, N., Asakura, K., Yamasaki, C., 2007. * EP001473574B1 * 1, 1–65.

Lane, P.N.J., Mackenzie, D.H., Nadler, A.D., 2002. Note of clarification about: Field and laboratory calibration and test of TDR and capacitance techniques for indirect measurement of soil water content, by P.N.J. Lane and D.H. Mackenzie, Vol. 39, pp. 1371-1386. Soil Res. 40.

Liang, H., Zhang, M., Wang, H., Gao, C., Zhao, Y., 2020. Variation Characteristics of Stem Water Content in Lagerstroemia indica and Its Response to Environmental Factors. J. Sensors 2020.

Looker, N., Martin, J., Jencso, K., Hu, J., 2016. Contribution of sapwood traits to uncertainty in conifer sap flow as estimated with the heat-ratio method. Agric. For. Meteorol.

López-Bernal, Á., Testi, L., Villalobos, F.J., 2012. Using the compensated heat pulse method to monitor trends in stem water content in standing trees. Tree Physiol. 32, 1420–1429.

Lotte, F., Bougrain, L., Cichocki, A., Clerc, M., Congedo, M., Rakotomamonjy, A., Yger, F., 2018. A review of classification algorithms for EEG-based brain–computer interfaces: a 10 year update. J. Neural Eng. 15, 031005.

Lu, P., 2002. Estimation of whole-plant transpiration of bananas using sap flow measurements. J. Exp. Bot.

Lu, P., Urban, L., Zhao, P., 2004. Granier's Thermal Dissipation Probe (TDP) Method for Measuring Sap Flow in Trees:Theory and Practice. ACTA ….

Lubczynski, M.W., Chavarro-Rincon, D., Roy, J., 2012. Novel, cyclic heat dissipation method for the correction of natural temperature gradients in sap flow measurements. Part 1. Theory and application. Tree Physiol. 32, 894–912.

Magh, R.K., Bonn, B., Grote, R., Burzlaff, T., Pfautsch, S., Rennenberg, H., 2019. Drought superimposes the positive effect of silver fir on water relations of european beech in mature forest stands. Forests 10.

Mahjoub, I., Masmoudi, M.M., Lhomme, J.P., Mechlia, N. Ben, 2009. Sap flow measurement by a single thermal dissipation probe: Exploring the transient regime. Ann. For. Sci. 66, 608–608.

Malavasi, U.C., Davis, A.S., de Matos Malavasi, M., 2016. Estimativa de água em caule lenhosos vivos – uma revisão. Cerne 22, 415–422.

Marshall, D.C., 1958. Measurement of Sap Flow in Conifers by Heat Transport. Plant Physiol.

Masmoudi, M.M., Mahjoub, I., Lhomme, J.P., Ben Mechlia, N., 2012. Sap flow measurement by a single thermal dissipation probe in transient regime: Implementation of the method and test under field conditions. Ann. For. Sci. 69, 773–781.

Matasov, V., Marchesini, L.B., Yaroslavtsev, A., Sala, G., Fareeva, O., Seregin, I., Castaldi, S., Vasenev, V., Valentini, R., 2020. IoT monitoring of urban tree ecosystem services: Possibilities and challenges. Forests 11.

Matheny, A.M., Bohrer, G., Garrity, S.R., Morin, T.H., Howard, C.J., Vogel, C.S., 2015. Observations of stem water storage in trees of opposing Hydraulic strategies. Ecosphere.

Matheny, A.M., Garrity, S.R., Bohrer, G., 2017. The calibration and use of capacitance sensors to monitor stem water content in trees. J. Vis. Exp. 2017, 1–10.

Matyssek, R., Wieser, G., Patzner, K., Blaschke, H., Häberle, K.H., 2009. Transpiration of forest trees and stands at different altitude: Consistencies rather than contrasts? Eur. J. For. Res. 128, 579–596.

McDowell, N.G., 2011. Mechanisms linking drought, hydraulics, carbon metabolism, and vegetation mortality. Plant Physiol.

Mitra, B., Papuga, S.A., Alexander, M.R., Swetnam, T.L., Abramson, N., 2020. Allometric relationships between primary size measures and sapwood area for six common tree species in snow-dependent ecosystems in the Southwest United States. J. For. Res. 31, 2171–2180.

Mousavi, S.M., Khademzadeh, A., Rahmani, A.M., 2022. The role of low-power wide-area network technologies in Internet of Things: A systematic and comprehensive review. Int. J. Commun. Syst. 35, e5036.

Nadezhdina, N., 1999. Sap flow index as an indicator of plant water status. Tree Physiol. 19, 885–891.

Nadezhdina, N., Vandegehuchte, M.W., Steppe, K., 2012. Sap flux density measurements based on the heat field deformation method. Trees - Struct. Funct.

Nadler, A., Raveh, E., Yermiyahu, U., Green, S., 2006. Stress Induced Water Content Variations in Mango Stem by Time Domain Reflectometry. Soil Sci. Soc. Am. J. 70.

Nadler, A., Raveh, E., Yermiyahu, U., Green, S.R., 2003. Evaluation of TDR use to monitor water content in stem of lemon trees and soil and their response to water stress. Soil Sci. Soc. Am. J.

Nadler, A., Tyree, M.T., 2008. Substituting stem's water content by electrical conductivity for monitoring water status changes. Soil Sci. Soc. Am. J. 72, 1006–1013.

Nalevanková, P., Sitková, Z., Kučera, J., Střelcová, K., 2020. Impact of water deficit on seasonal and diurnal dynamics of european beech transpiration and time-lag effect between stand transpiration and environmental drivers. Water (Switzerland) 12, 1–21.

Nelder, J.A., Mead, R., 1965. A Simplex Method for Function Minimization. Comput. J. 7, 308–313.

Neuwirth, B., Rabbel, I., Bendix, J., Bogena, H.R., Thies, B., 2021. The european heat wave 2018: The dendroecological response of oak and spruce in western germany. Forests 12, 1–17.

Nhean, S., Isarangkool Na Ayutthaya, S., Rocheteau, A., Do, F.C., Tognetti, R., 2019a. Multi-species test and calibration of an improved transient thermal dissipation system of sap flow measurement with a single probe. Tree Physiol. 39, 1061–1070.

Nhean, S., Isarangkool Na Ayutthaya, S., Rocheteau, A., Do, F.C., Tognetti, R., 2019b. Multi-species test and calibration of an improved transient thermal dissipation system of sap flow measurement with a single probe. Tree Physiol. 39, 1061–1070.

Nobel, P.S., 2009. Physicochemical and Environmental Plant Physiology. Physicochem. Environ. Plant

Physiol.

Nola, P., Bracco, F., Assini, S., Von Arx, G., Castagneri, D., n.d. Xylem anatomy of Robinia pseudoacacia L. and Quercus robur L. is differently affected by climate in a temperate alluvial forest.

Nourtier, M., Chanzy, A., Granier, A., Huc, R., 2011. Sap flow measurements by thermal dissipation method using cyclic heating: A processing method accounting for the non-stationary regime. Ann. For. Sci.

Pasqualetto, A., Presti, D.C. Lo, Junior, A.M., 2019. Availability and Demand of Water Resources in Brazil and Italy. Eur. J. Sci. Res. Vol. 153 N, 403–419.

Potter, B.E., Andresen, J.A., 2002. A finite-difference model of temperatures and heat flow within a tree stem. Can. J. For. Res. 32, 548–555.

Pretzsch, H., Hilmers, T., Uhl, E., Bielak, K., Bosela, M., del Rio, M., Dobor, L., Forrester, D.I., Nagel, T.A., Pach, M., Avdagić, A., Bellan, M., Binder, F., Bončina, A., Bravo, F., de-Dios-García, J., Dinca, L., Drozdowski, S., Giammarchi, F., Hoehn, M., Ibrahimspahić, A., Jaworski, A., Klopčič, M., Kurylyak, V., Lévesque, M., Lombardi, F., Matović, B., Ordóñez, C., Petráš, R., Rubio-Cuadrado, A., Stojanovic, D., Skrzyszewski, J., Stajić, B., Svoboda, M., Versace, S., Zlatanov, T., Tognetti, R., 2021. European beech stem diameter grows better in mixed than in mono-specific stands at the edge of its distribution in mountain forests. Eur. J. For. Res. 140, 127–145.

Pretzsch, H., Rötzer, T., Matyssek, R., Grams, T.E.E., Häberle, K.H., Pritsch, K., Kerner, R., Munch, J.C., 2014a. Mixed Norway spruce (Picea abies [L.] Karst) and European beech (Fagus sylvatica [L.]) stands under drought: from reaction pattern to mechanism. Trees - Struct. Funct. 28, 1305–1321.

Pretzsch, H., Rötzer, T., Matyssek, R., Grams, T.E.E., Häberle, K.H., Pritsch, K., Kerner, R., Munch, J.C., 2014b. Mixed Norway spruce (Picea abies [L.] Karst) and European beech (Fagus sylvatica [L.]) stands under drought: from reaction pattern to mechanism. Trees - Struct. Funct. 28, 1305–1321.

Ren, R., von der Crone, J., Horton, R., Liu, G., Steppe, K., 2020. An improved single probe method for sap flow measurements using finite heating duration. Agric. For. Meteorol. 280, 107788.

Reyer, C.P.O., Silveyra Gonzalez, R., Dolos, K., Hartig, F., Hauf, Y., Noack, M., Lasch-Born, P., Rötzer, T., Pretzsch, H., Meesenburg, H., Fleck, S., Wagner, M., Bolte, A., Sanders, T.G.M., Kolari, P., Mäkelä, A., Vesala, T., Mammarella, I., Pumpanen, J., Collalti, A., Collalti, A., Trotta, C., Matteucci, G., D'Andrea, E., Foltýnová, L., Krejza, J., Ibrom, A., Pilegaard, K., Loustau, D., Bonnefond, J.M., Berbigier, P., Picart, D., Lafont, S., Dietze, M., Cameron, D., Vieno, M., Tian, H., Palacios-Orueta, A., Cicuendez, V., Recuero, L., Wiese, K., Büchner, M., Lange, S., Volkholz, J., Kim, H., Horemans, J.A., Bohn, F., Steinkamp, J., Chikalanov, A., Weedon, G.P., Sheffield, J., Babst, F., Babst, F., Vega Del Valle, I., Suckow, F., Martel, S., Mahnken, M., Gutsch, M., Frieler, K., 2020. The PROFOUND Database for evaluating vegetation models and simulating climate impacts on European forests. Earth Syst. Sci. Data 12, 1295–1320.

Roderick, M.L., Berry, S.L., 2001. Linking wood density with tree growth and environment: A theoretical analysis based on the motion of water. New Phytol. 149, 473–485.

Rötzer, T., Häberle, K.H., Kallenbach, C., Matyssek, R., Schütze, G., Pretzsch, H., 2017. Tree species and size drive water consumption of beech/spruce forests - a simulation study highlighting growth under water limitation. Plant Soil 418, 337–356.

Saito, T., Yasuda, H., Sakurai, M., Acharya, K., Sueki, S., Inosako, K., Yoda, K., Fujimaki, H., Abd Elbasit, M.A.M., Eldoma, A.M., Nawata, H., 2016. Monitoring of Stem Water Content of Native and Invasive Trees in Arid Environments Using GS3 Soil Moisture Sensors. Vadose Zo. J. 15, vzj2015.04.0061.

Sakuratani, T., 1984. Improvement of the Probe for Measuring Water Flow Rate in Intact Plants with the Stem Heat Balance Method. J. Agric. Meteorol.

Salomón, R.L., Steppe, K., Ourcival, J.M., Villers, S., Rodríguez-Calcerrada, J., Schapman, R., Limousin, J.M., 2020. Hydraulic acclimation in a Mediterranean oak subjected to permanent throughfall exclusion results in increased stem hydraulic capacitance. Plant. Cell Environ. 43, 1528–1544.

Sánchez, J., Curt, M.D., Robert, N., Fernández, J., 2019. Biomass Resources. Role Bioenergy Emerg. Bioeconomy Resour. Technol. Sustain. Policy 25–111.

Saranya, T., Sridevi, S., Deisy, C., Chung, T.D., Khan, M.K.A.A., 2020. Performance Analysis of Machine Learning Algorithms in Intrusion Detection System: A Review. Procedia Comput. Sci. 171, 1251–1260.

Schermelleh-Engel, K., Moosbrugger, H., Müller, H., 2003. Evaluating the Fit of Structural Equation Models: Tests of Significance and Descriptive Goodness-of-Fit Measures. Methods Psychol. Res. Online 8, 23–74.

Senf, C., 2022. Seeing the System from Above: The Use and Potential of Remote Sensing for Studying Ecosystem Dynamics. Ecosyst. 2022 1–19.

Sevanto, S., Mcdowell, N.G., Dickman, L.T., Pangle, R., Pockman, W.T., 2014. How do trees die? A test of the hydraulic failure and carbon starvation hypotheses. Plant, Cell Environ.

Shah, M., 2020. A Comparison Of Numerical Solutions Of Diffusion And Advection Diffusion Equations using Python A Comparison Of Numerical Solutions Of Diffusion And Advection Diffusion Equations using Python Manan Shah.

Singh, R., Gehlot, A., Vaseem Akram, S., Kumar Thakur, A., Buddhi, D., Kumar Das, P., 2022. Forest 4.0: Digitalization of forest using the Internet of Things (IoT). J. King Saud Univ. - Comput. Inf. Sci. 34, 5587–5601.

Siqueira, J.M., Paço, T.A., da Silva, J.M., Silvestre, J.C., 2020. Biot-granier sensor: A novel strategy to measuring sap flow in trees. Sensors (Switzerland).

Skomarkova, M. V., Vaganov, E.A., Mund, M., Knohl, A., Linke, P., Boerner, A., Schulze, E.D., 2006. Inter-annual and seasonal variability of radial growth, wood density and carbon isotope ratios in tree rings of beech (Fagus sylvatica) growing in Germany and Italy. Trees - Struct. Funct. 20, 571–586.

Sousa, E.F., Santolin, M.A., Do, F.C., 2020. Estimation of steady water flux density in a porous medium by Fourier analysis of temperature variations in a cyclic heat pulse system. Acta Hortic. 1300, 187–192.

Steppe, K., 2004. Diurnal dynamics of water flow through trees: design and validation of a mathematical flow and storage model.

Stewart, S., Ivy, M.A., Anslyn, E. V., 2014. The use of principal component analysis and discriminant analysis in differential sensing routines. Chem. Soc. Rev. 43, 70–84.

Stott, L. V, Black, B., Bugbee, B., n.d. Quantifying Tree Hydration Using Electromagnetic Sensors.

Swanson, R.H. (Robert H. 1933-, 1983. Numerical and experimental analyses of implanted-probe heat pulse velocity theory.

Swanson, R.H., Whitfield, D.W.A.A., 1981. A numerical analysis of heat pulse velocity theory and practice. J. Exp. Bot.

Theses, D., Ray Ballard, J., 2011. Scholars Junction Scholars Junction A three-dimensional heat and mass transport model for a tree A three-dimensional heat and mass transport model for a tree within a forest within a forest Recommended Citation Recommended Citation.

Toledo, M., Poorter, L., Peña-Claros, M., Alarcón, A., Balcázar, J., Leaño, C., Licona, J.C., Llanque, O., Vroomans, V., Zuidema, P., Bongers, F., 2011. Climate is a stronger driver of tree and forest growth rates than soil and disturbance. J. Ecol. 99, 254–264.

Tomelleri, E., Belelli Marchesini, L., Yaroslavtsev, A., Asgharinia, S., Valentini, R., 2022. Toward a Unified TreeTalker Data Curation Process. Forests 13, 855.

Torresan, C., Garzón, M.B., O'grady, M., Robson, T.M., Picchi, G., Panzacchi, P., Tomelleri, E., Smith, M., Marshall, J., Wingate, L., Tognetti, R., Rustad, L.E., Kneeshaw, D., 2021. A new generation of sensors and monitoring tools to support climate-smart forestry practices. Can. J. For. Res. 51, 1751–1765.

Tvrdá, K., Minárová, M., 2018. Computation of definite integral over repeated integral. Tatra Mt. Math. Publ. 72, 141–154.

Valentini, R., Marchesini, L.B., Gianelle, D., Sala, G., Yarovslavtsev, A., Vasenev, V.I., Castaldi, S., 2019. New tree monitoring systems: From industry 4.0 to nature 4.0. Ann. Silvic. Res. 43, 84–88.

van As, H., Scheenen, T., Vergeldt, F.J., 2009. MRI of intact plants. Photosynth. Res.

Vandegehuchte, M.W., Steppe, K., 2012a. Sapflow+: A four-needle heat-pulse sap flow sensor enabling nonempirical sap flux density and water content measurements. New Phytol. 196, 306–317.

Vandegehuchte, M.W., Steppe, K., 2012b. Use of the correct heat conduction-convection equation as basis for heat-pulse sap flow methods in anisotropic wood. J. Exp. Bot. 63, 2833–2839.

Vandegehuchte, M.W., Steppe, K., 2013. Corrigendum to: Sap-flux density measurement methods: working principles and applicability. Funct. Plant Biol. 40, 1088.

Vergeynst, L.L., Vandegehuchte, M.W., McGuire, M.A., Teskey, R.O., Steppe, K., 2014. Changes in stem water content influence sap flux density measurements with thermal dissipation probes. Trees - Struct. Funct. 28, 949–955.

WARING, R.H., RUNNING, S.W., 1978. Sapwood water storage: its contribution to transpiration and effect upon water conductance through the stems of old-growth Douglas-fir. Plant. Cell Environ.

Whalley, W.R., Dean, T.J., Izzard, P., 1992. Evaluation of the capacitance technique as a method for dynamically measuring soil water content. J. Agric. Eng. Res. 52, 147–155.

Whitaker, S., 1986. Flow in porous media I: A theoretical derivation of Darcy's law. Transp. Porous Media 1986 11 1, 3–25.

Wiedemann, A., Marañón-Jiménez, S., Rebmann, C., Herbst, M., Cuntz, M., 2016. An empirical study of the wound effect on sap flux density measured with thermal dissipation probes. Tree Physiol. 36, 1471–1484.

Windt, C.W., Blümler, P., 2015. A portable NMR sensor to measure dynamic changes in the amount of water in living stems or fruit and its potential to measure sap flow. Tree Physiol. 35, 366–375.

Wolf, H., 2008. Determination of water density: Limitations at the uncertainty level of 1 × 10-6. Accredit. Qual. Assur. 13, 587–591.

Wullschleger, S.D., Hanson, P.J., Todd, D.E., 1996. Measuring stem water content in four deciduous hardwoods with a time- domain reflectometer. Tree Physiol. 16, 809–815.

Xue, J., Su, B., 2017. Significant remote sensing vegetation indices: A review of developments and applications. J. Sensors 2017.

Zhou, H., Sun, Y., Shan, G., Grantz, D.A., Cheng, Q., Schulze Lammers, P., Damerow, L., Wen, B., Xue, X., Chen, B., 2018. In situ measurement of stem water content and diurnal storage of an apricot tree with a high frequency inner fringing dielectric sensor. Agric. For. Meteorol. 250–251, 35–46.

Zhou, H., Sun, Y., Tyree, M.T., Sheng, W., Cheng, Q., Xue, X., Schumann, H., Schulze Lammers, P., 2015. An improved sensor for precision detection of in situ stem water content using a frequency domain fringing capacitor. New Phytol. 206, 471–481.

Zhu, Y., Irmak, S., Jhala, A.J., Vuran, M.C., Diotto, A., 2019. Time-domain and frequency-domain reflectometry type soil moisture sensor performance and soil temperature effects in fine- And coarse-textured soils. Appl. Eng. Agric. 35.

Zorzi, I., Francini, S., Chirici, G., Cocozza, C., 2021. The TreeTalkersCheck R package: An automatic daily routine to check physiological traits of trees in the forest. Ecol. Inform. 66.